ARL-TR-10317 • Apr 2026

Detailed Kinetic Modeling of the Pyrolysis of 1,5,9-Decatriene. Part I: Experimental and Automated Chemical Kinetics Mechanism Generation

by Joshua L. Lansford, Chiung-Chu Chen, Rodger E. Cornell, Christopher P. Stone, Michael J. McQuaid, Jeffrey D. Veals, Nimal Naser, Gina M. Fioroni, and Robert L. McCormick

NOTICES

Disclaimers

The findings in this report are not to be construed as an official Department of the Army position unless so designated by other authorized documents.

Citation of manufacturer's or trade names does not constitute an official endorsement or approval of the use thereof.

Destroy this report when it is no longer needed. Do not return it to the originator.

ARL-TR-10317 ● APR 2026

Detailed Kinetic Modeling of the Pyrolysis of 1,5,9-Decatriene. Part I: Experimental and Automated Chemical Kinetics Mechanism Generation

Joshua L. Lansford, Chiung-Chu Chen, Rodger E. Cornell, Christopher P. Stone, Michael J. McQuaid, and Jeffrey D. Veals
DEVCOM Army Research Laboratory

Nimal Naser, Gina M. Fioroni, and Robert L. McCormick
National Laboratory of the Rockies

REPORT DOCUMENTATION PAGE

1. REPORT DATE	2. REPORT TYPE	3. DATES COVERED	
		START DATE	END DATE
April 2026	Technical Report	01/29/2023	08/01/2025

4. TITLE AND SUBTITLE
Detailed Kinetic Modeling of the Pyrolysis of 1,5,9-Decatriene. Part I: Experimental and Automated Chemical Kinetics Mechanism Generation

5a. CONTRACT NUMBER	5b. GRANT NUMBER	5c. PROGRAM ELEMENT NUMBER
5d. PROJECT NUMBER	**5e. TASK NUMBER**	**5f. WORK UNIT NUMBER**

6. AUTHOR(S)
Joshua L. Lansford, Chiung-Chu Chen, Rodger E. Cornell, Christopher P. Stone, Michael J. McQuaid, Jeffrey D. Veals, Nimal Naser, Gina M. Fioroni, and Robert L. McCormick

7. PERFORMING ORGANIZATION NAME(S) AND ADDRESS(ES)	8. PERFORMING ORGANIZATION REPORT NUMBER
DEVCOM Army Research Laboratory ATTN: FCDD-RLA-WC Aberdeen Proving Ground, MD 21005	ARL-TR-10317

9. SPONSORING/MONITORING AGENCY NAME(S) AND ADDRESS(ES)	10. SPONSOR/MONITOR'S ACRONYM(S)	11. SPONSOR/MONITOR'S REPORT NUMBER(S)

12. DISTRIBUTION/AVAILABILITY STATEMENT
DISTRIBUTION STATEMENT A. Approved for public release: distribution unlimited.

13. SUPPLEMENTARY NOTES

14. ABSTRACT
As part of an ongoing effort leveraging machine learning techniques to accelerate the development of detailed chemical kinetics mechanisms for modeling the decomposition and combustion of energetic materials, this study investigates the application of Massachusetts Institute of Technology's Reaction Mechanism Generator (RMG) for autonomously producing chemical kinetics mechanisms for 1,5,9-decatriene (DTE)—a commercially available hydrocarbon with a well-defined molecular structure similar to hydroxyl-terminated polybutadiene. In this work, predictions using mechanisms generated with RMG for the pyrolysis of DTE were compared with measurements from flow reactor experiments conducted for this work as a case study of RMG's capabilities. The experiments were conducted by the National Laboratory of the Rockies' Fuels and Combustion Science Group using their laminar flow reactor that was set to a constant pressure of 5 bar, a constant residence time of 0.5 s, and explored temperatures ranging from 800 to 1200 K in 50 K increments. Predicted and measured mole fraction profiles show reasonable agreement for the decay of DTE, the formation of two primary products (1,5-hexadiene and 1,3-butadiene), and the formation of C_2 species, including ethane (C_2H_6) and ethene (C_2H_4). However, of the 26 product species observed experimentally, 7 were not predicted by the model. An analysis of the pyrolysis reaction pathways revealed that additional reactions must be incorporated into the mechanism to improve agreement with all experimental measurements. These results will be presented in greater detail in Part II of this three-part technical report.

15. SUBJECT TERMS
Weapons Sciences, automatic mechanism generation, reaction mechanism generator, decatriene pyrolysis, laminar flow reactor

16. SECURITY CLASSIFICATION OF:			17. LIMITATION OF ABSTRACT	18. NUMBER OF PAGES
a. REPORT	b. ABSTRACT	C. THIS PAGE		
UNCLASSIFIED	UNCLASSIFIED	UNCLASSIFIED	UU	75

19a. NAME OF RESPONSIBLE PERSON	19b. PHONE NUMBER *(Include area code)*
Joshua L. Lansford	(703) 400-3046

STANDARD FORM 298 (REV. 5/2020)
Prescribed by ANSI Std. Z39.18

Contents

List of Figures

List of Tables

1. Introduction

Revealing mechanisms underlying energetic material (EM) performance and vulnerability that are not obtainable from measurement-based methods alone, physics-based models with detailed chemical kinetics mechanisms are formulated and applied to accelerate the development of advanced gun and rocket propulsion systems. Examples abound, with models formulated and applied by U.S. Army Combat Capabilities Development Command (DEVCOM) Army Research Laboratory (ARL) researchers producing insights into phenomena ranging from the ignition delays observed in hydrazine-alternative hypergolic propulsion systems,[1] to burning-rate predictions for unconventional EMs that have yet to be produced in quantities that would allow them to be accurately measured.[2] However, the reliability of such models' predictions and the depth of insight obtainable from them depend critically on the capacity of chemical kinetics mechanisms to reasonably represent the relevant decomposition and combustion chemistry. Unfortunately, the time and cost required to create such mechanisms using currently available methods are considerable relative to the life cycles and funding levels typical of DoW-sponsored weapon propulsion system research programs. Therefore, proposals for their development are often difficult to fund.

The time and cost to create and validate mechanisms for modeling EM decomposition and combustion stems from several weaknesses of the only protocol ARL researchers have found to be sufficiently reliable for the objectives to which they aspire. That protocol involves a subject matter expert (SME) postulating reactions they believe may be important for the system of interest based on their experience and intuition. For each postulate, quantum mechanics-based electronic structure methods (QM-ESMs) are employed to produce estimates for the molecular structures, normal modes, and electronic energies of stationary points of minimum energy paths (MEPs) for it. Statistical mechanics is then applied to estimate thermodynamic properties for the structures. These results, in turn, are employed as input for implementations of transition state theory to parameterize reaction rate coefficients (k_i^g) as a function of temperature (T),

$$k_i^g = A_i T^{n_i} \, exp\left(\frac{-E_{a,i}}{RT}\right) \tag{1}$$

where A_i, n_i, and $E_{a,i}$ are constants. Due to the exponential dependence of k_i^g with respect to T, high-fidelity, computationally expensive QM-ESMs are required to obtain $E_{a,i}$ estimates with the ±2 kcal/mol accuracies needed for the parameterizations to be reliable.

Although the effort required to implement this protocol for a single reaction is generally modest (for an SME), the SME will characterize the MEP for any reaction considered potentially important to increase the likelihood that the mechanism will be an adequate representation of a process of interest. This approach typically leads to many hundreds of MEP characterizations being performed to create a new mechanism. For each MEP, the SME needs to construct starting molecular geometries, monitor calculation progress, and analyze output. The cumulative labor required to process a large number of MEPs is substantial. In addition, searches for transition states often require SME intervention, further increasing the labor required for the task. Combined, MEP characterizations are the most time-consuming and costly aspect of a mechanism's development. Indeed, when proposing the development of a new mechanism that we anticipate will take 1–2 years to complete, approximately 75% of the total number of person-hours and over 95% of the high-performance computing CPU hours (1–5 M/year) will be budgeted for them.

Contributing greatly to the number of MEP characterizations performed to create a new mechanism is the protocol's reliance on an SME's experience and intuition for "reaction enumeration" (i.e., the postulation of reactions with the potential to be important in the application of interest). Because an SME's experience and intuition may not encompass all the reaction types with the potential to be important, when discrepancies between experimental and modeling results are observed, there can be a lot of guesswork involved in reconciling them. For example, in the course of developing a mechanism for modeling the combustion of ammonium perchlorate (AP), we observed that our upgrade of a mechanism obtained from an open source produced burning rate predictions that were worse than those produced by the original, prompting an extensive search for missing critical reactions.[3] Unable to reconcile differences on that basis, we scrutinized all other model inputs, and found that the discrepancies were due to a combination of small "errors" that summed to produce a non-negligible error in the relative energies of the condensed and gas-phase manifolds.[4] (Based on our investigation, it was evident that A_i, n_i, and/or $E_{a,i}$ for a number of k_i^g in the open-source mechanism had been "tuned" to produce good agreement with measured burning rates; thus, the mechanism would likely have been a poor basis for studying AP's combustion.) We also note that if the discrepancies *had* been due to the absence of critical reactions, there was no guarantee they would have been discovered.

In addition, the SME's experience and intuition is usually insufficient to predict the relative importance of many of the reactions they will postulate prior to characterizing their MEPs with computationally expensive methods (and even then, it might not be obvious). This is important because species conservation requires

relevant multiscale finite element models to include a partial differential equation (PDE) for each species in the mechanism. Thus, every reaction in the mechanism adds a source term to each PDE, linearly increasing the computational cost of the simulation and limiting computationally tractable mechanisms to about 120 reactions. Since "full" mechanisms we develop for modeling the decomposition and combustion of propellant and explosive ingredients typically comprise more than 1000 reactions, and full mechanisms for formulations contain more, they must be reduced.

The fraction of postulates whose MEPs we have characterized that have proven to be unimportant is reflected in our group's efforts to produce mechanisms for use in computational fluid dynamics (CFD) models of rocket motor combustion chamber dynamics.[5–9] Over the past 10 years, we have routinely produced reduced or skeletal mechanisms with less than 120 reactions that in canonical combustion models are able to accurately reproduce all the salient features of solutions produced with full mechanisms containing more than 2000. This implies that over 90% of the reactions in the full mechanisms are unimportant when simulating many macroscale properties. Presuming a similar percentage of postulated reactions are generally unimportant, a method for ranking candidates that proscribed MEP characterizations for just two-thirds of them would cut the time and cost of mechanism development in half.

Attempting to address these issues, rules-based methods have been developed and implemented to systematically enumerate and evaluate the potential importance of chemical pathways, with Massachusetts Institute of Technology's Reaction Mechanism Generator (RMG) being perhaps the most comprehensive and widely used package for combustion applications.[10] As discussed by Liu et al.,[10] such methods are "largely . . . data-driven task[s], requiring good estimation algorithms for thermochemical and rate parameters, which in turn rely on accurate training data from experiments or quantum chemistry calculations." Unfortunately, their applicability is generally limited to the parameter space of the training data employed to create them, and to our knowledge, none have been adequately developed for the parameter space relevant to modeling the decomposition and combustion of conventional EMs, including nitrate esters and nitramines, let alone nonconventional EMs.

Interested, nonetheless, in whether RMG might serve as an aid in the creation of mechanisms for modeling the decomposition and combustion of conventional EMs, we applied it for that purpose. Unsurprisingly, in its current form, it does not reduce the time and cost of mechanism development for such applications. We find several reasons for this limitation. First, because it does not have reaction templates for many NO_x reaction types important in the decomposition and combustion of nitrate

esters and nitramines, it is unable generate those parts of the reaction mechanism. To overcome this obstacle, new reaction templates must be created, or the RMG-generated mechanism must be supplemented with additional SME-generated reactions. Current efforts by our group into automating the creation of new reaction templates are ongoing. Second, based on our experience in ranking the relative importance of reactions in a chemical kinetics mechanism, RMG's reaction elimination scheme is not sufficiently reliable or efficient. We are addressing this limitation through the development of our own in-house reaction ranking machine learning (ML) model and with the design of new uncertainty quantification (UQ) indices that can be used to improve RMG's own reaction elimination scheme. Third, the included sensitivity analysis is computationally prohibitive for large reaction systems. Alternative screening and ML methods are being explored.

Based on these conclusions, ARL researchers proposed an alternative method in which RMG, with added EM-specific reaction templates, would be employed for reaction enumeration, and ML-based methods would be employed to rank the potential importance of the reactions within an enumerated set for an intended application. Those rankings would then be employed as the basis for selecting MEPs to characterize using high-level QM-ESMs. To assess the suitability of this mechanism generation pipeline, RMG was applied to a mechanism relevant to the U.S. Army that does not contain EM-specific reaction types. Sponsored by an ARL mission program, the study of the pyrolysis of 1,5,9-decatriene (DTE, $C_{10}H_{16}$) summarized herein was undertaken to evaluate RMG's capacity to serve the function envisioned for it.

Our interest in studying the pyrolysis of DTE stemmed from ARL researchers' efforts to create mechanisms for representing the decomposition and combustion HTPB type R45M. Widely used as a binder in composite propellants, R45M polymer chains have an average molecular weight of approximately 2500 amu and comprise cis, trans, and vinyl C=C groups whose ratios are approximately 0.2:0.6:0.2, respectively. Believing that their pyrolysis would proceed through relatively large hydrocarbons with cis, trans, and vinyl ratios equivalent to R45M, McQuaid et al.[9] created a mechanism for modeling the decomposition and combustion of 6-ethenyl-2,8,12,16-octadectetraene (EODT) and in deflagration models specified EODT to represent the products volatilizing from HTPB's surface. Begun in 2009 and subsequently developed and employed for a variety of applications, that mechanism now comprises more than 1378 species and 5790 reactions.

Despite the extensive development of the EODT mechanism and the compelling results it has yielded, we would be hard-pressed to defend its "completeness," however one might define that property. A recent study by Zhao and Savoie[11]

mapped out an extensive reaction network for the pyrolysis of β-D-glucose—a molecule containing 11 heavy (non-hydrogen) atoms—identifying over 31,000 reactions generated through automated exploration. As such, it is obvious that the EODT mechanism includes only a miniscule fraction of the number of possibilities, which in principle would approach infinity if it were to include potential for modeling polymerization. Therefore, we cannot confidently state that it does not lack species and reactions whose inclusion could significantly change its predictions. Moreover, since EODT was a notional molecule with no chance of being affordably synthesized, there was no chance that measurement-based data would be available to inform the development of methods for addressing this issue. Therefore, we sought as an alternative a relatively inexpensive, commercially available hydrocarbon with a well-defined molecular structure having from 8 to 20 carbon atoms that like R45M had cis, trans, and vinyl C=C groups—DTE met these criteria.

Motivated by an interest in establishing the potential for experiments conducted with a high-throughput desorption/pyrolysis-gas-chromatograph/mass-spectroscopy (D/P-GC/MS) instrument to produce mechanism validating results, an initial study of DTE pyrolysis was conducted in which samples were rapidly heated in a pyroprobe, and relative product concentrations were derived from GC/MS chromatograms. The mechanism employed to represent the pyrolysis of DTE was a subset of the EODT mechanism.[12] Comparisons of predicted and measured results for product concentrations indicated that the mechanism/physics-based model combination was reasonably representative of the experiment. However, there were some discrepancies that could not be resolved. Moreover, from the standpoint of mechanism validation, the experimental system was less than ideal, with several fairly speculative assumptions having to be made about the gas-phase dynamics, process quenching, and product concentration quantification. Therefore, we had reservations about employing the results as the basis for an evaluation of an RMG-generated mechanism.

Offering a superior alternative, the Fuels and Combustion Science Group of the National Laboratory of the Rockies (NLR) employed a high-pressure laminar plug-flow reactor to study DTE's pyrolysis at 5 bar and temperatures ranging from 800 to 1200 K. Well-represented by a canonical closed-system, constant-pressure, constant-temperature homogeneous reactor model, such experiments represent a benchmark for mechanism validation. Summarized herein, the mole fractions of 26 different products were quantified at 50 K intervals within the temperature range considered and thus represent a demanding test of RMG's capacity to enumerate mechanisms for modeling the pyrolysis of polyenes with 8 or more carbon atoms.

Anticipating the key role we expect RMG to play in the mechanism creation protocol currently under development, we review herein the main methods it employs for reaction enumeration and species inclusion. The inputs we employed to create a mechanism for modeling DTE's pyrolysis are also provided. Comprising 377 species and 3968 reactions, that mechanism produced predictions for the concentrations of primary products (1,5-hexadiene and 1,3-butadiene) and a number of secondary products that are in reasonable agreement with measured values. However, there were also a fair number of products for which the predictions were significantly greater or less than measured values, confirming our skepticism of RMG's standalone capacity to generate mechanisms for the pyrolysis of relatively large hydrocarbons with the fidelity we seek.

As for RMG's potential to be used for reaction enumeration for the mechanism generation protocol we are developing, the results were encouraging. Areas where RMG could be improved are identified and discussed. Details of the RMG software are discussed extensively in the literature.[10,13,14]

Key features and functionality that we found to be important are discussed in Section 2 to aid in its application. The summarized information was collated from multiple open-source literature publications, the documentation provided with the software, and from our own analyses and implementation of the RMG source code.

2. Key Features of RMG

2.1 Molecular Representation

Adjacency lists are used to represent atom connectivity. Bond order, formal charge, and the number of radical and lone pair electrons are captured by this representation. Benzene bonds, hydrogen bonds, reaction bonds, and Van der Waal's interactions can be specified, which are given bonds with orders of 1.5, 0.1, 0.05, and 0, respectively. Adjacency lists are typically generated from an RMG molecule object. The molecule object can be generated from a number of standard chemical representations, such as SMILES, using open-source software, such as RDKit and Open Babel. Some of the properties, such as bond order, are identified with the open-source backend, while others, such as electronic information, are identified using rules predefined by RMG. An adjacency list for the methyl radical taken from a publication on the RMG software[13] is provided below in Figure 1.

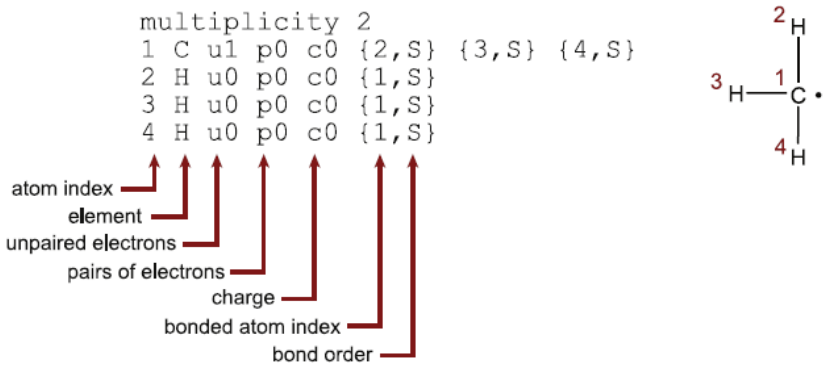

Figure 1. An adjacency list (left) given for a methyl radical (right).

As part of the adjacency list construction process, RMG identifies electronic resonance structures for a given molecule, as different resonance structures can match different reaction templates, and lumps these structures into a single species object. Figures 2a and 2b show two different resonance isomers of dioxohydrazine, including their 2D skeletal structures and adjacency lists.

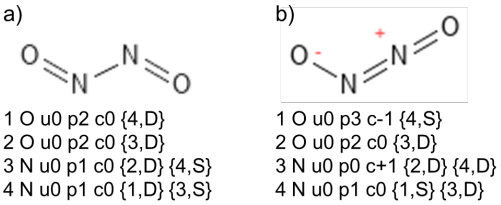

Figure 2. Resonance isomers of dioxohydrazine.

No 3D information is included in an adjacency list; therefore, it cannot distinguish between stereoisomers. This means that multiple mechanisms must be generated for DTE using different species' thermodynamic and kinetic libraries for molecules that have both cis and trans isomers that must be accounted for to obtain accurate predictions of kinetics and macroscale properties.

2.2 Reaction Enumeration

The first step RMG uses for reaction enumeration is to match portions of a molecule to predefined templates[13] via substructure matching algorithm implemented in the method "match_node_to_structure."[15] Every template is paired to a reaction recipe to determine bond rearrangement. Reaction templates are grouped into hierarchical trees, called reaction families, such that each level of the tree corresponds to more specific templates. The most specific template corresponds to an exact match. An example of a reaction template and recipe for a general hydrogen abstraction reaction, and the first level of a hierarchical tree, is provided in Figure 3. The second level of the tree might indicate the type of atom for X, such as carbon, and the third

level might indicate the chemical environment of the atom, such as whether it is a primary or secondary carbon atom.

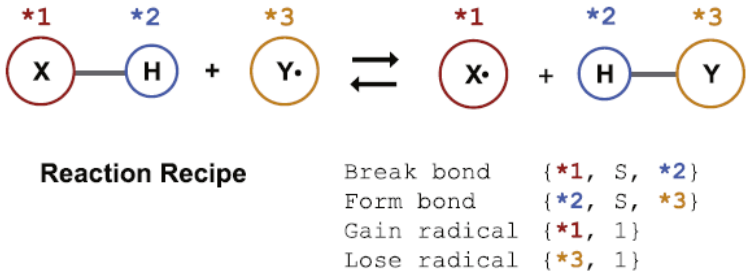

Figure 3. Reaction template and recipe for hydrogen abstraction.

2.3 Parameter Estimation

RMG primarily uses rate rules to estimate reaction rates. These rules are attached to specific templates. If a template does not have an associated rate rule, kinetics are averaged from directly connected templates further down the reaction tree, called child nodes. These child nodes can include reactions from a training set that can be modified.[13] Templates are organized into families and defined in the following files, which can be found on the RMG-database GitHub page.[16]

- *groups.py:* contains recipe, group definitions, and hierarchical trees
- *training.py:* contains specific kinetics that are matched to templates
- *rules.py:* contains parameters for a template

For the most general H-abstraction template mentioned previously, the rate rule entry in *rules.py* is provided in Figure 4 and includes the parameters used to calculate the rate constant.

```
entry(
    index = 1,
    label = "X_H;Y_rad_birad_trirad_quadrad",
    kinetics = ArrheniusEP(
        A = (100000, 'cm^3/(mol*s)'),
        n = 0,
        alpha = 0,
        E0 = (10, 'kcal/mol'),
        Tmin = (300, 'K'),
        Tmax = (1500, 'K'),
    ),
    rank = 0,
    shortDesc = u"""Default""",
)
```

Figure 4. Rate rule entry in *rules.py* for hydrogen abstraction.

The *training.py* file associated with this reaction includes over 3000 reactions that can be used to estimate rate parameters at deeper levels of the reaction family more accurately than the rate rule in Figure 4.

Each reaction family includes its own training set file. Generally, if the kinetics of a specific reaction are generalizable and very accurate, they should be added to a training set. Automatic child template generation from training reactions combined with decision trees for rate estimation in place of rate rules is currently being implemented.[10,17] In this scheme, the templates assigned to a reaction family depend on the training reactions available. A list of extensions is then generated, such as specifying an atom element or bond order, such that each extension matches some, but not all, of the training reactions. The extensions are selected such that the following equation is minimized,

$$\Pi = \sum_i N_i \sigma_i \tag{2}$$

where N_i is the number of training reactions matching an extension and σ_i is the standard deviation of the natural logarithm of rate constant (k) calculated for the training reactions in extension i at 1000 K. For example, if training reactions in the hydrogen abstraction class existed for the set of species (OH, OH_2, CH, CH_2, CH_3) reacting with hydrogen atom having $\log_{10}(k)$ values of (1, 2, 1.2, 2.2, 3.2), the extension selected would divide on number of hydrogen atoms bonded to X, rather than the element type of X such that the resulting leaf nodes would be (OH, CH), (OH_2, CH_2), and (CH_3) with a Π value of 0.4. Splitting on element type would have resulted in a Π value of 2.95. This process is repeated until each node generated by an extension contains only one training reaction. If the original list of extensions is not sufficient, additional extensions are added through subgraph isomorphism and can include the local environment of atoms bonded to X. The rates are then estimated at each node of the hierarchical tree by fitting a function that maps the activation heats of reactions for the training reactions associated with a node to their activation energies. The activation energy of a new reaction can then be predicted based on its heat of reaction. Figure 5 depicts how the decision tree of reaction templates is generated according to the scheme previously described.

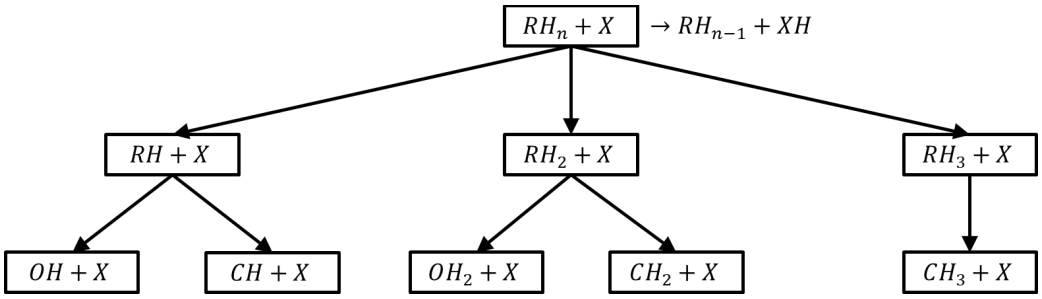

Figure 5. Automatically generated decision tree of reaction templates from five hydrogen abstraction training reactions.

RMG also hosts reaction depositories that can be added as a reaction library, which take precedence over rate rule estimates. Many of these depositories contain parameters that fit a specific mechanism and set of reaction conditions. In that case, caution should be used before using these if only part of the mechanism is relevant, or if the reaction will take place at different conditions than those for which the parameters were fit.

In the early versions of the program, thermodynamic parameters, such as heat of reaction (ΔH_{rxn}), were estimated using a group additivity scheme modeled after Bensen group additivity. Recently, an ML model has been developed that produces more accurate ΔH_{rxn} predictions for molecules with nitrogen, oxygen, and fused rings.[15,18] RMG applies ring strain and hydrogen bond corrections to estimate thermodynamic values. For any reversible reaction, thermodynamic consistency is maintained through the following relation between the forward and backward reaction rate:

$$\frac{k_f}{k_r} = K_{eq} = \left(\frac{RT}{P^o}\right)^{-\Delta n} exp\left(\frac{-\Delta G^o_{rxn}(T)}{RT}\right) \quad (3)$$

2.4 Computing Flux Rates

Species flux rates found in the solutions to closed, constant temperature, and constant pressure homogeneous reactor problems are the basis for mechanism filtering. RMG solves the differential equations for the problems via PyDAS wrapper that calls either DASPK or DASSL. Reverse reaction rates are calculated using Equation 2 to maintain thermodynamic consistency. Pressure corrections are available with a third body to thermally activate reacting species. CHEMKIN input files are produced at the end of each simulation step so that the generated mechanisms can be used with other modeling software.

RMG initializes the simulation at t = 0, followed by the next steps that determine if these "edge" species are important enough to be added to the "core" species. "Edge" species *i* are included into the "core" species if

$$R_i = \frac{dC_i}{dt} > \epsilon\, R_{core}, \tag{4}$$

where *Ri* is net flux of "edge" species *i*, defined as an infinitesimal change in the concentration of "edge" species (i.e., *dCi*) in an infinitesimal time (i.e., *dt*), ϵ is the user-specified error tolerance, and *Rcore* is the characteristic flux of the reaction system, defined by

$$R_{core} = \sqrt{\sum_j R_j^2} \tag{5}$$

ϵ is set to 0.3 in this work (as specified by toleranceMoveToCore = 0.3 in the RMG input file).

The reaction generation and integration continued until they met the termination criteria for reaction time (t_{term}) or the concentration of a specific species (X_{term}). This process results in the completed mechanism generation. The final model "core" for DTE pyrolysis comprised 377 species and 3968 reactions. The final model "edge" included 20,663 species and 106,668 reactions. The "core" mechanism of the final model, referred to as the DTE-RMG mechanism, was integrated into the homogeneous reactor to simulate NLR's experiment and is provided as an attachment to Appendix A.

2.5 Mechanism Growth, Reaction Filtering, and Termination Criteria

The first step in generating a mechanism is defining molecular species within the RMG input file. All species defined in the RMG input file are placed into the core mechanism. Species generated by reacting to these core species are placed in an expanded edge mechanism. If the flux of a species, as outlined in Section 2.4, in the edge mechanism exceeds a user-specified level, that species is added as a core species and the templates are used to identify possible reactions between the newly added species and the existing species in the core. A graphical depiction of the overall process taken from the *RMG Theory Guide*[19] is provided in Figure 6. The mechanism generation completes once there are no species in the edge with flux levels above the user-specified level.

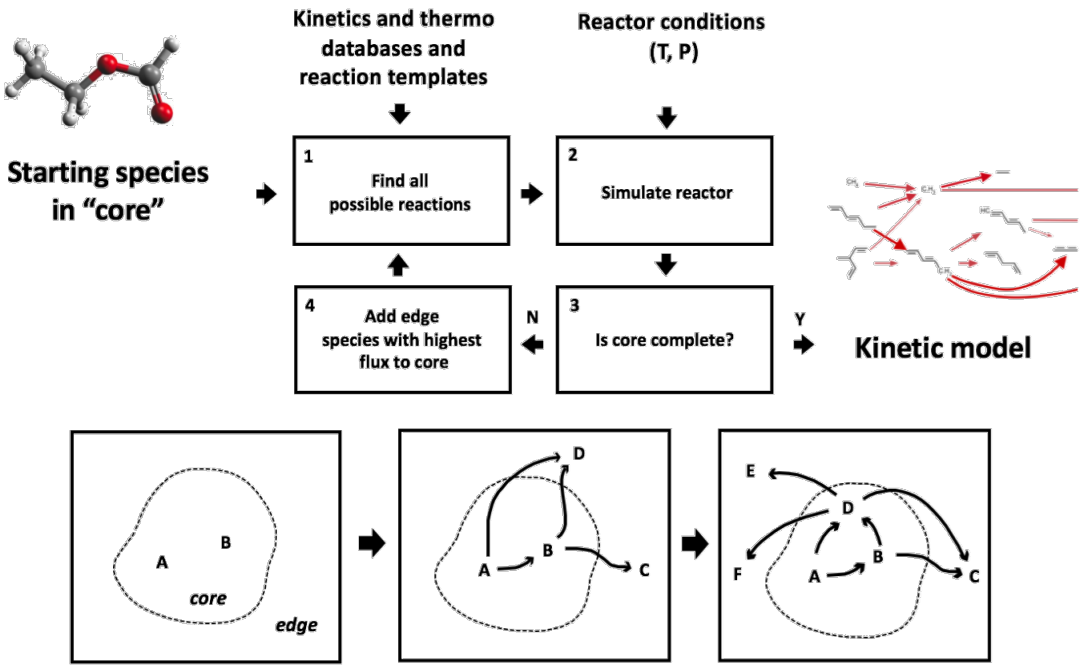

Figure 6. Illustration of rate-based enlargement algorithm taken from the *RMG Theory Guide*.[19]

There are three input parameters that control how molecules in the edge mechanism get moved into the core. These parameters are labeled in Figure 7, which depicts the tolerance criteria of edge species flux relative to the characteristic flux against the conversion of a species specified in the input file; it is reproduced from the RMG software documentation.[19] The characteristic flux is the root mean squared average of the core mechanism species' flux at any point in the simulation process. Parameters labeled in Figure 7 include *toleranceMoveToCore* (green line), *toleranceInterruptSimulation* (red line), *terminationConversion* (blue dashed line), and *toleranceKeepInEdge* (yellow line). As a simulation progresses, the first species to reach *toleranceMoveToCore* is moved from the edge to the core.

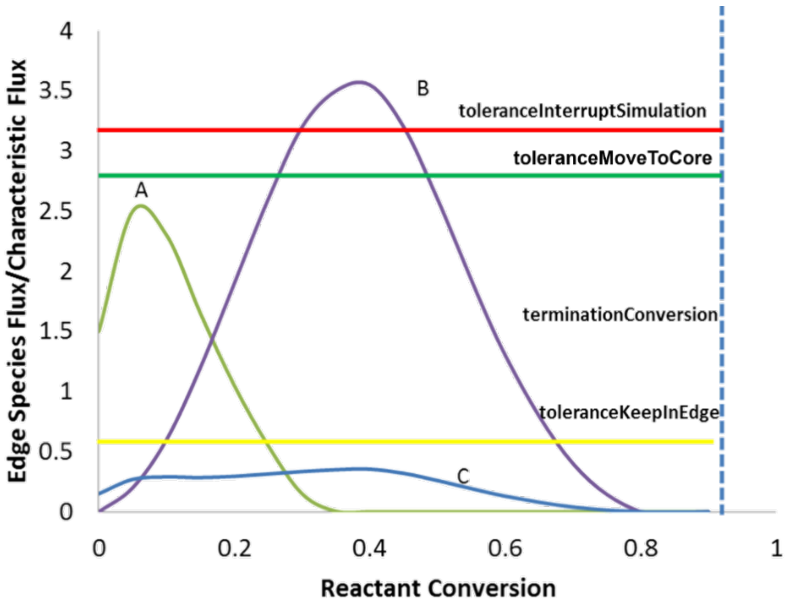

Figure 7. Example relative flux for three edge species (A, B, C) and RMG input parameters that determine mechanism growth.

The simulation ends once *toleranceInterruptSimulation* or a specified termination conversion is reached. Species with peak fluxes below *toleranceKeepInEdge* are removed from the edge mechanism, but only if the simulation reaches the termination conversion. For example, in Figure 7, species B (purple curve) would be moved to the core and the simulation would end at a reactant conversion of 0.3 as indicated by the red line. Because the termination conversion is never reached, species C (blue curve) is not removed from the edge mechanism even though its flux never reaches *toleranceKeepInEdge*. If the edge mechanism grows too large, the memory requirement may become too large. Generally, it is the reaction enumeration step that is the slowest part of RMG. This step can be accelerated by specifying the *filterThreshold* parameter, which instructs RMG to only apply templates to species if their predicted concentration is above the value specified by the user.[19]

Inclusion of a seed mechanism can influence both the mechanism's accuracy and the mechanism's growth rate. All species and reactions in the seed mechanism are automatically placed into the core mechanism. To limit reaction enumeration, no further reactions are explored between species in the seed mechanism beyond the reactions specified. As new species are moved from the edge to the core, additional bimolecular and trimolecular reactions are explored with the existing species in the core. This behavior can be changed with minor alterations to the source code. We have found that small changes in the seed mechanism can result in large changes in

total simulation time. We discuss the experimental flow reactor setup for DTE pyrolysis in Section 3.

3. Flow Reactor Experiment

The laminar flow reactor experiments were performed by the NLR Fuels and Combustion Science Group. The laminar flow reactor (Figure 8) consists of a SilcoTek-treated stainless-steel tube with an internal diameter of 13 mm and a length of 71 cm, heated within an insulated ceramic furnace to minimize spatial deviations in temperature from each specified reactor set point. Helium (He) was used as the diluent/carrier gas and its flow was precisely regulated by a mass flow controller. The experiments were conducted at a constant pressure of 5 bar using a step-down backpressure regulator.

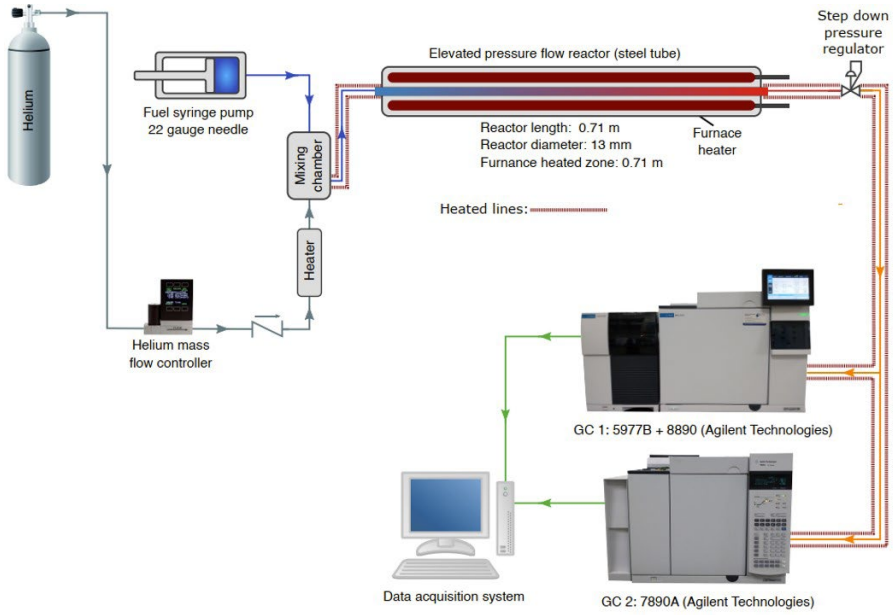

Figure 8. Schematic of the elevated pressure laminar flow reactor at NLR.

The DTE sample (>95% purity, CAS no.: 13393-64-1) was purchased from a commercial vendor (VWR) and employed as-received. Comprising a mixture of 5Z (cis) and 5E (trans) conformers whose composition was reported by the vendor to be nearly 50% cis and 50% trans, it is a liquid at 20 °C and 1 bar. Its normal boiling point is reported to be 170 °C.[20]

Samples were introduced into the He diluent flow using a syringe pump fuel delivery system that fed into a mixing chamber. Note that only the He diluent flow was heated prior to the mixing chamber to better control residence time of the DTE samples. DTE and He flows were independently controlled to produce an initial DTE mole fraction of 1000 ppm. Residence time of the DTE samples in the flow

reactor was controlled by the combined fuel and diluent flow rates and specified to 0.5 s for all temperature set points. The short residence time was chosen to prevent formation of high-carbon number soot and/or polycyclic aromatic hydrocarbons (PAHs) under pyrolysis conditions. These soot-precursor/soot compounds have high melting points that can condense in the transfer lines and GC sampling loops causing experimental difficulties, which include carbon balance issues and an increase in experimental uncertainties.

To prevent condensation of any products, the effluent transfer line and GC sampling loops were kept at 420 and 520 K, respectively. Two independent GC systems were used to analyze the effluent of the reactor. Heavy compounds (≥C5) were analyzed and quantified using GC1, which has a 60-m × 320-μm × 1-μm capillary column. GC1 column effluent was split between two parallel detectors: 1) a flame ionization detector (FID) equipped with a Polyarc methanizer and 2) mass spectrometer (MS). Polyarc methanizer is a catalytic microreactor that oxidizes all effluent components to methane prior to detection by FID. This enhances sensitivity and enables proper quantification of oxidation products. Calibration of the methanizer was performed using n-heptane, and identification of the compound was performed by MS spectral comparison with the National Institute of Standards and Technology database.[21] Quantification of identified species was performed by obtaining response factors from the FID and comparing them with the n-heptane calibration runs based on the effective carbon number method.[22] The lighter hydrocarbons (<C5) were analyzed on GC2, which has an FID and two thermal conductivity detectors (TCDs). The TCDs were used to analyze CO and CO_2. The FID of GC2 was calibrated by using standard gas mixtures with known concentrations of alkanes, alkenes, and alkynes, while the TCDs were calibrated using CO and CO_2 standards with each of 500-ppm concentrations.

Table 1 shows the DTE and He flow rates specified at each temperature set point to maintain the 0.5-s residence time. Estimates of all major experimental uncertainties are provided in Table 2. A more detailed description of the experiment is provided elsewhere.[23–27]

Table 1. Fuel and diluent flow rates for DTE flow reactor experiments as a function of temperature (P = 5 bar, τ [residence time] = 0.5 s, X_{fuel} = 1000 ppm).

T (K)	Fuel flow rate (mL/h)	Diluent flow rate (SLPM)
800	10.98	25.11
850	10.34	23.63
900	9.76	22.32
950	9.25	21.15
1000	8.79	20.09
1050	8.37	19.13
1100	7.99	18.26
1150	7.64	17.47
1200	7.32	16.74

Table 2. Estimated experimental uncertainties used for UQ.

Experimental parameter	Uncertainty value
Reactor length (m)	±0.020
Reactor diameter (m)	±0.020
Pressure (bar)	±0.1
Temperature uncertainty (K)]	±6
Fuel delivery uncertainty (μL/min)	1
Diluent flow uncertainty (SLPM)	0.1
Oxidizer flow uncertainty (SCCM)	1
Diluent density (kg/m^3)	0.01
Oxidizer density (kg/m^3)	0.01

4. DTE Pyrolysis Model

The DTE-RMG kinetic mechanism was integrated with a customized precommercial CHEMKIN-III version of SENKIN to simulate the experiments.[28] A zero-dimensional constant-pressure (CONP) reactor model was used to simulate all experiments. Initial simulation conditions consist of an initial reactor temperature set to each of the specified set points in Table 1, a constant pressure of 5 bar, a constant inlet fuel mole fraction of 1000-ppm DTE (with an He balance), and a fixed residence time of 0.5 s. RMG does not include 3D structural information in its adjacency list representation, which means it cannot differentiate between stereoisomers. As a result, the DTE-RMG kinetic mechanism does not distinguish between cis-DTE and trans-DTE isomers. Two analysis software packages (SREAD[29] and Elemap[30]) developed by Anderson et al. were used to postprocess data generated by CHEMKIN-CONP simulations to create diagrams illustrating the relative rates of reactions involved in the decomposition and formation of important species.

Several thermodynamic libraries available in RMG were used in the construction of the DTE-RMG kinetic mechanism. Included were parameters derived from Lai

et al.'s work on the pyrolysis of hexylbenzene (Lai_Hexylbenzene),[31–33] high-accuracy ab initio thermochemistry for various small molecules as calculated by Goldsmith et al.[34] (DFT_QCI_thermo), and the primaryThermoLibrary.[16] The kinetics depository used for rate estimation included only reaction families containing carbon and hydrogen elements in the RMG database. For required data that was not in the libraries, RMG used the Benson group additivity method for thermochemistry estimations, and the RMG training database for rate rules assignments. The RMG input for the reactor system defines operating conditions within a temperature range of 600–1500 K and a pressure of 5.0 bar. The reactor is simulated at a fixed number of times per cycle (nSims = 10), as described in Section 2.5.

5. Results and Discussion

Table 3 lists all of the species that were observed by NLR, including their formal name, label in the mechanism, molecular structure, maximum observed mole fraction and the corresponding temperature. All experimental data are also provided in Table B-1. Species labels and reaction numbers correspond to the DTE mechanism in Appendix B.

Table 3. Species observed by NLR.

Species	Molecular structure	Maximum (ppm)	Temp. (K)[b]
1,5,9-decatriene [$C_{10}H_{16}$(1)][a]	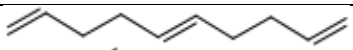	406.03 ± 28.80	800
1,5-hexadiene [C_6H_{10}(119)]	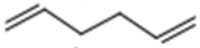	654.30 ± 56.49	900
1,3-butadiene [C_4H_6(57)]	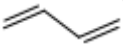	811.85 ± 98.75	1050
Ethene [C_2H_4(227)]		925.99 ± 44.06	1200
Acetylene [C_2H_2(501)]	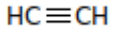	424.88 ± 10.25	1200
Methane [CH_4(1246)]		536.76 ± 18.55	1200
1-butene [C_4H_8(248)]	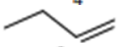	211.58 ± 9.22	1050
Propene [C_3H_6(84)]		520.43 ± 31.72	1050
Propyne [C_3H_4(759)]		1128.83 ± 43.35	800
Allene [ALLENE(51)]		181.24 ± 15.24	1150
Benzene [C_6H_6(5025)]		284.52 ± 25.65	1200
Toluene [C_7H_8(3291)]		33.00 ± 3.19	1150
Naphthalene [S(11344)]	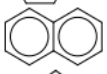	34.78 ± 2.55	1200
1,3-cyclopentadiene [S(14222)]		96.58 ± 9.93	1100
1,3-cyclohexadiene		42.84 ± 3.68	1000
1-butyne [C_4H_6(500)]		41.98 ± 1.98	1200
2-butyne	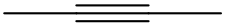	34.89 ± 2.34	1150
Ethane C_2H_6(1571)	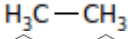	44.64 ± 1.85	1150
1-pentene		10.06 ± 0.87	950
1,3-pentadiene	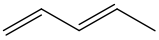	10.40 ± 0.80	1050
Butane	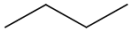	10.35 ± 0.40	1050
1,4,9-decatriene	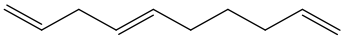	130.70 ± 9.17	800
1,9-decadiene	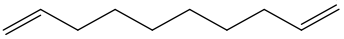	22.80 ± 2.08	850
1-buten-3-yne	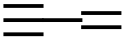	51.45 ± 6.60	1000
Styrene	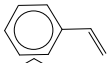	34.94 ± 2.69	1200
Indene	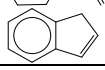	23.67 ± 1.80	1200

[a] Label in the mechanism.
[b] Temperature at which the maximum mole fraction occurred.

The profiles of all major and minor species predicted in the flow reactor simulations are presented in Figure 9, along with the corresponding experimental measurements. Figure 10 illustrates the species that were not predicted by the model yet were observed experimentally. Overall, the DTE-RMG model predictions exhibit reasonable qualitative agreement with the experimental data for the decay of DTE, the formation of the two primary products (1,5-hexadiene and 1,3-butadiene), and the formation of C_2 species, including ethane (C_2H_6) and ethene (C_2H_4).

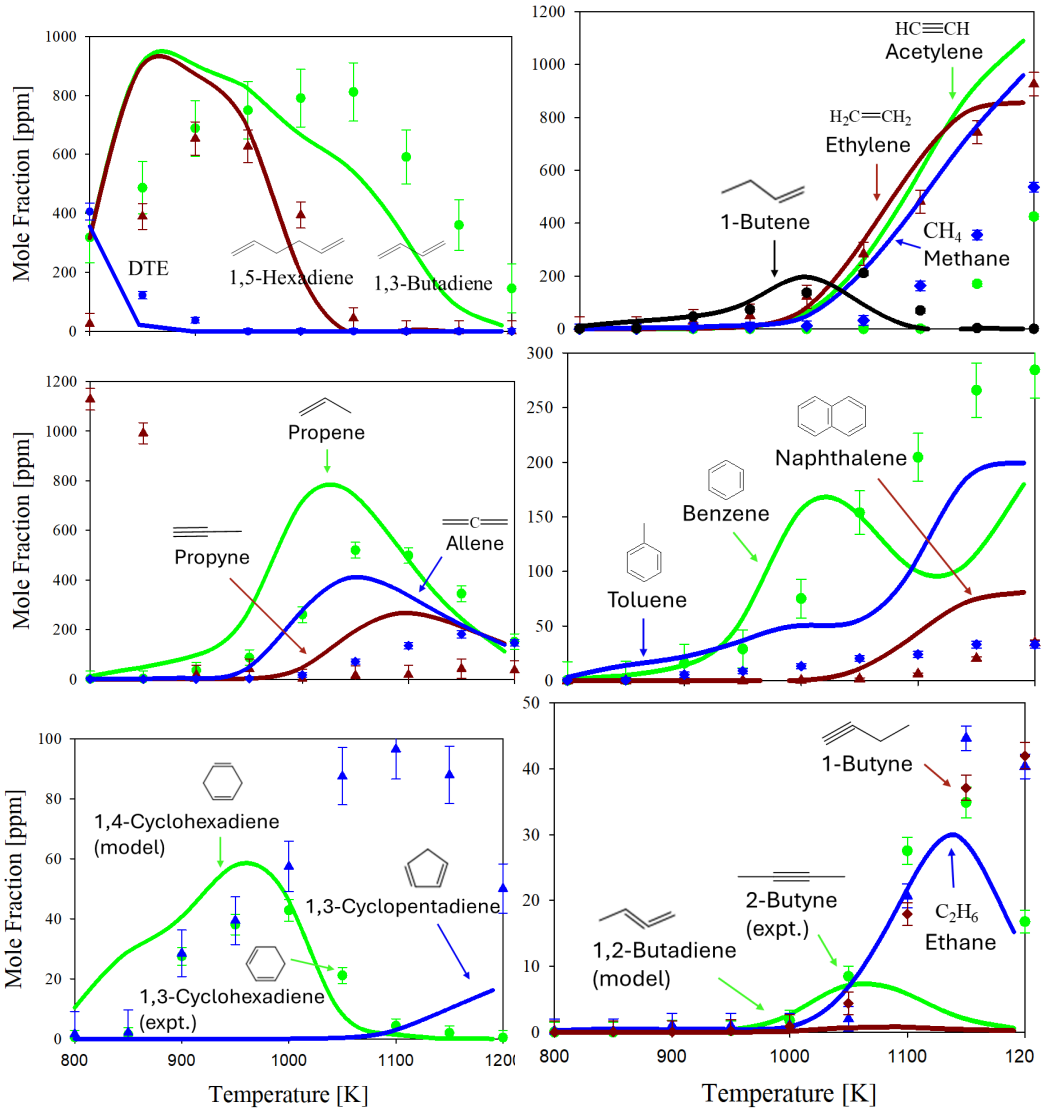

Figure 9. Mole fractions as function of temperature for 1,5,9-decatriene pyrolysis in a flow reactor, P = 5 bar, 1,5,9-decatriene = 1000 ppm: symbols, experimental mole fraction profile of molecule represented in graph; lines, mole fraction profiles calculated with CHEMKIN using the constant-pressure batch reactor model and the RMG-developed kinetic model.

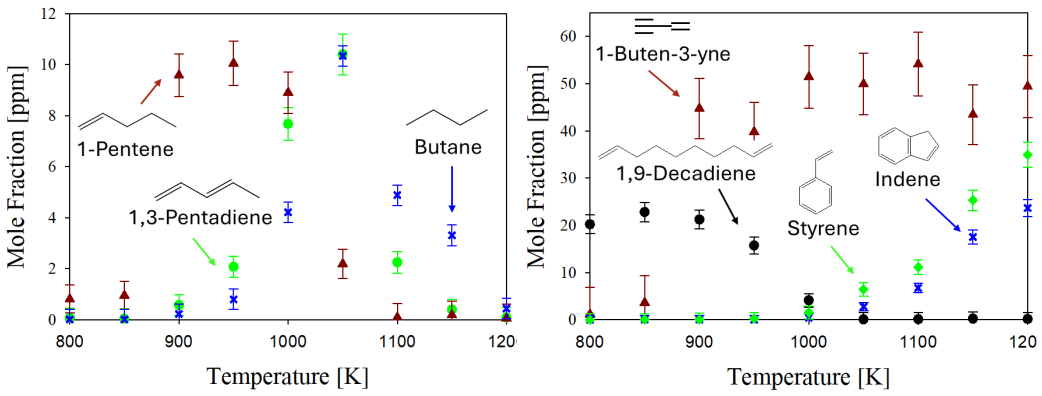

Figure 10. Mole fractions as function of temperature for 1,5,9-decatriene pyrolysis in a flow reactor, P = 5 bar, 1,5,9-decatriene = 1000 ppm: symbols, experimental mole fraction profile of molecule represented in graph. Seven species not predicted by the RMG model.

The predicted and measured amounts of cyclohexadiene are in close agreement; however, the model predicts the 1,4-isomer, while the experimental measurement indicates the presence of the 1,3-isomer. Because these isomers have similar GC-MS spectra, it is unclear what was measured in the experiments. Additional testing is needed to increase confidence in the identification of cyclohexadiene isomers using NLR's GC-MS diagnostic system. The model underestimates the concentrations of 1,3-cyclopentadiene and 2-butyne, but overpredicts the C_3 species (propene, propyne, and allene), as well as acetylene, methane, toluene, and naphthalene. In the experiment, 2-butyne was observed, while the model predicted the isomer 1,2-butadiene. It is possible that 1,2-butaidene isomerizes to 1,3-butadiene before it can be measured by the GCMS. Agreement between experimental results and model predictions are generally best below 1050 K.

The experimental data show that benzene levels increase with increasing temperature. In contrast, the model's predictions exhibit a more complex temperature dependence: benzene levels increase with temperature up to approximately 1025 K, then decrease with further temperature increase to a minimum around 1125 K, and finally increase again up to 1200 K.

Figures 11–17 present pathway diagrams for DTE pyrolysis at various temperatures, 5 bar, and a residence time of 0.5 s. Arrows indicate reactant–product connections. The widths of the arrows are proportional to the molar consumption rate of the reactant (species) in the box at the arrow's tail. Species listed next to the arrows are co-reactants, and the numbers associated with them indicate the consumption rate of the reactant in the box due to its reaction with the co-reactant relative to the rate of all other reactions at that spatial location. Absolute rates are scaled to a range in which the value for the largest molar consumption rate produced by any reaction at the location is 100. The absolute rate corresponding to 100 in

each diagram is provided in the figure captions. Relatively slow reactions are omitted to keep the diagrams clear and readable.

5.1 1,3-Butadiene [C_4H_6(57)] and 1,5-Hexadiene [C_6H_{10}(119)]: 800 K

As shown in Figure 11, the first step in DTE decomposition at 800 K is bond cleavage, producing allylic radical [ALLYL(3)] and 1,5-heptadiene-7-yl radical [C_7H_{11}(2)] (via R2, which denotes the reverse direction of reaction R2). DTE [$C_{10}H_{16}$(1)] can also undergo a Cope rearrangement,[35] in which two π bonds break and a new σ bond forms simultaneously, yielding 4-vinyl-1,7-octadiene [$C_{10}H_{16}$(17)] (via R1). Among the dissociation products, ALLYL(3) is the most abundant species, formed from the decomposition of $C_{10}H_{16}$(1) (via R2), $C_{10}H_{16}$(17) (via R3), and C_7H_{11}(2) (via R6). The recombination of two allylic radicals to form 1,5-hexadiene [C_6H_{10}(119)] (via R8) becomes the dominant pathway at 800 K. Experimentally, 1,5-hexadiene was identified as the primary product at temperatures between 800 and 1050 K. In addition, 1,3-butadiene [C_4H_6(57)] was observed, primarily arising from the dissociation of C_7H_{11}(2) (via R6).

$C_{10}H_{16}(17) \leftrightarrow C_{10}H_{16}(1)$ R1
$ALLYL(3) + C_7H_{11}(2) \leftrightarrow C_{10}H_{16}(1)$ R2
$ALLYL(3) + C_7H_{11}(2) \leftrightarrow C_{10}H_{16}(17)$ R3
$ALLYL(3) + C_4H_6(57) \leftrightarrow C_7H_{11}(2)$ R6
$ALLYL(3) + ALLYL(3) \leftrightarrow C_6H_{10}(119)$ R8

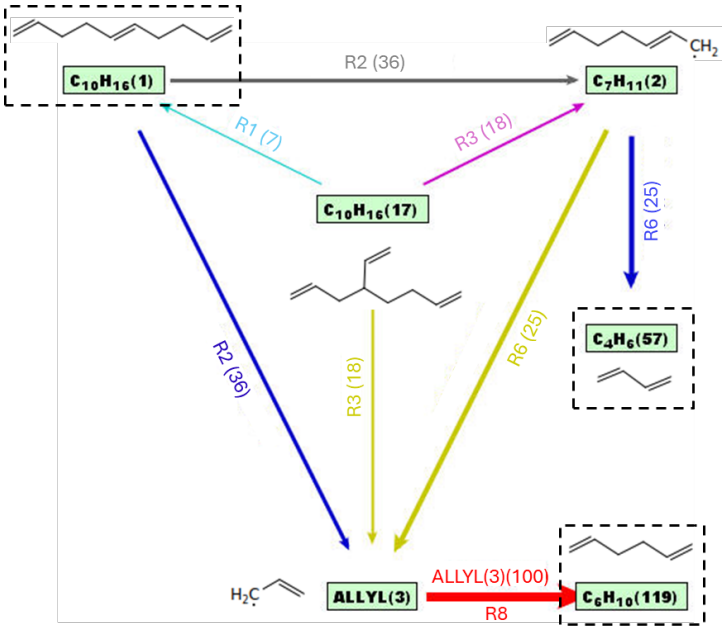

Figure 11. Primary decomposition pathway diagrams for DTE pyrolysis at 800 K, 5 bar, and a residence time of 0.5 s. The absolute rate corresponding to 100 is 8.07×10^{-8} mol/cm^3-s.

5.2 Propene [C_3H_6(84)] and 1,3-Butadiene [C_4H_6(57)]: 900 K

As the temperature increases, 1,5-hexadiene [C_6H_{10}(119)] dissociates back into two ALLYL(3) radicals through reaction R8. The major reaction pathways for DTE pyrolysis at 900 K are shown in Figure 12. The addition of a hydrogen atom to C_6H_{10}(119) at the terminal carbon of the C=C bond forms the hex-5-en-2-yl radical [C_6H_{11}(200)] (via R66). Subsequently, C_6H_{11}(200) undergoes β-scission to yield an ALLYL(3) radical and propene [C_3H_6(84)] (via R67). Propene [C_3H_6(84)] was observed experimentally, with its major production pathway identified as the disproportionation reaction R15, in which ALLYL(3) and but-3-en-2-yl radical [C_4H_7(181)] undergo an H-shift to form two stable products: propene [C_3H_6(84)] and 1,3-butadiene [C_4H_6(57)]. The but-3-en-2-yl radical [C_4H_7(181)] is formed by the addition of a hydrogen atom to C_4H_6(57) at the terminal carbon of the C=C bond.

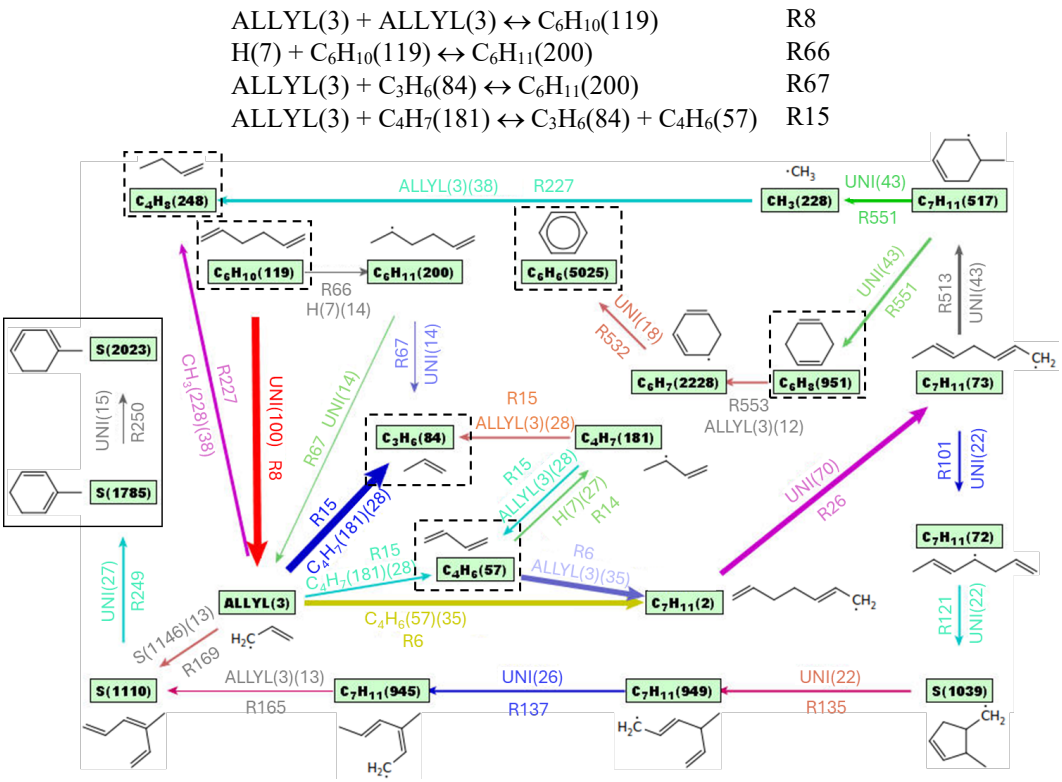

Figure 12. Pathway diagrams for DTE pyrolysis at 900 K, 5 bar, and a residence time of 0.5 s. The absolute rate corresponding to 100 is 5.89 × 10^{-9} mol/cm^3-s.

5.3 1,4-Cyclohexadiene [C_6H_8(951)] and Benzene [C_6H_6(5025)]: 900 K

As shown in Figure 12, the primary pathway for benzene formation begins with the addition of ALLYL(3) to C_4H_6(57) (via R6), yielding a 1,5-heptadiene-7-yl radical [C_7H_{11}(2)]. This radical then undergoes a 1,5 H-shift to form a 1,5-heptadiene-3-yl radical [C_7H_{11}(73)] (via R26). Subsequently, C_7H_{11}(73) cyclizes to produce C_7H_{11}(517) through reaction R513, which then eliminates a methyl radical to generate 1,4-cyclohexadiene [C_6H_8(951)] via reaction R551. ALLYL(3) abstracts a hydrogen atom from C_6H_8(951), forming C_6H_7(2228) (via R553). Finally, the loss of a hydrogen atom from C_6H_7(2228) results in the formation of benzene [C_6H_6(5025)] (via R532).

ALLYL(3) + C_4H_6(57) ↔ C_7H_{11}(2)	R6
C_7H_{11}(2) ↔ C_7H_{11}(73)	R26
C_7H_{11}(73) ↔ C_7H_{11}(517)	R513
CH_3(228) + C_6H_8(951) ↔ C_7H_{11}(517)	R551
ALLYL(3) + C_6H_8(951) ↔ C_3H_6(84) + C_6H_7(2228)	R553
H(7) + C_6H_6(5025) ↔ C_6H_7(2228)	R532

5.4 1-Butene [C_4H_8(248)]: 900 K

The 1-butene [C_4H_8(248)] was also observed experimentally, and its primary formation pathway involves the recombination of two dominant radicals: CH_3(228) and ALLYL(3) (see Figure 12).

$$CH_3(228) + \text{ALLYL}(3) \leftrightarrow C_4H_8(248) \quad \text{R227}$$

5.5 Toluene [C_7H_8(3291)]: 900 K

The precursor 3-methyl-1,3,5-hexatriene [S(1110)] in toluene production originates from the 1,5-heptadiene-3-yl radical [C_7H_{11}(73)] (see Figure 12). This radical undergoes a 1,4-hydrogen shift to form the 1,5-heptadiene-4-yl radical [C_7H_{11}(72)] (via R101). Subsequent cyclization yields the five-membered–ring 1,5-dimethylcyclopentene radical [S(1039)] (via R121). Ring opening of S(1039) produces C_7H_{11}(949) (via R135), which then undergoes a 1,4-hydrogen shift to form C_7H_{11}(945) (via R137). Finally, C_7H_{11}(945) undergoes disproportionation with ALLYL(3), producing propene [C_3H_6(84)] and S(1110) (via R165).

C_7H_{11}(72) ↔ C_7H_{11}(73)	R101
C_7H_{11}(72) ↔ S(1039)	R121
C_7H_{11}(949) ↔ S(1039)	R135
C_7H_{11}(949) ↔ C_7H_{11}(945)	R137
ALLYL(3) + C_7H_{11}(945) ↔ C_3H_6(84) +S (1110)	R165

Figure 13 illustrates the toluene formation pathways originating from the S(1110) precursor. The 2-methyl-1,3-cyclohexadiene [S(1785)] is produced through an intramolecular Diels–Alder cycloaddition reaction of S(1110) (R249). S(1785) then undergoes an intramolecular ene reaction to form 1-methyl-1,3-cyclohexadiene [S(2023)]. This process involves a concerted shift of an allylic hydrogen and the rearrangement of the double bond position without breaking the cyclic structure. Toluene formation proceeds via hydrogen abstraction by ALLYL(3) from S(1785) and S(2023), producing methyl-cyclohexadiene radicals [C_7H_9(2024), C_7H_9(2025), and C_7H_9(2151)]. Subsequently, the loss of one hydrogen atom from the methyl-cyclohexadiene radicals leads to toluene formation.

S(1110) ↔ S(1785)	R249
S(1785) ↔ S(2023)	R250
C_3H_6(84) + C_7H_9(2024) ↔ ALLYL(3) + S(1785)	R289
C_3H_6(84) + C_7H_9(2151) ↔ ALLYL(3) + S(2023)	R371
C_3H_6(84) + C_7H_9(2025) ↔ ALLYL(3) + S(1785)	R313
H(7) + C_7H_8(3291) ↔ C_7H_9(2024)	R438
H(7) + C_7H_8(3291) ↔ C_7H_9(2151)	R451
H(7) + C_7H_8(3291) ↔ C_7H_9(2025)	R443

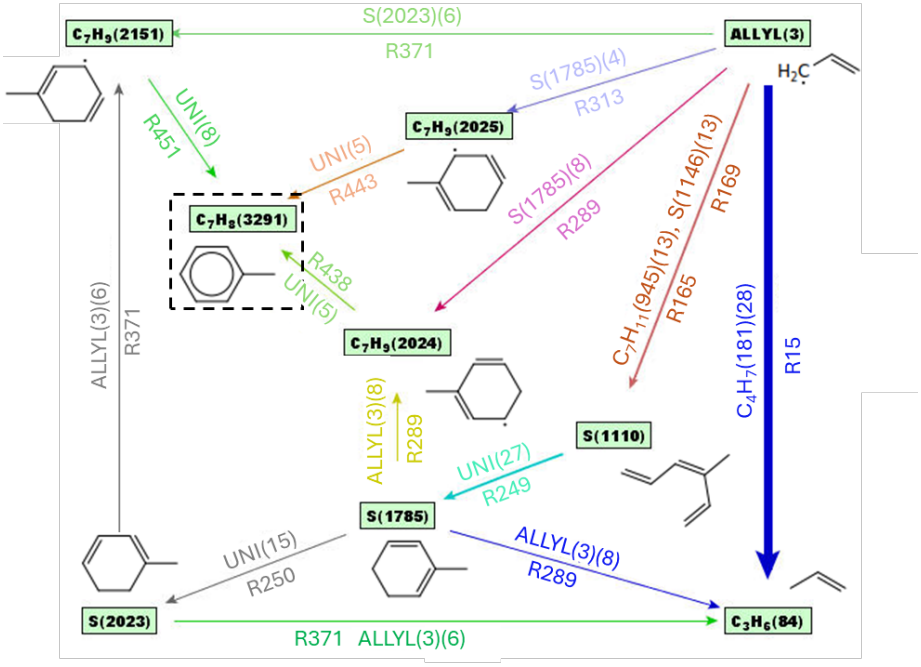

Figure 13. Pathway diagrams for the reaction of methyl cyclohexadiene S(1785) and S(2023) leading to toluene formation in DTE pyrolysis at 900 K, 5 bar, and a residence time of 0.5 s. The absolute rate corresponding to 100 is 5.89 × 10^{-9} mol/cm^3-s.

5.6 Allene [ALLENE(51)], Propyne [C_3H_4(759)], Ethylene [C_2H_4(227)], Acetylene [C_2H_2(501)], and Methane [CH_4(1246)]: 1100 K

At elevated temperatures, the hydrogen atom plays a significant role in the decomposition of 1,3-butadiene and propene. As shown in Figure 14, it can add to the C=C double bond of 1,3-butadiene and propene, yielding the but-3-en-1-yl radical [C_4H_7(9)] and the propyl radical [C_3H_7(231)], respectively. These radicals can further react to form the vinyl radical [C_2H_3(5)] and the methyl radical [CH_3(228)], accompanied by the formation of ethylene [C_2H_4(227)]. The vinyl radical [C_2H_3(5)] can subsequently dissociate, releasing a hydrogen atom and producing acetylene [C_2H_2(501)].

The resulting active methyl radicals promote the conversion to methane [CH_4(1246)] as a dominant reaction pathway. Specifically, methyl radical abstraction of a hydrogen atom from toluene is the most significant reaction. The reactions involved in the above processes are shown below and illustrated in Figure 14.

$H(7) + C_4H_6(57) \leftrightarrow C_4H_7(181)$	R14
$H(7) + C_4H_6(57) \leftrightarrow C_4H_7(9)$	R20
$C_4H_7(9) \leftrightarrow C_4H_7(181)$	R22
$C_2H_3(5) + C_2H_4(227) \leftrightarrow C_4H_7(9)$	R48
$H(7) + C_2H_2(501) \leftrightarrow C_2H_3(5)$	R58
$H(7) + C_3H_6(84) \leftrightarrow C_3H_7(231)$	R113
$CH_3(228) + C_2H_4(227) \leftrightarrow C_3H_7(231)$	R140

Alternatively, hydrogen atoms and methyl radicals can abstract a hydrogen atom from propene [C_3H_6(84)], yielding the allyl radical [ALLYL(3)]. Subsequent loss of a hydrogen atom from the allyl radical produces allene [ALLENE(51)]. Propyne [C_3H_4(759)] is then formed through hydrogen atom addition to the terminal C=C bond of allene, generating the 2-propenyl radical [C_3H_5(53)], which subsequently eliminates a vinyl hydrogen atom.

$H(7) + C_3H_6(84) \leftrightarrow H_2(219) + ALLYL(3)$ R2025
$CH_3(228) + C_3H_6(84) \leftrightarrow CH_4(1246) + ALLYL(3)$ R146
$H(7) + ALLENE(51) \leftrightarrow C_3H_5(53)$ R30
$H(7) + C_3H_4(759) \leftrightarrow C_3H_5(53)$ R42

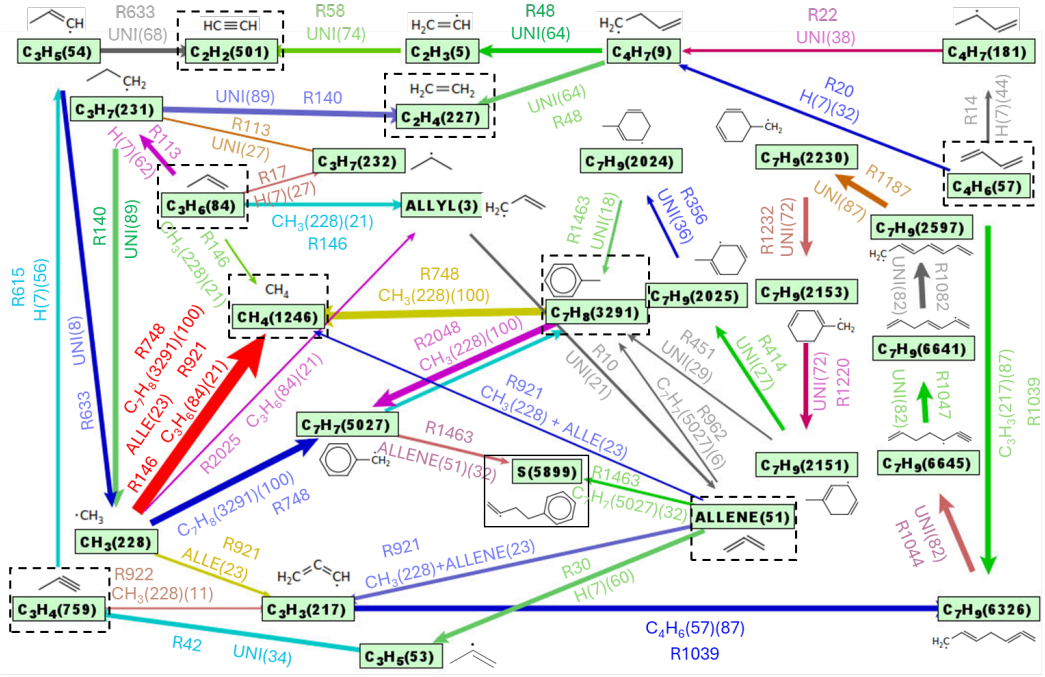

Figure 14. Pathway diagrams for DTE pyrolysis at 1100 K, 5 bar, and a residence time of 0.5 s. The absolute rate corresponding to 100 is 1.37×10^{-8} mol/cm^3-s.

Methane [CH_4(1246)] formation predominates at high temperatures, mainly through the abstraction of a hydrogen atom from toluene, propene, and allene by the methyl radical [CH_3(228)].

$CH_3(228) + C_7H_8(3291) \leftrightarrow CH_4(1246) + C_7H_7(5027)$ R748
$CH_4(1246) + C_3H_3(217) \leftrightarrow CH_3(228) + ALLENE(51)$ R921
$CH_3(228) + C_3H_6(84) \leftrightarrow CH_4(1246) + ALLENE(51)$ R146

5.7 Toluene [C_7H_8(3291)] and Naphthalene [S(11344)]: 1100 K

The propargyl radical [C_3H_3(217)] is a highly significant intermediate in combustion chemistry. It is resonance-stabilized and plays a role in the formation of PAHs. At relatively high temperatures (~1100 K), the toluene formation pathway proceeds through the C_3H_3(217) radical rather than via the S(1110) pathway observed at 900 K.

As illustrated in Figure 14, the primary pathways at 1100 K involve the formation of C_3H_3(217) from the hydrogen abstraction of propyne [C_3H_4(759)] and allene [ALLENE(51)], mainly by the CH_3 radical. The C_3H_3(217) radical reacts with 1,3-butadiene to form heptatriene radicals [C_7H_9(6326), C_7H_9(6645), C_7H_9(6641), and

$C_7H_9(2597)$]. The $C_7H_9(2597)$ radical then undergoes a six-member ring cyclization to produce methyl-cyclohexadiene radicals [$C_7H_9(2230)$, $C_7H_9(2153)$, $C_7H_9(2151)$, $C_7H_9(2025)$, and $C_7H_9(2024)$]. Toluene is formed from the loss of one hydrogen atom from the methyl-cyclohexadiene radicals, as previously mentioned in Section 5.5.

$CH_4(1246) + C_3H_3(217) \leftrightarrow CH_3(228) + ALLENE(51)$	R921
$CH_4(1246) + C_3H_3(217) \leftrightarrow CH_3(228) + C_3H_4(759)$	R922
$C_3H_3(217) + C_4H_6(57) \leftrightarrow C_7H_9(6326)$	R1039
$C_7H_9(6645) \leftrightarrow C_7H_9(6326)$	R1044
$C_7H_9(6645) \leftrightarrow C_7H_9(6641)$	R1047
$C_7H_9(6641) \leftrightarrow C_7H_9(2597)$	R1082
$C_7H_9(2597) \leftrightarrow C_7H_9(2230)$	R1187
$C_7H_9(2230) \leftrightarrow C_7H_9(2153)$	R1232
$C_7H_9(2153) \leftrightarrow C_7H_9(2151)$	R1220
$C_7H_9(2025) \leftrightarrow C_7H_9(2151)$	R414
$C_7H_9(2025) \leftrightarrow C_7H_9(2024)$	R356

The CH_3 radical then abstracts one of the hydrogen atoms in the methyl group of toluene, leading to the formation of a strongly resonance-stabilized benzyl radical [$C_7H_7(5027)$]. The naphthalene formation pathway illustrated in Figure 15 is initiated by the reaction of the benzyl radical with allene, forming the 3-butenylbenzene-3-yl radical [S(5899)]. This radical (S5899) undergoes intramolecular addition, leading to the formation of a two-ring structure that ultimately produces naphthalene.

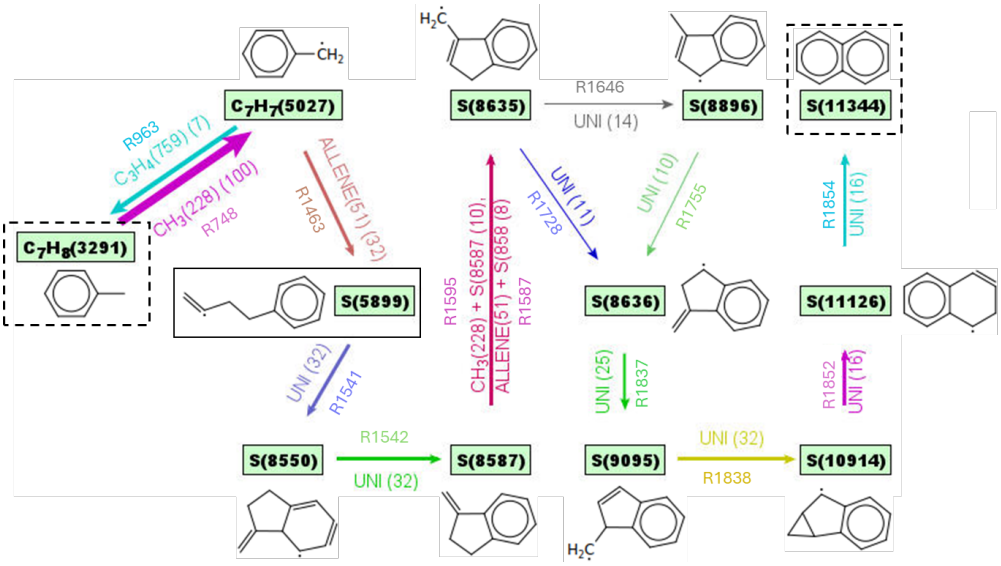

Figure 15. Pathway diagrams for the reaction of benzyl radical [$C_7H_7(5027)$] and allene leading to naphthalene formation in DTE pyrolysis at 1100 K, 5 bar, and a residence time of 0.5 s. The absolute rate corresponding to 100 is 1.37×10^{-8} mol/cm^3-s.

5.8 1,3-Cyclopentadiene [S(14222)]: 1200 K

The model predicted minimal 1,3-cyclopentadiene formation at lower temperatures, with appreciable amounts observed only up to approximately 1100 K. The formation pathways (as shown in Figure 16) suggest that it forms through the addition of the propargyl radical [C_3H_3(217)] to acetylene [C_2H_2(501)], resulting in a 1-buten-3-yne radical [C_5H_5(6350)]. This radical then undergoes cyclization to form the 1,3-cyclopentadiene-1-yl radical [C_5H_5(7360)], followed by a 1,2-H shift isomerization to produce the 1,3-cyclopentadiene-5-yl radical [S(14220)]. Subsequently, the abstraction of one hydrogen atom (mainly from allene) leads to the production of 1,3-cyclopentadiene.

$C_2H_2(501) + C_3H_3(217) \leftrightarrow C_5H_5(6350)$ R1972

$C_5H_5(6350) \leftrightarrow C_5H_5(7360)$ R2892

$C_5H_5(7360) \leftrightarrow S(14220)$ R2894

$H(7) + S(14222) \leftrightarrow H_2(219) + S(14220)$ R3047

However, the model significantly underestimates the production of 1,3-cyclopentadiene across all temperature set points. This underprediction might result from the absence of pathways for the formation of 1,5-hexadiene radicals in the RMG-generated mechanisms. One plausible pathway involves the cyclization of 1,5-hexadiene radicals to form the 4-methylcyclopentene-3-yl radical, which can subsequently lose a methyl radical to yield 1,3-cyclopentadiene.

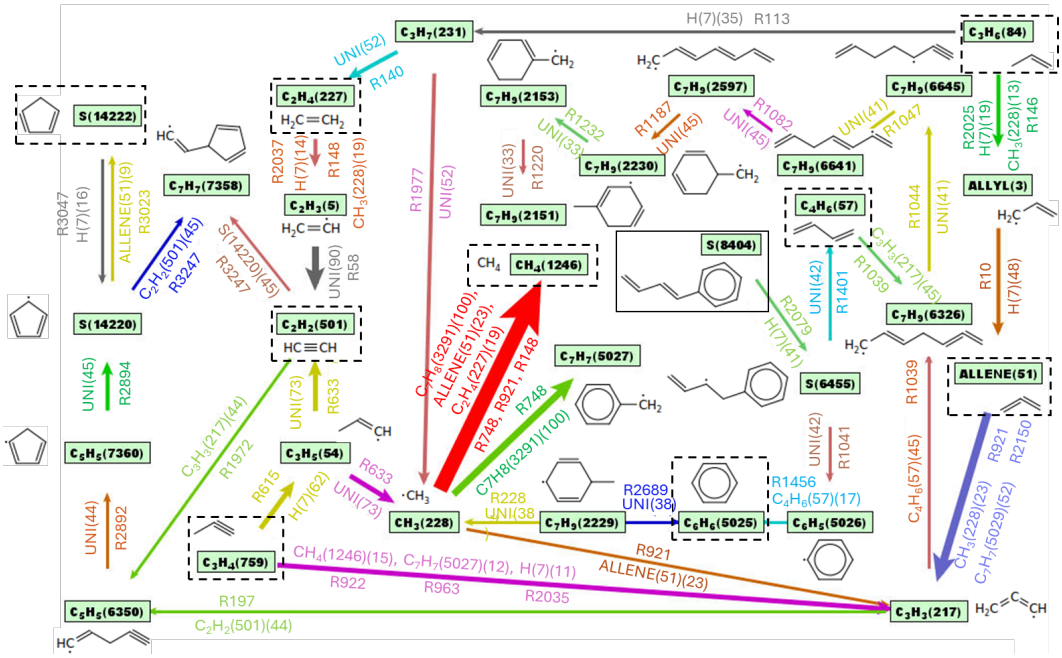

Figure 16. Pathway diagrams for DTE pyrolysis at 1200 K, 5 bar, and a residence time of 0.5 s. The absolute rate corresponding to 100 is 1.08 × 10^{-8} mol/cm^3-s.

5.9 Benzene [C_6H_6(5025)] Reformation: 1200 K

Figure 17 illustrates the reaction pathways for 1,3-butadienylbenzene [S(8404)]—shown in the solid box—and its subsequent reformation to benzene at 1200 K. The process initiates with methyl radical [CH_3(228)] abstraction of hydrogen atoms from toluene [C_7H_8(3291)] and propyne [C_3H_4(759)], yielding benzyl radical [C_7H_7(5027)] and propargyl radical [C_3H_3(217)]. 1,3-butadienylbenzene then forms via combination of these radicals, involving singlet carbene intra-disproportionation. Subsequent hydrogen addition to the central carbon–carbon double bond is followed by β-scission, producing 1,3-butadiene and phenyl radical [C_6H_5(5026)]. Further reaction of phenyl radical include addition with acetylene [C_2H_2(501)] and abstraction of a vinyl hydrogen of 1,3-butadiene, producing styrene radical [C_8H_7(8283)] and benzene [C_6H_6(5025)].

$CH_3(228) + C_7H_8(3291) \leftrightarrow CH_4(1246) + C_7H_7(5027)$	R748
$C_3H_4(759) + C_7H_7(5027) \leftrightarrow C_3H_3(217) + C_7H_8$	R963
$C_3H_3(217) + C_7H_7(5027) \leftrightarrow$ S(6420)	R1977
S(11912) ↔ S(6420)	R2077
S(11912) ↔ S(8404)	R2080
S(6455) ↔ H(7) + S(8404)	R2079
$C_4H_6(57) + C_6H_5(5026) \leftrightarrow$ S(6455)	R1401
$C_2H_2(501) + C_6H_5(5026) \leftrightarrow C_8H_7(8283)$	R2234

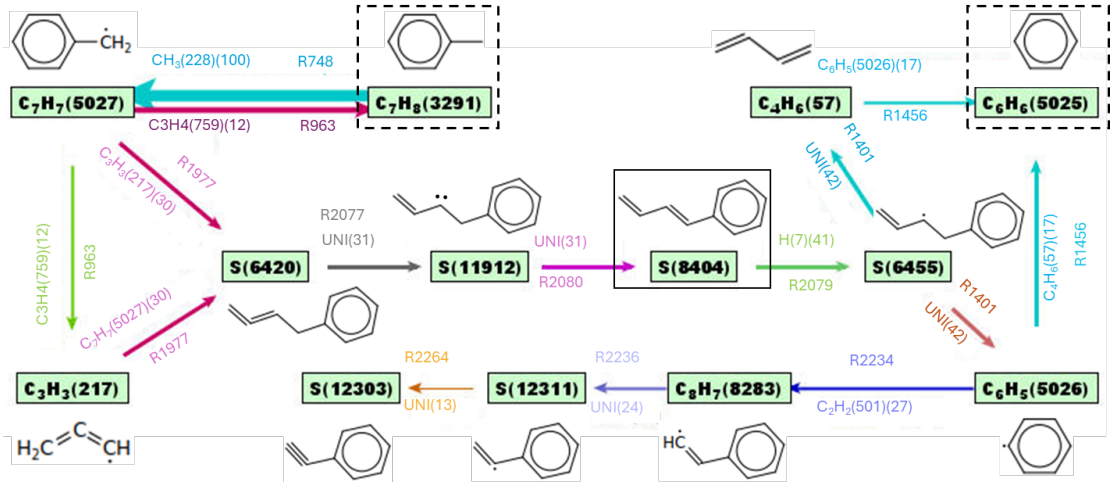

Figure 17. Pathway diagram for the decomposition of 1,3-butadienylbenzene leading to benzene reformation at 1200 K, 5 bar, and a residence time of 0.5 s. The absolute rate corresponding to 100 is 1.08×10^{-8} mol/cm^3-s.

5.10 Discrepancies between Experiment and Model

1,4,9-decatriene was observed experimentally to exhibit similar decay behavior to DTE, but it was not predicted by the model. In contrast, the isomer 4-vinyl-1,7-octadiene [$C_{10}H_{16}$(17)] was predicted by the model and showed reasonable

agreement with the experimental measurements of 1,4,9-decatriene. Further experimental investigation is necessary to ascertain that the GCMS peak attributed to 1,4,9-decatriene is not an isomer of 1,5,9-dectatriene or another more stable species. Although the species 1,3-pentadiene, 1-buten-3-yne, 1-pentene, butane, and 1,9-decadiene were not predicted by the DTE-RMG mechanism, they were detected in trace amounts in the experiment. The model was able to predict the formation of ethynylbenzene [S(12303)] at 1200 K (as shown in Figure 17), but it failed to predict styrene. This discrepancy can be attributed to the reaction of the benzyl radical with acetylene to form styrene radical isomers [C_8H_7(8283)] and [S(12311)], which subsequently lose one hydrogen atom to produce phenyl ethyne [S(12303)]. The mechanism overlooked the disproportionation reactions of styrene radicals with other radicals, which would lead to the production of styrene. Additionally, another pathway, involving the combination of benzyl radical with the CH_3 radical, followed by the elimination of H_2 to produce styrene, was also absent from the DTE-RMG mechanism.

The failure of the model to predict indene can be attributed to the complexity of the formation pathways of the simplest PAHs, including indene and naphthalene. These pathways involve a variety of species and reactions, such as phenyl radical + C_3H_4 (including allene and propyne), benzene + propargyl radical, benzyl radical + acetylene, phenyl radical + propene, benzene + allyl radical, and phenyl radical + allyl radical. Clearly, substantial improvements are required to enhance the accuracy of the RMG model in capturing the formation pathways of indene and naphthalene.

6. Conclusions

This study utilized a high-pressure laminar flow reactor system to study the pyrolysis of DTE over a range of intermediate temperatures. While temperature set point varied, all experiments were conducted at 5 bar with a constant inlet DTE mole fraction of 1000 ppm and a fixed residence time of 0.5 s.

A new kinetic mechanism for DTE pyrolysis was developed using RMG software. The final mechanism consisted of 377 species and 3968 reactions. The model was used to simulate the pyrolysis of DTE at various reactor temperature set points that ranged from 800 to 1200 K. The experimental and modeling results showed reasonable agreement for the decay of DTE and the formation of primary products, such as 1,5-hexadiene and 1,3-butadiene.

The model predicted the formation of multiple pyrolysis products, including cyclohexadiene, propene, 1-butene, toluene, and naphthalene. However, the model underpredicted the formation of 1,3-cyclopentadiene and overpredicted the

formation of C_3 species, acetylene, methane, toluene, and naphthalene. The model also failed to predict the formation of certain species, such as styrene and indene. These discrepancies highlight the complexity of pyrolysis reaction pathways for larger hydrocarbons and the challenges of developing accurate kinetic mechanisms for these materials that can reproduce experiments within uncertainties.

This study emphasizes the importance of experimental validation of modeling results to ensure the accuracy of kinetic mechanisms. The results suggest that the RMG-generated model requires refinement to better capture the formation pathways of certain species (e.g., indene and naphthalene). While the mechanism shows reasonable agreement for major products, discrepancies in predicting specific intermediates highlight the complexity of pyrolysis chemistry and the challenges of modeling larger hydrocarbons. By acknowledging the limitations of the current model, the study paves the way for future improvements and a deeper understanding of the pyrolysis process. Analysis of the pyrolysis reaction pathways indicated that additional reactions are required in the mechanism to better align with experimental results—findings that will be presented in Part II. Importantly, DTE serves as a model compound for certain hydrocarbon linkages within HTPB. Thus, the discrepancies and successes observed in predicting DTE pyrolysis products directly inform our approach to modeling the much more complex HTPB system. This improved understanding of DTE pyrolysis, and the identified areas for model refinement, will be essential for developing more accurate and predictive kinetic mechanisms for HTPB pyrolysis.

7. References

1. Chen CC, McQuaid MJ. A thermochemical kinetic-based study of ignition delays for 2-azidoethanamine-red fuming nitric acid systems: 2-azido-N-methylethanamine (MMAZ) vs. 2-azido-N,N-dimethylethanamine. Army Research Laboratory (US); 2014. Report No.: ARL-TR-6787.

2. Chen CC, McQuaid MJ. Predictions for the deflagration of notional extended solids of carbon monoxide with (C2O4H2)n stoichiometry: burning rates and other properties. Army Research Laboratory (US); 2017. Report No.: ARL-TR-7984.

3. Chen CC, McQuaid MJ. Modeling the deflagration of ammonium perchlorate at pressures from 300 to 30,000 psia. Part I: gas-phase, finite-rate chemical kinetics mechanism development. Proceedings of the 46th JANNAF Combustion Science Subcommittee Meeting; 2014.

4. McQuaid MJ, Chen CC. Modeling the deflagration of ammonium perchlorate at pressures from 300 to 30,000 psia. Part II: consideration besides the gas-phase, finite-rate chemical kinetics mechanism. Proceedings of the 46th JANNAF Combustion Science Subcommittee Meeting; 2014.

5. McQuaid MJ. Chemical kinetics mechanism reduction based on principle component analysis: development and testing of some new implementations. Army Research Laboratory (US); 2013. Report No.: ARL-TR-6449.

6. McQuaid MJ. The trial mechanism method for chemical kinetics mechanism reduction: an approach to generating reduced mechanisms with wider ranges of applicability. Proceedings of the 7th JANNAF Liquid Propulsion Subcommittee Meeting; 2013.

7. McQuaid MJ. An opposed-flow diffusion flame simulation-based implementation of the trial mechanism method for chemical kinetics mechanism reduction: application to the San Diego mechanism for HTPB-air combustion modeling. DEVCOM Army Research Laboratory (US); 2020. Report No.: ARL-TR-9032.

8. Chen CC, McQuaid MJ. A skeletal, gas-phase, finite-rate, chemical kinetics mechanism for modeling the deflagration of ammonium perchlorate-hydroxyl terminated polybutadiene composite propellants. Army Research Laboratory (US); 2016. Report No.: ARL-TR-7655.

9. McQuaid MJ, Chen C-C, Stone C, Veals JD. On modeling the pyrolysis of hydroxyl-terminated polybutadiene (HTPB) type R45M at temperatures in the range 465–600 °C. DEVCOM Army Research Laboratory (US); 2023 May. Report No.: ARL-TR-9681.

10. Liu MJ et al. Reaction mechanism generator v3.0: advances in automatic mechanism generation. J Chem Inf Model. 2021;61(6):2686–2696. https://doi.org/10.1021/acs.jcim.0c01480

11. Zhao QY, Savoie BM. Deep reaction network exploration of glucose pyrolysis. Proc Natl Acad Sci USA. 2023;120(34). https://doi.org/10.1073/pnas.2305884120

12. McQuaid MJ et al. On simulating the pyroprobe-induced pyrolysis of hydrocarbons with a model having a detailed finite-rate chemical kinetics mechanism: results for 1,5,9-decatriene. DEVCOM Army Research Laboratory (US); 2023. Report No.: ARL-TR-9869.

13. Gao CW, Allen JW, Green WH, West RH. Reaction mechanism generator: automatic construction of chemical kinetic mechanisms. Comput Phys Commun. 2016;203:212–225. https://doi.org/10.1016/j.cpc.2016.02.013

14. Faravelli T, Manenti F, Ranzi E. Mathematical modelling of gas-phase complex reaction systems: pyrolysis and combustion. Elsevier Science Ltd; 2019.

15. Machine Learning-based Thermo Estimation. Green WH, West RH, RMG Team; c2025. https://reactionmechanismgenerator.github.io/RMG-Py/users/rmg/input.html

16. Green WH, West RH, RMG Team. ReactionMechanismGenerator/RMG-database. Last updated 2025 Oct 1 [accessed 2025 Oct 10]. https://github.com/ReactionMechanismGenerator/RMG-database

17. Johnson MS, Green WH. A machine learning based approach to reaction rate estimation. React Chem Eng. 2024;9(6):1364–1380. https://doi.org/10.1039/d3re00684k

18. Li YP, Han KH, Grambow CA, Green WH. Self-evolving machine: a continuously improving model for molecular thermochemistry. J Phys Chem A. 2019;123(10):2142–2152. https://doi.org/10.1021/acs.jpca.8b10789

19. RMG Theory Guide. Green WH, West RH, RMG Team; c2025. https://reactionmechanismgenerator.github.io/RMGPy/theory/rmg/index.html

20. Bykov VI, Goletiani AR, Butenko TA, Finkelshtein ES. A new synthesis of (Z,E)-undec-5-enoic acids, the sex pheromone of the varied carpet beetle *Anthrenus verbasci*. Russ Chem Bull. 2004;53(11):2650–2652. https://doi.org/10.1007/s11172-005-0169-8

21. Stein S. The NIST 14 mass spectral library. National Institute of Standards and Technology (US); 2014.

22. Scanlon JT, Willis DE. Calculation of flame ionization detector relative response factors using the effective carbon number concept. J Chromatogr Sci. 1985;23(8):333–340.

23. Johnson MS et al. Oxidation and pyrolysis of methyl propyl ether. Int J Chem Kinet. 2021;53(8):915–938. https://doi.org/10.1002/kin.21489

24. Lokachari N et al. A comprehensive experimental and kinetic modeling study of di-isobutylene isomers: part 2. Combust Flame. 2023;251. https://doi.org/10.1016/j.combustflame.2022.112547

25. Song HS. Isomeric effects on the reactivity of branched alkenes: an experimental and kinetic modeling study of methylbutenes. Combust Flame. 2023;254. https://doi.org/10.1016/j.combustflame.2023.112849

26. Mohamed SY et al. Effect of the *β*-hydroxy group on ester reactivity: combustion kinetics of methyl hexanoate and methyl 3-hydroxyhexanoate. Combust Flame. 2023;258. https://doi.org/10.1016/j.combustflame.2023.113071.

27. Cooper SP et al. An experimental and chemical kinetic modeling study of 4-butoxyheptane combustion. Combust Flame. 2024;267. https://doi.org/10.1016/j.combustflame.2024.113568

28. Lutz AE, Kee RJ, Miller JA. SENKIN: a FORTRAN program for predicting homogeneous gas phase chemical kinetics with sensitivity analysis. 1988.

29. Anderson WR, Haga SW, Nuzman JF, Kotlar AJ, Anderson RJ. SREAD computer code: a versatile, portable FORTRAN computer code for interpreting the complex chemical kinetics of a homogeneous reacting gas mixture in a closed system. Army Research Laboratory (US); 2002.

30. Anderson RJ, Anderson WR. ELEMAP: an interactive, portable, JAVA computer code for rapid visualization of chemical pathways diagrams related to complex chemical kinetic code outputs. Army Research Laboratory (US); 2002.

31. Lai L, Gudiyella S, Liu MJ, Green WH. Chemistry of alkylaromatics reconsidered. Energ Fuel. 2018;32(4):5489–5500. https://doi.org/10.1021/acs.energyfuels.8b00069

32. Lai L, Green WH. Thermochemistry and kinetics of intermolecular addition of radicals to toluene and alkylaromatics. J Phys Chem A. 2019;123(14):3176–3184. https://doi.org/10.1021/acs.jpca.9b00817

33. Lai L, Pang HW, Green WH. Formation of two-ring aromatics in hexylbenzene pyrolysis. Energ Fuel. 2020:34(2):1365–1377. https://doi.org/10.1021/acs.energyfuels.9b03223

34. Goldsmith CF, Magoon GR, Green WH. Database of small molecule thermochemistry for combustion. J Phys Chem A. 2012;116(36):9033–9057. https://doi.org/10.1021/jp303819e

35. Tomiczek BM, Grenning AJ. Aromatic cope rearrangements. Org Biomol Chem. 2021;19(11):2385–2398. https://doi.org/10.1039/d1ob00094b

Appendix A. DTE Mechanism Generated with RMG

This appendix was not edited and appears as a PDF attachment in original form.

Appendix B. Representative Reactions and Molecular Structures of Species Generated by RMG for 1,5,9-Decatriene Pyrolysis

This appendix presents the reactions displayed in the pathway diagrams for the pyrolysis of 1,5,9-decatriene. Table B-1 lists maximum experimental measurement in parts per million (ppm) for the laminar flow reactor. Table B-2 summarizes the reactions and their corresponding rate coefficient parameterizations. Table B-3 provides the coefficients used to calculate the thermodynamic properties of the species involved in the pathway diagrams of 1,5,9-decatriene pyrolysis. Lastly, Table B-4 lists the SMILES strings and molecular structures of the species in these reactions.

Table B-1. Maximum concentration from laminar flow reactor experiments (ppm).

Temperature (K)	**1,5,9-Decatriene $C_{10}H_{16}$(1)** 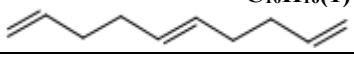	**1,5-Hexadiene C_6H_{10}(119)** 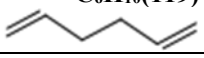	**1,3-Butadiene C_4H_6(57)** 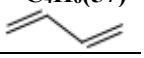
800	**406.0349 ± 28.80**	25.8238 ± 35.66	318.3907 ± 85.13
850	122.7858 ± 12.52	389.7152 ± 44.17	487.3259 ± 88.65
900	37.2253 ± 9.76	**654.3027 ± 56.49**	688.6867 ± 94.45
950	0.1385 ± 9.44	627.2327 ± 55.09	749.7822 ± 96.52
1000	0.0210 ± 9.44	394.5381 ± 44.36	791.0430 ± 97.99
1050	0.0041 ± 9.44	44.8823 ± 35.74	**811.8453 ± 98.75**
1100	0.0062 ± 9.44	0.5261 ± 35.62	591.4756 ± 91.45
1150	0.0689 ± 9.44	0.0231 ± 35.62	360.4738 ± 85.88
1200	0.0371 ± 9.44	0.0010 ± 35.62	145.6270 ± 82.99
Temperature (K)	**Ethene C_2H_4(227)** $H_2C=CH_2$	**Acetylene C_2H_2(501)** $HC\equiv CH$	**Methane CH_4(1246)** CH_4
800	1.3440 ± 44.03	0.0053 ± 9.95	0.3288 ± 18.54
850	2.2447 ± 44.03	0.0052 ± 9.95	0.5337 ± 18.54
900	29.4548 ± 44.03	0.0311 ± 9.95	5.7067 ± 18.54
950	50.1655 ± 44.03	0.0248 ± 9.95	6.8554 ± 18.54
1000	122.2046 ± 44.03	0.0143 ± 9.95	11.0034 ± 18.54
1050	283.8391 ± 44.03	0.1070 ± 9.95	32.3995 ± 18.54
1100	481.8351 ± 44.03	1.2779 ± 9.95	163.5506 ± 18.54
1150	744.4766 ± 44.05	170.7478 ± 10.00	355.3358 ± 18.54
1200	**925.9898 ± 44.06**	**424.8774 ± 10.25**	**536.7621 ± 18.55**
Temperature (K)	**1-Butene C_4H_8(248)** 	**Propene C_3H_6(84)** 	**Propyne C_3H_4(759)** 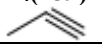
800	0.9145 ± 9.11	1.5370 ± 31.71	**1128.8300 ± 43.35**
850	2.3957 ± 9.11	2.5474 ± 31.71	991.8623 ± 42.24
900	47.2733 ± 9.12	35.4948 ± 31.71	17.5407 ± 38.25
950	73.4327 ± 9.13	87.1614 ± 31.71	42.2101 ± 38.25
1000	137.3177 ± 9.16	260.6746 ± 31.71	2.1563 ± 38.25
1050	**211.5782 ± 9.22**	**520.4318 ± 31.72**	15.4247 ± 38.25
1100	70.0274 ± 9.13	498.6107 ± 31.72	18.0629 ± 38.25
1150	3.3233 ± 9.11	344.6854 ± 31.71	42.0602 ± 38.25
1200	0.6158 ± 9.11	151.2468 ± 31.71	36.6485 ± 38.25

Note: Units are in ppm.

Table B-1. The laminar flow reactor experimental data (continued).

Temperature (K)	Allene ALLENE(51) 	Benzene C_6H_6(5025) 	Toluene C_7H_8(3291) 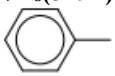
800	0.0051 ± 9.21	0.2373 ± 17.16	0.1125 ± 2.30
850	0.0103 ± 9.21	0.5492 ± 17.16	0.2981 ± 2.30
900	0.0564 ± 9.21	15.9089 ± 17.19	5.4194 ± 2.32
950	1.7847 ± 9.21	28.9494 ± 17.27	8.7628 ± 2.37
1000	17.4622 ± 9.29	75.1036 ± 17.88	13.2953 ± 2.46
1050	71.0139 ± 10.37	153.8589 ± 20.02	20.1999 ± 2.66
1100	134.9630 ± 12.91	204.5643 ± 21.96	23.8715 ± 2.80
1150	**181.2384 ± 15.24**	265.8895 ± 24.74	**33.0001 ± 3.19**
1200	146.2506 ± 13.45	**284.5211 ± 25.65**	32.7518 ± 3.18
Temperature (K)	**Naphthalene S(11344)** 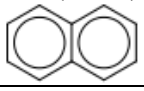	**1,3-Cyclopentadiene S(14222)** 	**1,3-Cyclohexadiene** 
800	0.0078 ± 1.04	1.6348 ± 7.53	0.4960 ± 2.31
850	0.0067 ± 1.04	2.1653 ± 7.53	1.4050 ± 2.31
900	0.0228 ± 1.04	28.5186 ± 7.76	27.5281 ± 2.95
950	0.0161 ± 1.04	39.4462 ± 7.98	38.1072 ± 3.44
1000	0.1187 ± 1.04	57.5312 ± 8.46	**42.8380 ± 3.68**
1050	1.5195 ± 1.05	87.5667 ± 9.54	21.1449 ± 2.71
1100	5.9335 ± 1.12	**96.5771 ± 9.93**	4.3513 ± 2.32
1150	20.2018 ± 1.71	87.9582 ± 9.56	1.9991 ± 2.31
1200	**34.7784 ± 2.55**	50.1123 ± 8.24	0.4564 ± 2.31
Temperature (K)	**1-Butyne C_4H_6(500)** 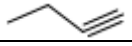	**2-Butyne** 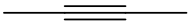	**Ethane C_2H_6(1571)** 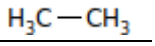
800	0.0003 ± 1.71	0.0022 ± 1.50	0.1699 ± 1.85
850	0.0009 ± 1.71	0.0010 ± 1.50	0.1962 ± 1.85
900	0.0440 ± 1.71	0.2757 ± 1.50	1.0227 ± 1.85
950	0.2140 ± 1.71	0.2429 ± 1.50	0.9627 ± 1.85
1000	0.9424 ± 1.71	1.7951 ± 1.50	1.0560 ± 1.85
1050	4.4093 ± 1.71	8.4801 ± 1.56	2.0164 ± 1.85
1100	17.9357 ± 1.76	27.5352 ± 2.06	20.6963 ± 1.85
1150	37.0957 ± 1.93	**34.8854 ± 2.34**	**44.6373 ± 1.85**
1200	**41.9820 ± 1.98**	16.7857 ± 1.73	40.3497 ± 1.85

Note: Units are in ppm.

Table B-1. The laminar flow reactor experimental data (continued).

Temperature (K)	1-Pentene 	1,3-Pentadiene 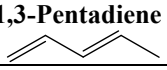	Butane 
800	0.8035 ± 0.55	0.0630 ± 0.39	0.0007 ± 0.40
850	0.9471 ± 0.55	0.0292 ± 0.39	0.0053 ± 0.40
900	9.5876 ± 0.84	0.5673 ± 0.39	0.2126 ± 0.40
950	**10.0563 ± 0.87**	2.0697 ± 0.42	0.7946 ± 0.40
1000	8.9085 ± 0.81	7.6744 ± 0.65	4.2073 ± 0.40
1050	2.1853 ± 0.57	**10.4039 ± 0.80**	**10.3483 ± 0.40**
1100	0.0913 ± 0.55	2.2431 ± 0.42	4.8761 ± 0.40
1150	0.1790 ± 0.55	0.3927 ± 0.39	3.3042 ± 0.40
1200	0.0538 ± 0.55	0.0780 ± 0.39	0.4315 ± 0.40
Temperature (K)	**1,4,9-Decatriene** 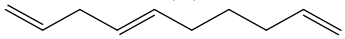	**1,9-Decadiene** 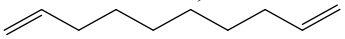	**1-Buten-3-yne** 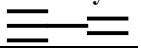
800	**130.6977 ± 9.17**	20.2200 ± 1.96	1.1666 ± 5.63
850	23.6092 ± 3.14	**22.8033 ± 2.08**	3.6507 ± 5.64
900	8.3723 ± 2.77	21.2100 ± 2.00	44.7495 ± 6.38
950	0.1015 ± 2.72	15.7145 ± 1.76	39.8470 ± 6.23
1000	0.0475 ± 2.72	4.1056 ± 1.44	**51.4492 ± 6.60**
1050	0.0731 ± 2.72	0.0895 ± 1.41	49.9401 ± 6.55
1100	0.0475 ± 2.72	0.1219 ± 1.41	54.1470 ± 6.70
1150	0.0334 ± 2.72	0.2413 ± 1.41	43.4629 ± 6.34
1200	0.0210 ± 2.72	0.1591 ± 1.41	49.4028 ± 6.53
Temperature (K)	**Styrene** 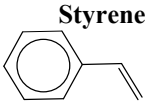	**Indene** 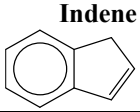	
800	0.0046 ± 1.33	0.0326 ± 0.85	
850	0.0193 ± 1.33	0.0376 ± 0.85	
900	0.0419 ± 1.33	0.0706 ± 0.85	
950	0.1872 ± 1.33	0.0197 ± 0.85	
1000	1.5549 ± 1.33	0.3818 ± 0.85	
1050	6.4108 ± 1.39	2.7702 ± 0.87	
1100	11.1325 ± 1.52	6.7590 ± 0.97	
1150	25.2874 ± 2.15	17.5295 ± 1.45	
1200	**34.9362 ± 2.69**	**23.6734 ± 1.80**	

Note: Units are in ppm.

Table B-2. Reactions and rate coefficient parameterizations shown in pathway diagrams of 1,5,9-decatriene (DTE) pyrolysis.

	Reactions	A	b	E
R1	$C_{10}H_{16}(17) = C_{10}H_{16}(1)$	6.21E + 10	0.3	35.1
R2	$ALLYL(3) + C_7H_{11}(2) = C_{10}H_{16}(1)$	6.96E + 13	–0.2	0.0
R3	$ALLYL(3) + C_7H_{11}(2) = C_{10}H_{16}(17)$	6.96E + 13	–0.2	0.0
R4	$ALLYL(3) + C_7H_{11}(2) = C_{10}H_{16}(1)$	6.96E + 13	–0.2	0.0
R6	$ALLYL(3) + C_4H_6(57) = C_7H_{11}(2)$	9.96E + 04	2.4	8.8
R7	$ALLYL(3) + C_4H_6(57) = C_7H_{11}(2)$	9.96E + 04	2.4	8.8
R8	$ALLYL(3) + ALLYL(3) = C_6H_{10}(119)$	2.04E + 13	0.0	–0.3
R10	$H(7) + ALLENE(51) = ALLYL(3)$	4.42E + 08	1.6	2.8
R11	$H(7) + ALLENE(51) = ALLYL(3)$	4.42E + 08	1.6	2.8
R12	$ALLYL(3) + ALLYL(3) = ALLENE(51) + C_3H_6(84)$	1.69E + 11	0.0	6.0
R13	$H(7) + ALLYL(3) = C_3H_6(84)$	5.84E + 13	0.2	0.1
R14	$H(7) + C_4H_6(57) = C_4H_7(181)$	4.62E + 08	1.6	–0.5
R15	$ALLYL(3) + C_4H_7(181) = C_3H_6(84) + C_4H_6(57)$	1.37E + 14	–0.3	–0.1
R17	$H(7) + C_3H_6(84) = C_3H_7(232)$	1.84E + 09	1.6	1.6
R18	$ALLYL(3) + C_3H_7(232) = C_3H_6(84) + C_3H_6(84)$	2.75E + 14	–0.3	–0.1
R19	$ALLYL(3) + C_3H_7(232) = C_3H_6(84) + C_3H_6(84)$	2.75E + 14	–0.3	–0.1
R20	$H(7) + C_4H_6(57) = C_4H_7(9)$	3.24E + 08	1.6	2.4
R21	$ALLYL(3) + C_4H_7(9) = C_3H_6(84) + C_4H_6(57)$	5.80E + 12	0.0	–0.1
R22	$C_4H_7(9) = C_4H_7(181)$	1.72E + 06	2.0	27.2
R25	$C_4H_7(246) = C_4H_7(9)$	1.11E + 05	2.2	10.6
R26	$C_7H_{11}(2) = C_7H_{11}(73)$	2.52E + 05	1.9	21.1
R27	$C_7H_{11}(73) = C_7H_{11}(523)$	5.72E + 12	0.2	20.1
R29	$C_3H_5(53) = ALLYL(3)$	7.32E + 09	1.1	41.3
R30	$H(7) + ALLENE(51) = C_3H_5(53)$	4.18E + 08	1.6	1.2
R32	$C_3H_5(53) + C_3H_6(84) = ALLYL(3) + C_3H_6(84)$	3.78E – 03	4.3	–0.2
R35	$ALLYL(3) + C_3H_5(53) = ALLENE(51) + C_3H_6(84)$	1.37E + 14	–0.3	–0.1
R39	$ALLYL(3) + C_3H_5(53) = ALLENE(51) + C_3H_6(84)$	1.37E + 14	–0.3	–0.1
R42	$H(7) + C_3H_4(759) = C_3H_5(53)$	1.50E + 09	1.6	3.1
R43	$ALLYL(3) + C_3H_5(53) = C_3H_4\ (759) + C_3H_6(84)$	1.64E + 07	1.9	–1.1
R45	$H(7) + C_3H_4(759) = C_3H_5(53)$	1.50E + 09	1.6	3.1
R48	$C_2H_3(5) + C_2H_4\ (227) = C_4H_7(9)$	2.86E + 04	2.4	1.8
R51	$C_2H_3(5) + C_3H_6(84) = C_2H_4(227) + ALLYL(3)$	6.66E – 03	4.3	0.1
R58	$H(7) + C_2H_2(501) = C_2H_3(5)$	1.03E + 09	1.6	2.1
R59	$C_2H_3\ (5) + ALLYL(3) = C_2H_2(501) + C_3H_6(84)$	1.64E + 07	1.9	–1.1
R62	$C_7H_{11}(683) = C_7H_{11}(523)$	1.68E + 09	0.8	9.2
R66	$H(7) + C_6H_{10}(119) = C_6H_{11}(200)$	6.72E + 08	1.6	0.6
R67	$ALLYL(3) + C_3H_6(84) = C_6H_{11}(200)$	1.56E+ 03	2.5	11.0
R73	$C_3H_6(84) + C_7H_{11}(2) = ALLYL(3) + C_7H_{12}(93)$	4.35E – 03	4.3	13.6
R75	$ALLYL(3) + C_4H_7(181) = C_7H_{12}(93)$	6.96E + 13	–0.2	0.0
R81	$C_3H_6(84) + C_7H_{11}(73) = ALLYL(3) + C_7H_{12}(93)$	2.69E – 03	4.3	14.3
R96	$ALLYL(3) + C_4H_7(181) = C_7H_{12}(257)$	6.96E + 13	–0.2	0.0
R97	$C_7H_{12}(257) = C_7H_{12}(93)$	6.21E + 10	0.3	35.1
R101	$C_7H_{11}(72) = C_7H_{11}(73)$	1.17E + 11	0.7	27.7
R113	$H(7) + C_3H_6(84) = C_3H_7(231)$	1.36E + 08	1.6	1.9

Notes: $k = A\ T^b \exp(–E/RT)$; A unit is mole-cm-sec-K, E unit is kcal/mole.

Table B-2. Reactions and rate coefficient parameterizations shown in pathway diagrams of DTE pyrolysis (continued).

	Reactions	A	b	E
R116	C3H7(232)=C3H7(231)	4.86E + 09	1.3	40.3
R121	C7H11(72)=S(1039)	1.13E + 11	0.2	22.1
R123	C7H11(683)=C7H11(949)	1.21E + 05	1.9	13.3
R135	C7H11(949)=S(1039)	5.25E + 08	0.8	19.3
R136	C7H11(683)=C7H11(945)	4.52E + 08	1.1	20.9
R137	C7H11(949)=C7H11(945)	1.81E – 03	4.2	9.1
R139	CH3(228)+C2H3(5)=C3H6(84)	7.23E + 13	0.0	0.0
R140	CH3(228)+C2H4(227)=C3H7(231)	4.18E + 04	2.4	5.6
R142	S(1146)=C7H11(945)	1.63E + 03	2.3	19.7
R144	CH3(228)+C2H3(5)=C3H6(84)	7.23E + 13	0.0	0.0
R145	CH3(228)+ALLYL(3)=CH4(1246)+ALLENE(51)	3.01E + 12	0.0	6.0
R146	CH3(228)+C3H6(84)=CH4(1246)+ALLYL(3)	7.20E – 02	4.2	7.5
R148	CH4(1246)+C2H3(5)=CH3(228)+C2H4(227)	2.24E – 02	4.3	5.7
R151	CH3(228)+C7H12(93)=CH4(1246)+C7H11(2)	7.20E – 02	4.2	7.5
R153	H(7)+CH3(228)=CH4(1246)	1.93E +14	0.0	0.3
R163	H(7)+S(1110)=C7H11(945)	2.31E + 08	1.6	–0.5
R165	ALLYL(3)+C7H11(945)=C3H6(84)+S(1110)	1.37E + 14	–0.3	–0.1
R167	H(7)+S(1110)=S(1146)	2.31E + 08	1.6	–0.5
R169	ALLYL(3)+S(1146)=C3H6(84)+S(1110)	1.37E + 14	–0.3	–0.1
R192	ALLYL(3)+C4H7(181)=ALLENE(51)+C4H8(248)	1.87E + 12	0.0	2.7
R193	C3H6(84)+C4H7(181)=ALLYL(3)+C4H8(248)	2.69E – 03	4.3	14.3
R194	C3H5(53)+C4H8(248)=C3H6(84)+C4H7(181)	7.82E – 03	4.3	–1.6
R200	C3H6(84)+C4H7(9)=ALLYL(3)+C4H8(248)	2.96E – 04	4.5	4.6
R221	C2H3(5)+C4H8(248)=C2H4(227)+C4H7(181)	1.69E – 02	4.3	–1.2
R227	CH3(228)+ALLYL(3)=C4H8(248)	2.04E + 14	–0.3	–0.1
R229	CH3(228)+C4H8(248)=CH4(1246)+C4H7(181)	2.04E – 01	4.0	6.3
R239	CH3(228)+C4H8(248)=CH4(1246)+C4H7(9)	6.00E + 12	0.0	12.6
R249	S(1110)=S(1785)	5.67E + 12	–0.1	39.3
R250	S(1785)=S(2023)	2.03E + 09	1.1	27.6
R253	S(2150)=S(2023)	2.12E + 09	1.0	11.0
R257	H(7)+C7H10(507)=C7H11(73)	4.52E + 06	2.0	2.5
R258	ALLYL(3)+C7H11(73)=C3H6(84)+C7H10(507)	5.80E + 12	0.0	–0.1
R266	ALLYL(3)+C7H11(72)=C3H6(84)+C7H10(507)	5.80E + 12	0.0	–0.1
R267	C7H10(507)=S(2150)	5.67E + 12	–0.1	39.3
R289	C3H6(84)+C7H9(2024)=ALLYL(3)+S(1785)	5.38E – 03	4.3	14.3
R291	C4H7(181)+C7H9(2024)=C4H6(57)+S(1785)	3.00E + 11	0.0	0.0
R294	ALLYL(3)+C7H9(2024)=ALLENE(51)+S(1785)	3.74E + 12	0.0	2.7
R302	CH4(1246)+C7H9(2024)=CH3(228)+S(1785)	8.48E – 02	4.3	30.3
R303	C4H8(248)+C7H9(2024)=C4H7(181)+S(1785)	9.16E – 03	4.3	11.7
R313	C3H6(84)+C7H9(2025)=ALLYL(3)+S(1785)	2.69E – 03	4.3	14.3
R315	C4H7(181)+C7H9(2025)=C4H6(57)+S(1785)	1.50E + 11	0.0	0.0
R318	ALLYL(3)+C7H9(2025)=ALLENE(51)+S(1785)	1.87E + 12	0.0	2.7
R326	C3H6(84)+C7H9(2025)=ALLYL(3)+S(2023)	2.69E – 03	4.3	14.3
R328	C4H7(181)+C7H9(2025)=C4H6(57)+S(2023)	1.50E + 11	0.0	0.0
R331	ALLYL(3)+C7H9(2025)=ALLENE(51)+S(2023)	1.87E + 12	0.0	2.7
R337	CH4(1246)+C7H9(2025)=CH3(228)+S(1785)	4.24E – 02	4.3	30.2
R338	CH4(1246)+C7H9(2025)=CH3(228)+S(2023)	4.24E – 02	4.3	29.6
R342	C4H8(248)+C7H9(2025)=C4H7(181)+S(1785)	4.58E – 03	4.3	11.7
R343	C4H8(248)+C7H9(2025)=C4H7(181)+S(2023)	4.58E – 03	4.3	11.7
R356	C7H9(2025)=C7H9(2024)	4.02E + 08	1.4	19.8
R371	C3H6(84)+C7H9(2151)=ALLYL(3)+S(2023)	2.69E – 03	4.3	14.3

Notes: k = A T^b exp(–E/RT); A unit is mole-cm-sec-K, E unit is kcal/mole.

Table B-2. Reactions and rate coefficient parameterizations shown in pathway diagrams of DTE pyrolysis (continued).

	Reactions	A	b	E
R373	C4H7(181)+C7H9(2151)=C4H6(57)+S(2023)	1.50E + 11	0.0	0.0
R376	ALLYL(3)+C7H9(2151)=ALLENE(51)+S(2023)	1.87E + 12	0.0	2.7
R381	CH4(1246)+C7H9(2151)=CH3(228)+S(2023)	4.24E – 02	4.3	30.8
R388	C4H7(181)+C7H9(2151)=C4H6(57)+S(2150)	8.58E + 15	–1.1	0.0
R390	ALLYL(3)+C7H9(2151)=ALLENE(51)+S(2150)	2.89E + 13	0.0	6.0
R400	C4H8(248)+C7H9(2151)=C4H7(181)+S(2023)	4.58E – 03	4.3	11.7
R414	C7H9(2025)=C7H9(2151)	4.02E + 08	1.4	19.8
R420	C7H9(2025)=C7H9(2151)	4.02E + 08	1.4	19.8
R421	ALLYL(3)+C7H9(2151)=ALLENE(51)+S(2023)	1.87E + 12	0.0	2.7
R423	C4H7(181)+C7H9(2151)=C4H6(57)+S(2023)	1.50E + 11	0.0	0.0
R438	H(7)+C7H8(3291)=C7H9(2024)	1.12E + 09	1.4	5.4
R443	H(7)+C7H8(3291)=C7H9(2025)	1.08E + 09	1.4	5.4
R451	H(7)+C7H8(3291)=C7H9(2151)	1.02E + 09	1.4	4.5
R452	ALLYL(3)+C7H9(2151)=C3H6(84)+C7H8(3291)	5.80E + 12	0.0	–0.1
R464	H(7)+C7H8(3291)=C7H9(2024)	1.12E + 09	1.4	5.4
R477	C2H2(501)+C2H5(502)=C4H7(246)	1.36E + 04	2.4	6.2
R478	H(7)+C2H4(227)=C2H5(502)	4.62E + 08	1.6	1.0
R479	C2H5(502)+ALLYL(3)=C2H4(227)+C3H6(84)	1.37E + 14	–0.3	–0.1
R510	C2H2(501)+C2H5(502)=C4H7(246)	1.36E + 04	2.4	6.2
R511	CH3(228)+C4H6(57)=C5H9(1283)	4.72E + 04	2.4	2.5
R513	C7H11(73)=C7H11(517)	8.19E + 10	0.2	24.1
R530	H(7)+S(2150)=C7H11(517)	1.14E + 09	1.4	1.3
R531	CH3(228)+C6H7(2228)=S(2150)	3.60E + 16	–1.0	0.0
R532	H(7)+C6H6(5025)=C6H7(2228)	9.22E + 08	1.6	4.6
R551	CH3(228)+C6H8(951)=C7H11(517)	4.04E + 04	2.4	6.8
R552	ALLYL(3)+C6H7(2228)=ALLENE(51)+C6H8(951)	4.58E + 12	0.0	6.0
R553	ALLYL(3)+C6H8(951)=C3H6(84)+C6H7(2228)	1.54E – 02	4.3	6.7
R554	C3H5(53)+C6H8(951)=C3H6(84)+C6H7(2228)	2.12E – 02	4.3	–4.2
R555	C4H7(181)+C6H7(2228)=C4H6(57)+C6H8(951)	1.50E + 11	0.0	0.0
R556	C2H3(5)+C6H8(951)=C2H4(227)+C6H7(2228)	4.56E – 02	4.3	–2.8
R563	CH3(228)+C6H8(951)=CH4(1246)+C6H7(2228)	4.24E – 02	4.3	1.7
R564	C4H7(181)+C6H8(951)=C4H8(248)+C6H7(2228)	3.92E – 03	4.3	6.3
R573	H(7)+C6H7(2228)=C6H8(951)	4.02E + 13	0.2	0.0
R590	C5H9(984)=C5H9(1283)	1.21E + 05	1.9	13.3
R597	C3H5(54)=ALLYL(3)	1.53E + 10	1.0	37.7
R599	ALLYL(3)+C3H6(84)=C3H5(54)+C3H6(84)	9.28E – 02	4.3	29.6
R610	C3H5(54)+C4H6(57)=C7H11(73)	3.91E + 04	2.4	0.4
R615	H(7)+C3H4(759)=C3H5(54)	6.92E + 08	1.6	3.4
R633	CH3(228)+C2H2(501)=C3H5(54)	1.34E + 05	2.4	6.8
R660	C2H4(227)+C3H5(54)=C5H9(984)	2.86E + 04	2.4	1.8
R661	C7H11(2)=C7H11(77)	4.11E + 10	0.2	23.0
R662	CH3(228)+CH3(228)=C2H6(1571)	9.45E + 14	–0.5	0.1
R667	CH3(228)+C2H6(1571)=CH4(1246)+C2H5(502)	3.50E + 01	3.4	10.4
R689	C4H6(177)=C4H6(57)	7.00E + 13	–1.3	6.3
R690	CH3(228)+C3H6(84)=C4H9(1337)	2.10E + 04	2.4	5.3
R699	H(7)+C4H8(248)=C4H9(1337)	3.36E + 08	1.6	0.6
R714	H(7)+C4H6(239)=C4H7(181)	5.46E + 08	1.6	3.8
R715	ALLYL(3)+C4H7(181)=C3H6(84)+C4H6(239)	1.69E + 11	0.0	6.0
R717	C4H7(181)+C4H7(181)=C4H6(239)+C4H8(248)	1.87E + 12	0.0	2.7
R729	C4H7(181)+C6H7(2228)=C4H6(239)+C6H8(951)	4.58E + 12	0.0	6.0
R730	C4H6(177)=C4H6(239)	6.15E + 14	–1.1	13.6

Notes: k = A T^b exp(–E/RT); A unit is mole-cm-sec-K, E unit is kcal/mole.

Table B-2. Reactions and rate coefficient parameterizations shown in pathway diagrams of DTE pyrolysis (continued).

	Reactions	A	b	E
R735	H(7)+C7H7(5027)=C7H8(3291)	7.23E + 13	0.1	–0.0
R736	C3H6(84)+C7H7(5027)=ALLYL(3)+C7H8(3291)	4.02E – 03	4.3	11.5
R738	C4H7(181)+C7H7(5027)=C4H6(57)+C7H8(3291)	3.45E + 13	–0.2	–0.0
R740	ALLYL(3)+C7H7(5027)=ALLENE(51)+C7H8(3291)	2.85E + 11	0.0	6.0
R745	C2H3(5)+C7H8(3291)=C2H4(227)+C7H7(5027)	5.64E – 03	4.3	2.0
R748	CH3(228)+C7H8(3291)=CH4(1246)+C7H7(5027)	1.07E + 06	2.3	4.4
R754	C4H8(248)+C7H7(5027)=C4H7(181)+C7H8(3291)	8.38E – 03	4.3	9.1
R756	C7H7(5027)+S(1146)=C7H8(3291)+S(1110)	3.45E + 13	–0.2	–0.0
R757	C7H7(5027)+C7H11(945)=C7H8(3291)+S(1110)	3.45E + 13	–0.2	–0.0
R761	C2H6(1571)+C7H7(5027)=C2H5(502)+C7H8(3291)	8.10E – 02	4.3	17.6
R762	C3H5(53)+C7H8(3291)=C3H6(84)+C7H7(5027)	3.21E – 03	4.3	1.7
R763	C6H8(951)+C7H7(5027)=C6H7(2228)+C7H8(3291)	7.16E – 03	4.3	4.6
R768	ALLYL(3)+C7H7(5027)=ALLENE(51)+C7H8(3291)	2.85E + 11	0.0	6.0
R774	C7H8(3291)+C7H9(2024)=C7H7(5027)+S(1785)	4.57E – 03	4.3	16.2
R775	C7H8(3291)+C7H9(2025)=C7H7(5027)+S(1785)	2.28E – 03	4.3	16.2
R776	C7H8(3291)+C7H9(2025)=C7H7(5027)+S(2023)	2.28E – 03	4.3	16.1
R777	C7H8(3291)+C7H9(2151)=C7H7(5027)+S(2023)	2.28E – 03	4.3	16.7
R781	C7H7(5790)=C7H7(5027)	1.24E + 12	0.3	3.6
R783	C3H6(84)+C7H7(5030)=ALLYL(3)+C7H8(3291)	7.80E – 01	4.0	1.7
R792	C2H4(227)+C7H7(5030)=C2H3(5)+C7H8(3291)	2.20E – 02	4.4	4.7
R795	CH3(228)+C7H8(3291)=CH4(1246)+C7H7(5030)	1.05E + 08	1.8	14.7
R801	C4H8(248)+C7H7(5030)=C4H7(181)+C7H8(3291)	2.16E – 02	4.3	–3.9
R810	C6H8(951)+C7H7(5030)=C6H7(2228)+C7H8(3291)	5.80E – 02	4.3	–5.6
R815	C7H7(5030)=C7H7(5027)	2.16E + 03	2.5	3.7
R818	H(7)+C4H6(239)=C4H7(181)	5.46E + 08	1.6	3.8
R819	C4H8(2010)=C4H8(248)	4.85E + 16	–0.9	20.9
R821	C4H7(181)+C7H7(5027)=C4H6(57)+C7H8(3291)	3.45E + 13	–0.2	–0.0
R823	ALLYL(3)+C4H7(181)=ALLENE(51)+C4H8(251)	8.43E + 10	0.0	6.0
R824	C3H6(84)+C4H7(181)=ALLYL(3)+C4H8(251)	4.35E – 03	4.3	13.6
R827	H(7)+C4H7(181)=C4H8(251)	1.63E + 13	0.3	0.0
R828	C4H7(181)+C4H7(181)=C4H6(57)+C4H8(251)	6.87E + 13	–0.3	–0.1
R840	C4H7(181)+C7H11(945)=C4H8(251)+S(1110)	6.87E + 13	–0.3	–0.1
R841	CH3(228)+C4H8(251)=CH4(1246)+C4H7(181)	1.44E – 01	4.2	7.5
R857	C4H7(181)+C6H8(951)=C4H8(251)+C6H7(2228)	7.72E – 03	4.3	6.7
R859	H(7)+C4H8(251)=C4H9(1337)	2.92E + 08	1.6	1.4
R860	C4H8(2010)=C4H8(251)	2.90E + 13	–0.3	8.9
R877	H(7)+C3H3(217)=ALLENE(51)	2.05E + 13	0.2	–0.2
R878	C3H3(217)+C3H6(84)=ALLENE(51)+ALLYL(3)	4.92E – 03	4.3	10.9
R881	C3H3(217)+C4H7(181)=ALLENE(51)+C4H6(57)	4.56E + 14	–0.7	0.0
R884	C3H3(217)+ALLYL(3)=ALLENE(51)+ALLENE(51)	2.41E + 12	0.0	6.0
R887	C3H3(217)+C4H8(248)=ALLENE(51)+C4H7(181)	1.02E – 02	4.3	8.5
R888	ALLENE(51)+C4H7(181)=C3H3(217)+C4H8(251)	1.09E – 01	4.3	14.5
R893	H(7)+C3H3(217)=C3H4(759)	6.40E + 13	0.1	–0.0
R894	C3H3(217)+C3H6(84)=C3H4(759)+ALLYL(3)	2.22E – 03	4.3	9.8
R913	C2H4(227)+C3H3(217)=C2H3(5)+ALLENE(51)	1.05E – 01	4.3	22.2
R914	C2H3(5)+C3H4(759)=C2H4(227)+C3H3(217)	2.08E – 02	4.3	0.6
R921	CH4(1246)+C3H3(217)=CH3(228)+ALLENE(51)	6.36E – 02	4.3	20.5
R922	CH4(1246)+C3H3(217)=CH3(228)+C3H4(759)	2.86E – 02	4.3	19.3
R955	C3H3(217)+C6H8(951)=ALLENE(51)+C6H7(2228)	8.72E – 03	4.3	4.1
R956	C3H3(217)+C6H8(951)=C3H4(759)+C6H7(2228)	3.94E – 03	4.3	2.9
R962	C3H3(217)+C7H8(3291)=ALLENE(51)+C7H7(5027)	4.17E – 03	4.3	12.8

Notes: k = A T^b exp(–E/RT); A unit is mole-cm-sec-K, E unit is kcal/mole.

Table B-2. Reactions and rate coefficient parameterizations shown in pathway diagrams of DTE pyrolysis (continued).

	Reactions	A	b	E
R963	C3H4(759)+C7H7(5027)=C3H3(217)+C7H8(3291)	1.25E – 02	4.3	12.0
R964	ALLENE(51)+C7H7(5030)=C3H3(217)+C7H8(3291)	2.12E – 01	4.3	–1.7
R969	C3H3(217)+ALLYL(3)=ALLENE(51)+ALLENE(51)	2.41E + 12	0.0	6.0
R980	C4H7(181)+S(1146)=C4H8(251)+S(1110)	6.87E + 13	–0.3	–0.1
R989	C3H4(759)+C7H7(5030)=C3H3(217)+C7H8(3291)	2.64E – 02	4.3	–2.1
R992	ALLYL(3)+C7H7(5027)=S(5864)	7.26E + 13	–0.1	0.0
R995	ALLYL(3)+C7H11(24)=C10H16(17)	6.96E + 13	–0.2	0.0
R997	ALLYL(3)+C4H6(57)=C7H11(24)	5.60E + 04	2.4	13.3
R1032	C7H11(24)=C7H11(77)	6.65E + 07	0.8	13.4
R1038	H(7)+C3H3(217)=ALLENE(51)	2.05E + 13	0.2	–0.2
R1039	C3H3(217)+C4H6(57)=C7H9(6326)	5.34E + 04	2.5	1.2
R1044	C7H9(6645)=C7H9(6326)	7.42E + 04	2.2	10.6
R1046	C7H9(6326)=C7H9(6641)	1.17E + 11	0.7	27.7
R1047	C7H9(6645)=C7H9(6641)	7.42E + 04	2.2	10.6
R1082	C7H9(6641)=C7H9(2597)	7.42E + 04	2.2	10.6
R1176	C7H9(2151)=C7H9(2230)	2.31E + 09	1.3	48.6
R1187	C7H9(2597)=C7H9(2230)	3.95E + 10	0.5	31.5
R1192	C4H7(181)+C7H9(2153)=C4H6(57)+S(2023)	6.87E + 13	–0.3	–0.1
R1220	C7H9(2153)=C7H9(2151)	5.16E + 04	2.0	25.3
R1232	C7H9(2230)=C7H9(2153)	2.12E + 09	1.0	11.0
R1237	C7H7(5027)=C7H7(5801)	2.52E + 12	–0.2	37.5
R1238	H(7)+C7H7(5027)=C7H8(3291)	7.23E + 13	0.1	–0.0
R1248	C7H7(6190)=C7H7(5790)	2.10E + 12	0.1	0.3
R1249	C7H7(7251)=C7H7(5801)	2.10E + 12	0.1	0.3
R1258	C3H3(217)+C3H3(217)=C6H6(6621)	1.31E + 12	0.2	–0.7
R1262	C6H6(7615)=C6H6(6621)	1.62E + 16	–0.9	20.9
R1272	C7H7(5027)+C7H7(5027)=S(6149)	3.38E + 16	–1.3	0.0
R1276	C6H6(7615)=C6H6(7686)	5.66E + 12	–0.4	5.2
R1291	C6H6(7686)=C6H6(3530)	3.18E + 12	–0.3	37.3
R1294	CH3(228)+C7H7(5027)=S(6287)	6.75E + 16	–1.3	0.0
R1305	C3H6(84)+C6H5(5026)=ALLYL(3)+C6H6(5025)	2.60E – 01	4.0	1.7
R1319	CH3(228)+C6H6(5025)=CH4(1246)+C6H5(5026)	5.15E + 03	2.9	15.3
R1332	C2H4(227)+C6H5(5026)=C2H3(5)+C6H6(5025)	4.72E – 02	4.3	3.4
R1335	C6H5(5026)+C7H8(3291)=C6H6(5025)+C7H7(5027)	7.20E – 03	4.3	–0.8
R1337	C3H3(217)+C6H6(5025)=ALLENE(51)+C6H5(5026)	1.93E – 01	4.3	25.9
R1338	C3H4(759)+C6H5(5026)=C3H3(217)+C6H6(5025)	2.64E – 02	4.3	–2.1
R1344	H(7)+C6H5(5026)=C6H6(3530)	8.03E + 13	0.2	0.0
R1358	C6H5(5026)+C6H8(951)=C6H6(5025)+C6H7(2228)	5.80E – 02	4.3	–5.6
R1367	C3H6(84)+S(6455)=ALLYL(3)+S(5864)	2.69E – 03	4.3	14.3
R1401	C4H6(57)+C6H5(5026)=S(6455)	8.13E + 05	2.6	0.0
R1404	ALLYL(3)+C4H6(57)=C3H6(84)+C4H5(176)	1.86E – 01	4.3	29.6
R1424	C2H2(501)+C2H3(5)=C4H5(176)	1.17E + 07	2.0	5.5
R1456	C4H6(57)+C6H5(5026)=C4H5(176)+C6H6(5025)	3.16E + 04	3.1	4.0
R1463	ALLENE(51)+C7H7(5027)=S(5899)	2.22E + 04	2.4	10.2
R1499	C7H7(6190)=C7H7(7340)	4.25E + 09	1.0	11.0
R1505	C3H6(84)+S(6457)=ALLYL(3)+S(5864)	7.80E – 01	4.0	1.7
R1519	CH3(228)+S(5864)=CH4(1246)+S(6457)	3.21E + 07	1.8	14.2
R1541	S(5899)=S(8550)	4.70E + 09	0.8	14.1
R1542	H(7)+S(8587)=S(8550)	1.34E + 08	1.6	2.3
R1585	C3H6(84)+S(8635)=ALLYL(3)+S(8587)	2.69E – 03	4.3	14.3
R1587	ALLYL(3)+S(8635)=ALLENE(51)+S(8587)	1.87E + 12	0.0	2.7

Notes: k = A T^b exp(–E/RT); A unit is mole-cm-sec-K, E unit is kcal/mole.

Table B-2. Reactions and rate coefficient parameterizations shown in pathway diagrams of DTE pyrolysis (continued).

	Reactions	A	b	E
R1595	CH4(1246)+S(8635)=CH3(228)+S(8587)	4.24E – 02	4.3	24.9
R1603	C7H8(3291)+S(8635)=C7H7(5027)+S(8587)	2.28E – 03	4.3	16.1
R1606	ALLENE(51)+S(8635)=C3H3(217)+S(8587)	6.76E – 02	4.3	15.2
R1607	C3H4(759)+S(8635)=C3H3(217)+S(8587)	8.37E – 03	4.3	14.8
R1619	S(8635)=H(7)+S(8877)	1.23E + 12	0.8	43.6
R1646	S(8635)=S(8896)	2.56E + 05	2.0	28.1
R1650	ALLYL(3)+S(8896)=C3H6(84)+S(8877)	1.37E + 14	–0.3	–0.1
R1659	C7H7(5027)+S(8896)=C7H8(3291)+S(8877)	3.45E + 13	–0.2	–0.0
R1728	S(8636)=S(8635)	1.18E + 10	1.0	32.1
R1755	S(8636)=S(8896)	7.07E – 16	8.1	14.6
R1837	S(9095)=S(8636)	1.14E + 10	0.6	16.6
R1838	S(9095)=S(10914)	2.59E + 10	0.5	9.6
R1852	S(11126)=S(10914)	4.53E + 12	0.2	29.2
R1853	S(11126)=S(10914)	4.53E + 12	0.2	29.2
R1854	S(11126)=H(7)+S(11344)	2.57E + 11	0.8	28.2
R1887	S(11126)=H(7)+S(11344)	2.57E + 11	0.8	28.2
R1909	C3H6(84)+C7H7(5028)=ALLYL(3)+C7H8(3291)	7.80E – 01	4.0	1.7
R1918	C2H4(227)+C7H7(5028)=C2H3(5)+C7H8(3291)	2.20E – 02	4.4	4.7
R1921	CH3(228)+C7H8(3291)=CH4(1246)+C7H7(5028)	3.21E + 07	1.8	14.2
R1927	C4H8(248)+C7H7(5028)=C4H7(181)+C7H8(3291)	2.16E – 02	4.3	–3.9
R1937	C6H8(951)+C7H7(5028)=C6H7(2228)+C7H8(3291)	5.80E – 02	4.3	–5.6
R1942	C7H7(5028)=C7H7(5027)	4.71E + 10	0.7	41.9
R1946	ALLENE(51)+C7H7(5028)=C3H3(217)+C7H8(3291)	2.12E – 01	4.3	–1.7
R1947	C3H4(759)+C7H7(5028)=C3H3(217)+C7H8(3291)	2.64E – 02	4.3	–2.1
R1972	C2H2(501)+C3H3(217)=C5H5(6350)	1.27E + 06	2.1	10.4
R1977	C3H3(217)+C7H7(5027)=S(6420)	3.14E + 19	–2.2	1.2
R2022	H(7)+C4H6(57)=H2(219)+C4H5(176)	2.40E + 02	3.6	11.3
R2023	H2(219)+C3H3(217)=H(7)+ALLENE(51)	7.50E – 02	3.9	16.2
R2025	H(7)+C3H6(84)=H2(219)+ALLYL(3)	3.36E + 03	3.1	4.3
R2026	H(7)+C3H6(84)=H2(219)+C3H5(53)	4.09E + 05	2.5	9.8
R2035	H2(219)+C3H3(217)=H(7)+C3H4(759)	3.06E + 00	3.5	15.0
R2037	H(7)+C2H4(227)=H2(219)+C2H3(5)	2.40E + 02	3.6	11.3
R2039	H(7)+CH4(1246)=H2(219)+CH3(228)	4.10E + 03	3.2	8.8
R2040	H(7)+C4H8(248)=H2(219)+C4H7(181)	4.50E + 04	2.7	3.5
R2041	H(7)+C4H8(248)=H2(219)+C4H7(9)	1.60E + 13	0.0	8.2
R2048	H(7)+C7H8(3291)=H2(219)+C7H7(5027)	7.54E + 04	2.6	3.1
R2049	H(7)+C7H8(3291)=H2(219)+C7H7(5028)	2.81E + 05	2.4	8.8
R2050	H(7)+C7H8(3291)=H2(219)+C7H7(5030)	1.57E + 06	2.4	9.4
R2051	H(7)+C6H6(5025)=H2(219)+C6H5(5026)	4.57E + 08	1.9	14.8
R2053	H(7)+C2H6(1571)=H2(219)+C2H5(502)	1.15E + 08	1.9	7.5
R2054	H2(219)+S(8635)=H(7)+S(8587)	4.58E – 02	4.3	24.2
R2064	H(7)+C6H8(951)=H2(219)+C6H7(2228)	1.79E + 00	4.3	–0.4
R2077	S(11912)=S(6420)	1.62E + 16	–0.9	20.9
R2079	S(6455)=H(7)+S(8404)	6.61E + 07	2.1	38.6
R2080	S(11912)=S(8404)	5.66E + 12	–0.4	5.2
R2112	C3H6(84)+C7H7(5029)=ALLYL(3)+C7H8(3291)	7.80E – 01	4.0	1.7
R2117	H(7)+C7H8(3291)=H2(219)+C7H7(5029)	1.16E + 06	2.4	9.1
R2122	C2H4(227)+C7H7(5029)=C2H3(5)+C7H8(3291)	2.20E – 02	4.4	4.7
R2125	CH3(228)+C7H8(3291)=CH4(1246)+C7H7(5029)	1.11E + 08	1.8	14.4
R2131	C4H8(248)+C7H7(5029)=C4H7(181)+C7H8(3291)	2.16E – 02	4.3	–3.9
R2141	C6H8(951)+C7H7(5029)=C6H7(2228)+C7H8(3291)	5.80E – 02	4.3	–5.6

Notes: k = A T^b exp(–E/RT); A unit is mole-cm-sec-K, E unit is kcal/mole.

Table B-2. Reactions and rate coefficient parameterizations shown in pathway diagrams of DTE pyrolysis (continued).

	Reactions	A	b	E
R2146	C7H7(5029)=C7H7(5027)	2.84E + 04	2.2	33.2
R2150	ALLENE(51)+C7H7(5029)=C3H3(217)+C7H8(3291)	2.12E – 01	4.3	–1.7
R2151	C3H4(759)+C7H7(5029)=C3H3(217)+C7H8(3291)	2.64E – 02	4.3	–2.1
R2234	C2H2(501)+C6H5(5026)=C8H7(8283)	2.95E + 07	1.6	3.4
R2236	C8H7(8283)=S(12311)	1.19E + 07	1.4	7.3
R2246	S(12337)=S(12311)	7.42E + 04	2.2	10.6
R2264	H(7)+S(12303)=S(12311)	6.97E + 07	1.9	4.8
R2265	H(7)+S(12303)=S(12337)	5.31E + 07	1.6	0.1
R2378	C7H7(7355)=C7H7(7340)	1.17E + 11	0.7	27.7
R2383	C7H7(7340)=C7H7(7355)	8.03E + 08	1.4	25.6
R2410	C7H7(7355)=C7H7(7354)	7.42E + 04	2.2	10.6
R2624	C3H6(84)+C7H9(2229)=ALLYL(3)+S(2150)	5.38E – 03	4.3	14.3
R2628	ALLYL(3)+C7H9(2229)=ALLENE(51)+S(2150)	3.74E + 12	0.0	2.7
R2635	CH4(1246)+C7H9(2229)=CH3(228)+S(2150)	8.48E – 02	4.3	30.2
R2642	C4H8(248)+C7H9(2229)=C4H7(181)+S(2150)	9.16E – 03	4.3	11.7
R2651	C7H9(2229)=C7H9(2151)	1.66E + 08	1.6	30.1
R2656	C7H9(2229)=H(7)+C7H8(3291)	1.03E + 09	1.4	26.5
R2689	C7H9(2229)=CH3(228)+C6H6(5025)	2.07E + 11	0.8	22.8
R2762	CH3(228)+C3H4(759)=C4H7(247)	1.78E + 05	2.4	7.2
R2794	H(7)+C4H6(239)=C4H7(247)	1.73E + 09	1.5	1.3
R2867	C3H3(217)+C3H3(217)=C6H6(6622)	2.94E + 13	–0.3	–0.3
R2868	C3H3(217)+C3H3(217)=C6H6(6617)	2.14E + 09	0.8	–1.0
R2869	C6H6(6617)=C6H6(7686)	2.08E + 09	0.8	39.1
R2871	C6H6(6622)=C6H6(6617)	2.31E + 10	0.4	34.6
R2887	C6H6(5543)=C6H6(5025)	2.91E + 12	0.2	0.2
R2892	C5H5(6350)=C5H5(7360)	2.88E + 10	0.3	12.1
R2894	C5H5(7360)=S(14220)	1.15E + 10	1.0	26.9
R2902	C3H6(84)+C7H7(5027)=S(5910)	1.03E + 04	2.4	9.3
R2946	H(7)+S(5864)=S(5910)	3.36E + 08	1.6	0.6
R3023	C3H3(217)+S(14222)=ALLENE(51)+S(14220)	4.36E – 03	4.3	4.1
R3024	ALLYL(3)+S(14222)=C3H6(84)+S(14220)	7.72E – 03	4.3	6.7
R3025	C3H5(53)+S(14222)=C3H6(84)+S(14220)	1.06E – 02	4.3	–4.2
R3027	C3H3(217)+S(14222)=C3H4(759)+S(14220)	1.97E – 03	4.3	2.9
R3028	C2H3(5)+S(14222)=C2H4(227)+S(14220)	2.28E – 02	4.3	–2.8
R3029	CH3(228)+S(14222)=CH4(1246)+S(14220)	2.12E – 02	4.3	1.7
R3033	S(14222)+C7H7(5027)=S(14220)+C7H8(3291)	3.58E – 03	4.3	4.6
R3034	S(14222)+C7H7(5028)=S(14220)+C7H8(3291)	2.90E – 02	4.3	–5.6
R3035	S(14222)+C7H7(5029)=S(14220)+C7H8(3291)	2.90E – 02	4.3	–5.6
R3036	S(14222)+C7H7(5030)=S(14220)+C7H8(3291)	2.90E – 02	4.3	–5.6
R3037	S(14222)+C6H5(5026)=S(14220)+C6H6(5025)	2.90E – 02	4.3	–5.6
R3045	S(14222)+S(8635)=S(14220)+S(8587)	1.96E – 03	4.3	6.3
R3046	S(14222)+S(8636)=S(14220)+S(8587)	1.24E – 03	4.3	3.2
R3047	H(7)+S(14222)=H2(219)+S(14220)	8.94E – 01	4.3	–0.4
R3050	H(7)+S(14220)=S(14222)	2.50E + 15	0.0	0.0
R3245	C7H7(7358)=C7H7(7251)	1.01E + 10	1.0	19.2
R3247	C2H2(501)+S(14220)=C7H7(7358)	4.08E + 05	2.2	10.8
R3258	C7H7(8876)=C7H7(7354)	4.51E + 12	0.3	25.2
R3260	C7H7(7358)=C7H7(8876)	9.25E + 11	0.2	9.8
R3326	CH3(228)+S(6287)=CH4(1246)+C8H9(6454)	6.00E + 12	0.0	12.6
R3392	CH3(228)+S(6287)=CH4(1246)+C8H9(8217)	3.21E + 07	1.8	14.2
R3449	CH3(228)+S(12303)=CH4(1246)+S(12511)	3.21E + 07	1.8	14.2

Notes: k = A T^b exp(–E/RT); A unit is mole-cm-sec-K, E unit is kcal/mole.

Table B-2. Reactions and rate coefficient parameterizations shown in pathway diagrams of DTE pyrolysis (continued).

	Reactions	A	b	E
R3460	ALLENE(51)+S(12511)=C3H3(217)+S(12303)	2.12E – 01	4.3	–1.7
R3586	CH3(228)+S(12303)=CH4(1246)+S(12512)	1.60E + 07	1.8	14.2
R3597	ALLENE(51)+S(12512)=C3H3(217)+S(12303)	2.12E – 01	4.3	–1.7
R3655	CH3(228)+S(12303)=CH4(1246)+S(12510)	3.21E + 07	1.8	14.2
R3666	ALLENE(51)+S(12510)=C3H3(217)+S(12303)	2.12E – 01	4.3	–1.7

Notes: k = A T^b exp(–E/RT); A unit is mole-cm-sec-K, E unit is kcal/mole.

Table B-3. Coefficients for calculating the thermodynamic properties of species in the pathway diagrams of DTE pyrolysis.

```
THERMO
   300.000  1500.000  5000.000
ALLENE(51)              C   3H   4          G   100.000  5000.000  949.70      1
 6.79951692E+00 9.59986429E-03-3.02072703E-06 5.37837787E-10-3.92614717E-14    2
 1.97722894E+04-1.27579867E+01 3.37448426E+00 7.04603491E-03 2.78312131E-05    3
-3.99452792E-08 1.55732731E-11 2.11885602E+04 7.62043021E+00                   4
ALLYL(3)                C   3H   5          G   100.000  5000.000  942.16      1
 8.06840722E+00 1.01840441E-02-2.84817142E-06 5.00933642E-10-3.79673181E-14    2
 1.69147746E+04-1.95259079E+01 3.29621577E+00 5.79137321E-03 4.33952241E-05    3
-5.99933663E-08 2.33834346E-11 1.89082117E+04 9.01969380E+00                   4
C10H16(1)               C  10H  16          G   100.000  5000.000 1145.81      1
 1.84921014E+01 5.29108577E-02-2.15085167E-05 3.96090714E-09-2.73981208E-13    2
 4.35260816E+03-6.18502248E+01-1.09394286E+00 9.67839280E-02-4.68682058E-05    3
 5.35082806E-11 4.65045450E-12 1.04493534E+04 4.23254939E+01                   4
C10H16(17)              C  10H  16          G   100.000  5000.000 1095.80      1
 1.89720450E+01 5.20611196E-02-2.09215524E-05 3.85813240E-09-2.68377506E-13    2
 4.70441725E+03-6.39953730E+01-1.13082934E+00 9.68134345E-02-4.29916642E-05    3
-6.55723671E-09 7.54736001E-12 1.08290222E+04 4.26714399E+01                   4
C2H2(501)               C   2H   2          G   100.000  5000.000  897.94      1
 5.89067162E+00 2.09057452E-03 4.88323382E-08-5.66869966E-11 4.15056951E-15    2
 2.54158944E+04-1.07351021E+01 3.08745059E+00 5.78565574E-03 8.56356418E-06    3
-1.72827849E-08 7.83609784E-12 2.62737790E+04 4.46078104E+00                   4
C2H3(5)                 C   2H   3          G   100.000  5000.000  933.66      1
 5.36081257E+00 5.27352358E-03-1.31964328E-06 2.21574674E-10-1.68776994E-14    2
 3.36586028E+04-4.76300481E+00 3.83071491E+00-1.47646348E-03 3.09009114E-05    3
-3.80485348E-08 1.43174967E-11 3.45242392E+04 5.61943330E+00                   4
C2H4(227)               C   2H   4          G   100.000  5000.000  946.02      1
 4.59027216E+00 8.72714078E-03-2.66488192E-06 4.81698247E-10-3.60680089E-14    2
 4.12699879E+03-3.32486536E+00 3.98874461E+00-6.74693776E-03 5.04391044E-05    3
-5.70734797E-08 2.04940710E-11 5.04704816E+03 3.80499481E+00                   4
C2H5(502)               C   2H   5          G   100.000  5000.000  967.56      1
 4.21409736E+00 1.22658184E-02-4.37067389E-06 7.87986108E-10-5.56038842E-14    2
 1.24800844E+04 1.53824771E+00 3.69275531E+00 1.87277548E-03 3.11950013E-05    3
-3.71210965E-08 1.32026605E-11 1.31683444E+04 7.07155492E+00                   4
C2H6(1571)              C   2H   6          G   100.000  5000.000  981.60      1
 3.34696252E+00 1.61750145E-02-6.00966161E-06 1.09622982E-09-7.72310606E-14    2
-1.20941964E+04 3.10404244E+00 3.74672845E+00 4.52321117E-05 4.07972227E-05    3
-4.57425453E-08 1.56847718E-11-1.14740722E+04 4.74132231E+00                   4
C3H3(217)               C   3H   3          G   100.000  5000.000  949.37      1
 6.99888511E+00 7.24413979E-03-2.36570305E-06 3.98587730E-10-2.69780619E-14    2
 3.97273455E+04-1.20479082E+01 3.09017772E+00 1.73589434E-02-8.30808651E-06    3
-2.47806058E-09 2.58688945E-12 4.07558459E+04 8.11430183E+00                   4
C3H4(759)               C   3H   4          G   100.000  5000.000  969.98      1
 5.80051735E+00 1.13536392E-02-4.03493954E-06 7.19070516E-10-5.02190641E-14    2
 1.97499748E+04-7.36949349E+00 3.30524258E+00 1.09263675E-02 1.31992209E-05    3
-2.25168350E-08 8.87438780E-12 2.07382226E+04 7.19159787E+00                   4
C3H5(53)                C   3H   5          G   100.000  5000.000 1030.45      1
 5.02495284E+00 1.54866219E-02-6.07291199E-06 1.11597857E-09-7.79103403E-14    2
 2.79427600E+04-9.11377563E-01 3.26240010E+00 1.20170332E-02 1.39879076E-05    3
-2.15738725E-08 7.78299526E-12 2.88534509E+04 1.03011437E+01                   4
C3H5(54)                C   3H   5          G   100.000  5000.000  988.72      1
 5.81117011E+00 1.40189058E-02-5.21090817E-06 9.48998006E-10-6.67718876E-14    2
 2.95131350E+04-5.37297240E+00 3.22799964E+00 1.18522806E-02 1.72178565E-05    3
-2.70808862E-08 1.02841620E-11 3.06406475E+04 1.01787412E+01                   4
C3H6(84)                C   3H   6          G   100.000  5000.000  983.76      1
 5.36765118E+00 1.70741321E-02-6.35097810E-06 1.16617206E-09-8.27600983E-14    2
-4.87179929E+02-4.54523482E+00 3.31909503E+00 8.17990024E-03 3.34724870E-05    3
-4.36178753E-08 1.58206875E-11 7.49326441E+02 9.54034329E+00                   4
```

Table B-3. Coefficients for calculating the thermodynamic properties of species in the pathway diagrams of DTE pyrolysis (continued).

```
C3H7(231)               C   3H   7          G   100.000  5000.000  984.47      1
 6.16551720E+00 1.84493164E-02-6.79021113E-06 1.23047232E-09-8.63849946E-14    2
 9.09502531E+03-6.67653316E+00 3.02813337E+00 1.47025993E-02 2.40500275E-05    3
-3.66725789E-08 1.38605931E-11 1.05120556E+04 1.24699506E+01                   4
C3H7(232)               C   3H   7          G   100.000  5000.000 1029.98      1
 4.36582811E+00 2.14399422E-02-8.48558174E-06 1.56801566E-09-1.09812925E-13    2
 8.03956499E+03 2.70055246E+00 3.23518579E+00 1.11016010E-02 2.80213867E-05    3
-3.59458757E-08 1.23657295E-11 9.05375554E+03 1.19813575E+01                   4
C4H5(176)               C   4H   5          G   100.000  5000.000  937.72      1
 1.29704389E+01 6.69132397E-03-1.00073711E-06 1.67609542E-10-1.71443095E-14    2
 3.82796987E+04-4.39473732E+01 2.64256537E+00 1.63335672E-02 3.86229728E-05    3
-6.71383146E-08 2.83605805E-11 4.17296359E+04 1.32819832E+01                   4
C4H6(177)               C   4H   6          G   100.000  5000.000 2271.41      1
 1.33025358E+01 1.41307445E-02-5.59060021E-06 9.21122762E-10-5.59689127E-14    2
 4.39065751E+04-3.81494587E+01 2.68371726E+00 2.99287474E-02-1.41069342E-05    3
 2.85822979E-09-2.07267310E-13 4.94791197E+04 2.34397759E+01                   4
C4H6(239)               C   4H   6          G   100.000  5000.000 1025.61      1
 6.82083672E+00 1.92337227E-02-7.45616219E-06 1.36534765E-09-9.53184301E-14    2
 1.60280062E+04-1.04336045E+01 2.74634069E+00 2.18190533E-02 8.22301897E-06    3
-2.14761560E-08 8.55596082E-12 1.75635646E+04 1.27381119E+01                   4
C4H6(57)                C   4H   6          G   100.000  5000.000  946.05      1
 1.24693326E+01 1.00554583E-02-2.41210852E-06 4.57086790E-10-3.93168493E-14    2
 8.01079412E+03-4.36372511E+01 2.80600520E+00 1.02582985E-02 6.17265730E-05    3
-9.01650174E-08 3.59120322E-11 1.16584967E+04 1.20621004E+01                   4
C4H7(181)               C   4H   7          G   100.000  5000.000  995.01      1
 7.60270618E+00 2.07982091E-02-7.87779566E-06 1.45013878E-09-1.02663239E-13    2
 1.27543966E+04-1.45508965E+01 2.68514595E+00 2.07744562E-02 2.19958332E-05    3
-3.85571097E-08 1.49722721E-11 1.47127821E+04 1.40723604E+01                   4
C4H7(246)               C   4H   7          G   100.000  5000.000 1012.54      1
 7.74082444E+00 2.03541139E-02-7.74605049E-06 1.41034649E-09-9.84410712E-14    2
 2.60852963E+04-1.37520923E+01 2.52157313E+00 2.59936051E-02 6.08981132E-06    3
-2.23097735E-08 9.36554870E-12 2.79100802E+04 1.52845057E+01                   4
C4H7(247)               C   4H   7          G   100.000  5000.000 1477.84      1
 7.04126999E+00 2.22766296E-02-9.06111359E-06 1.61291806E-09-1.06960450E-13    2
 2.31356240E+04-1.08437965E+01 2.61024550E+00 2.78343500E-02-8.17014102E-06    3
-1.73566633E-09 9.57979855E-13 2.51480554E+04 1.46416800E+01                   4
C4H7(9)                 C   4H   7          G   100.000  5000.000 1051.00      1
 7.36559182E+00 2.10619473E-02-8.19314352E-06 1.49014840E-09-1.03098946E-13    2
 2.14330321E+04-1.12172301E+01 2.48601576E+00 2.77402230E-02-7.50642659E-07    3
-1.39976065E-08 6.14206980E-12 2.31155594E+04 1.56914714E+01                   4
C4H8(2010)              C   4H   8          G   100.000  5000.000 1802.44      1
 1.05026352E+01 2.26351107E-02-8.93619334E-06 1.52845623E-09-9.75139237E-14    2
 3.05114758E+04-2.16464092E+01 2.23551121E+00 3.62128221E-02-1.62669897E-05    3
 2.77200357E-09-6.63967431E-14 3.42663131E+04 2.52570554E+01                   4
C4H8(248)               C   4H   8          G   100.000  5000.000 1007.28      1
 7.20513157E+00 2.36362247E-02-9.03153930E-06 1.65393585E-09-1.16020021E-13    2
-3.79732241E+03-1.24423997E+01 2.58773856E+00 2.32776837E-02 1.93416352E-05    3
-3.55501549E-08 1.36908232E-11-1.91872967E+03 1.45750278E+01                   4
C4H8(251)               C   4H   8          G   100.000  5000.000 1157.78      1
 6.04218302E+00 2.60073541E-02-1.04844033E-05 1.90882434E-09-1.30601730E-13    2
-4.86273162E+03-7.52672959E+00 2.51999295E+00 2.76811719E-02 9.44131595E-07    3
-1.25013178E-08 4.67160143E-12-3.34374810E+03 1.30195272E+01                   4
C4H9(1337)              C   4H   9          G   100.000  5000.000 1083.85      1
 6.12698235E+00 2.82086390E-02-1.13016940E-05 2.07331211E-09-1.43451009E-13    2
 4.72410286E+03-4.53091277E+00 2.48182356E+00 2.70986277E-02 1.03886696E-05    3
-2.36649548E-08 8.65274961E-12 6.36961857E+03 1.72942972E+01                   4
```

Table B-3. Coefficients for calculating the thermodynamic properties of species in the pathway diagrams of DTE pyrolysis (continued).

```
C5H5(6350)              C   5H   5          G   100.000  5000.000 1020.59      1
 9.61238432E+00 1.62441042E-02-6.07929102E-06 1.08940714E-09-7.51981484E-14    2
 5.87667369E+04-2.17848185E+01 2.17298418E+00 3.48443927E-02-1.79010171E-05    3
-1.32354622E-09 2.99850502E-12 6.08350664E+04 1.69512042E+01                   4
C5H5(7360)              C   5H   5          G   100.000  5000.000  952.66      1
 1.11869168E+01 1.28538609E-02-3.79077348E-06 7.28245619E-10-5.85262083E-14    2
 4.39233946E+04-3.56087259E+01 2.96708931E+00 6.72428900E-03 6.98542076E-05    3
-9.55907560E-08 3.69698311E-11 4.73338179E+04 1.33282152E+01                   4
C5H9(1283)              C   5H   9          G   100.000  5000.000  999.84      1
 1.02289046E+01 2.64699429E-02-1.01084593E-05 1.86963519E-09-1.32726211E-13    2
 9.04334050E+03-2.68358860E+01 1.97338755E+00 3.36989468E-02 1.77498410E-05    3
-4.25119106E-08 1.74170325E-11 1.19836903E+04 1.94394605E+01                   4
C5H9(984)               C   5H   9          G   100.000  5000.000 1100.04      1
 8.32449920E+00 2.92565718E-02-1.18105792E-05 2.17377436E-09-1.50622522E-13    2
 1.61365943E+04-1.44346278E+01 1.97546717E+00 3.72871499E-02-2.23074582E-06    3
-1.60741418E-08 6.82415664E-12 1.84443802E+04 2.09416726E+01                   4
C6H10(119)              C   6H  10          G   100.000  5000.000 1029.51      1
 1.11942591E+01 3.14218098E-02-1.24028041E-05 2.30465179E-09-1.62630037E-13    2
 4.43826770E+03-3.01757997E+01 1.48890581E+00 4.41329564E-02 5.49845143E-06    3
-3.28724153E-08 1.41067931E-11 7.76134915E+03 2.33629693E+01                   4
C6H11(200)              C   6H  11          G   100.000  5000.000 1482.98      1
 1.09172302E+01 3.48274057E-02-1.37979939E-05 2.42685690E-09-1.60043792E-13    2
 1.20329133E+04-2.61778130E+01 1.31776112E+00 5.25265931E-02-2.34131145E-05    3
 3.02382836E-09 3.67353556E-13 1.57810152E+04 2.69543698E+01                   4
C6H5(5026)              C   6H   5          G   100.000  5000.000  938.83      1
 1.25685360E+01 1.27451771E-02-2.83419519E-06 4.97055539E-10-4.18298117E-14    2
 3.50253496E+04-4.35190683E+01 2.84113463E+00 6.98532706E-03 8.17889423E-05    3
-1.13150490E-07 4.44827109E-11 3.89321368E+04 1.38752987E+01                   4
C6H6(3530)              C   6H   6          G   100.000  5000.000  957.77      1
 1.29094396E+01 1.68727210E-02-5.38408426E-06 1.02583478E-09-7.96378154E-14    2
 4.27725605E+04-4.56031893E+01 2.45863180E+00 1.64127261E-02 6.44130811E-05    3
-9.56389411E-08 3.77025166E-11 4.67974462E+04 1.49259384E+01                   4
C6H6(5025)              C   6H   6          G   100.000  5000.000  949.24      1
 1.25210218E+01 1.65024545E-02-4.66524109E-06 8.85737097E-10-7.16100728E-14    2
 4.05217497E+03-4.72612521E+01 2.88774574E+00 3.39715127E-03 1.00900052E-04    3
-1.32850650E-07 5.08461968E-11 8.30030931E+03 1.14551653E+01                   4
C6H6(5543)              C   6H   6          G   100.000  5000.000  993.89      1
 1.21082454E+01 2.33013908E-02-9.76382022E-06 1.99589171E-09-1.52848104E-13    2
 4.72446390E+04-4.44493733E+01 2.55946800E+00 1.21813072E-02 8.18014619E-05    3
-1.09584930E-07 4.05315637E-11 5.15900205E+04 1.38711911E+01                   4
C6H6(6617)              C   6H   6          G   100.000  5000.000  987.88      1
 1.36930956E+01 1.73399932E-02-6.25060131E-06 1.13246749E-09-8.01954813E-14    2
 4.18530373E+04-4.55041846E+01 1.42952374E+00 4.78179887E-02-2.34083742E-05    3
-6.94025516E-09 6.93591150E-12 4.52118284E+04 1.82473403E+01                   4
C6H6(6621)              C   6H   6          G   100.000  5000.000 1502.12      1
 1.25077416E+01 1.89812604E-02-7.11301182E-06 1.23032535E-09-8.11002763E-14    2
 4.47346587E+04-3.78003520E+01 1.46995331E+00 4.83736318E-02-3.64637118E-05    3
 1.42565865E-08-2.24906577E-12 4.80506965E+04 1.99416940E+01                   4
C6H6(6622)              C   6H   6          G   100.000  5000.000 1299.70      1
 1.14107105E+01 1.82241310E-02-5.01899259E-06 6.85817142E-10-3.82981055E-14    2
 4.53977275E+04-3.05410218E+01 1.28113154E+00 5.30770234E-02-4.94877181E-05    3
 2.56727669E-08-5.26338253E-12 4.77201839E+04 1.97886482E+01                   4
C6H6(7615)              C   6H   6          G   100.000  5000.000  835.73      1
 6.89878964E+00 3.03193282E-02-1.29505235E-05 2.35259137E-09-1.58445586E-13    2
 7.82256050E+04 5.30918716E+00 1.38461915E+00 6.10807906E-02-7.60046187E-05    3
 5.89070029E-08-1.89474653E-11 7.89946887E+04 3.00094562E+01                   4
```

Table B-3. Coefficients for calculating the thermodynamic properties of species in the pathway diagrams of DTE pyrolysis (continued).

```
C6H6(7686)              C   6H   6          G   100.000  5000.000  951.74      1
 1.59979655E+01 1.30901626E-02-3.81647746E-06 6.83741365E-10-5.19524656E-14    2
 3.46450872E+04-5.85086523E+01 1.52699624E+00 4.10807193E-02 3.80793558E-06    3
-4.08985181E-08 2.03904899E-11 3.88864337E+04 1.84006917E+01                   4
C6H7(2228)              C   6H   7          G   100.000  5000.000 1051.47      1
 8.26337564E+00 2.94390959E-02-1.26582762E-05 2.45533605E-09-1.76992261E-13    2
 1.95763521E+04-2.13932081E+01 2.41083212E+00 2.38204806E-02 3.51340819E-05    3
-5.30665374E-08 1.90203780E-11 2.23484544E+04 1.44651576E+01                   4
C6H8(951)               C   6H   8          G   100.000  5000.000  966.34      1
 1.18944285E+01 2.41863328E-02-8.47109335E-06 1.61955304E-09-1.22272240E-13    2
 7.20885789E+03-4.04075955E+01 2.50805353E+00 1.30896172E-02 8.62888709E-05    3
-1.17244972E-07 4.44674771E-11 1.13551350E+04 1.66220082E+01                   4
C7H10(507)              C   7H  10          G   100.000  5000.000  964.44      1
 1.71632635E+01 2.51950051E-02-8.49305347E-06 1.52030237E-09-1.08851877E-13    2
 8.47076522E+03-6.32351509E+01 7.07372803E-01 5.73831712E-02-2.46688147E-06    3
-4.14167980E-08 2.10715791E-11 1.33220536E+04 2.42541381E+01                   4
C7H11(2)                C   7H  11          G   100.000  5000.000 1035.81      1
 1.36593143E+01 3.48944505E-02-1.38111996E-05 2.56422379E-09-1.80696975E-13    2
 1.75671801E+04-4.08412120E+01 8.15581564E-01 5.75166911E-02-7.50527644E-06    3
-2.66382474E-08 1.29362105E-11 2.16750647E+04 2.85598890E+01                   4
C7H11(24)               C   7H  11          G   100.000  5000.000  994.87      1
 1.31760510E+01 3.38944735E-02-1.24346334E-05 2.21897286E-09-1.53505262E-13    2
 2.49281909E+04-3.55668162E+01 8.34971040E-01 5.82884879E-02-1.11817051E-05    3
-2.41066151E-08 1.28662234E-11 2.86320721E+04 3.01821293E+01                   4
C7H11(517)              C   7H  11          G   100.000  5000.000  989.11      1
 1.21352107E+01 3.66012012E-02-1.41638178E-05 2.71508032E-09-1.99255974E-13    2
 1.23809468E+04-3.97388285E+01 1.89741718E+00 2.52493600E-02 8.30540556E-05    3
-1.16733111E-07 4.36207672E-11 1.69867466E+04 2.25853065E+01                   4
C7H11(523)              C   7H  11          G   100.000  5000.000  983.68      1
 1.40004095E+01 3.26378462E-02-1.21797332E-05 2.29012327E-09-1.66619954E-13    2
 2.57864159E+04-4.46510903E+01 1.40265125E+00 3.86972220E-02 4.74563928E-05    3
-8.48063044E-08 3.38322696E-11 3.04501074E+04 2.70261227E+01                   4
C7H11(683)              C   7H  11          G   100.000  5000.000 1340.99      1
 1.01563327E+01 3.96645698E-02-1.59103294E-05 2.85556214E-09-1.92740213E-13    2
 2.45936793E+04-2.02883989E+01 8.75379436E-01 6.73484216E-02-4.68768003E-05    3
 1.82503742E-08-3.06278279E-12 2.70828154E+04 2.72099542E+01                   4
C7H11(72)               C   7H  11          G   100.000  5000.000 1082.71      1
 1.18913900E+01 3.76739792E-02-1.53686270E-05 2.85993520E-09-2.00085414E-13    2
 1.67123138E+04-3.31191744E+01 9.95398767E-01 5.49609569E-02-7.49873248E-06    3
-2.15783490E-08 9.96670768E-12 2.04179517E+04 2.65303559E+01                   4
C7H11(73)               C   7H  11          G   100.000  5000.000 1061.31      1
 1.28481562E+01 3.60557677E-02-1.44535493E-05 2.67848035E-09-1.87560710E-13    2
 1.64792102E+04-3.68189505E+01 8.57179875E-01 5.76691461E-02-1.16746245E-05    3
-2.00009402E-08 1.00858529E-11 2.03524336E+04 2.80004636E+01                   4
C7H11(77)               C   7H  11          G   100.000  5000.000  972.83      1
 1.04880284E+01 3.68609009E-02-1.33504762E-05 2.46626831E-09-1.77897921E-13    2
 1.61661084E+04-2.63913146E+01 2.08975509E+00 2.26565120E-02 8.36971480E-05    3
-1.15536073E-07 4.33805390E-11 2.01062733E+04 2.57469911E+01                   4
C7H11(945)              C   7H  11          G   100.000  5000.000 1011.64      1
 1.32525197E+01 3.50663883E-02-1.32012036E-05 2.37832188E-09-1.64861368E-13    2
 8.65365745E+03-4.12150953E+01 7.55848202E-01 5.99969483E-02-1.38676983E-05    3
-2.11034792E-08 1.15495084E-11 1.24347903E+04 2.54102154E+01                   4
C7H11(949)              C   7H  11          G   100.000  5000.000 1202.28      1
 1.37648655E+01 3.52079810E-02-1.40389783E-05 2.53977115E-09-1.73150289E-13    2
 1.65850803E+04-4.30391448E+01 5.12788332E-01 6.70279954E-02-3.84304660E-05    3
 7.57656638E-09 5.44548410E-13 2.06584120E+04 2.70237057E+01                   4
```

Table B-3. Coefficients for calculating the thermodynamic properties of species in the pathway diagrams of DTE pyrolysis (continued).

```
C7H12(257)              C   7H  12          G   100.000  5000.000 1021.05      1
 1.35813307E+01 3.69460497E-02-1.43791789E-05 2.65836206E-09-1.87419984E-13    2
-2.18388458E+02-4.11247242E+01 8.05786866E-01 5.67087327E-02 1.08051489E-06    3
-3.64859558E-08 1.65097973E-11 3.96922000E+03 2.85068790E+01                   4
C7H12(93)               C   7H  12          G   100.000  5000.000 1118.33      1
 1.21603689E+01 3.96570005E-02-1.61063029E-05 2.97092262E-09-2.05965912E-13    2
-3.39676722E+02-3.33473553E+01 7.68978355E-01 6.04854781E-02-1.73306387E-05    3
-1.22232066E-08 6.75038953E-12 3.45359643E+03 2.84516249E+01                   4
C7H7(5027)              C   7H   7          G    10.000  3000.000  549.06      1
-6.62671000E-01 5.80793000E-02-3.73415000E-05 1.14394000E-08-1.33771000E-12    2
 2.32703000E+04 2.56807000E+01 4.13967000E+00-1.41725000E-02 2.61854000E-04    3
-4.75457000E-07 2.76642000E-10 2.33046000E+04 1.05067000E+01                   4
C7H7(5028)              C   7H   7          G   100.000  5000.000  990.22      1
 1.12442130E+01 2.55942517E-02-9.68541662E-06 1.84053218E-09-1.34500249E-13    2
 3.08763952E+04-3.41760145E+01 2.10443259E+00 2.74497213E-02 4.06207322E-05    3
-6.77892840E-08 2.64735116E-11 3.44055763E+04 1.85087437E+01                   4
C7H7(5029)              C   7H   7          G   100.000  5000.000  990.22      1
 1.12442130E+01 2.55942517E-02-9.68541662E-06 1.84053218E-09-1.34500249E-13    2
 3.08763952E+04-3.41760145E+01 2.10443259E+00 2.74497213E-02 4.06207322E-05    3
-6.77892840E-08 2.64735116E-11 3.44055763E+04 1.85087437E+01                   4
C7H7(5030)              C   7H   7          G   100.000  5000.000  990.22      1
 1.12442130E+01 2.55942517E-02-9.68541662E-06 1.84053218E-09-1.34500249E-13    2
 3.08763952E+04-3.48691616E+01 2.10443259E+00 2.74497213E-02 4.06207322E-05    3
-6.77892840E-08 2.64735116E-11 3.44055763E+04 1.78155965E+01                   4
C7H7(5790)              C   7H   7          G   100.000  5000.000 1059.88      1
 9.46524888E+00 3.17526245E-02-1.39245403E-05 2.72431357E-09-1.97129432E-13    2
 3.20229958E+04-2.77307477E+01 2.13793636E+00 2.85238657E-02 3.43509220E-05    3
-5.51321026E-08 1.99342515E-11 3.53107800E+04 1.62282727E+01                   4
C7H7(5801)              C   7H   7          G   100.000  5000.000 1005.50      1
 1.12143970E+01 2.82319886E-02-1.18048035E-05 2.35146083E-09-1.75498810E-13    2
 3.81950078E+04-4.00452238E+01 2.34964485E+00 1.85114693E-02 6.98051506E-05    3
-9.62519279E-08 3.54032000E-11 4.22518091E+04 1.40789785E+01                   4
C7H7(6190)              C   7H   7          G   100.000  5000.000  953.78      1
 1.84321868E+01 1.64272725E-02-4.91567617E-06 8.81336530E-10-6.62534115E-14    2
 4.35657348E+04-7.42074334E+01 9.45055335E-01 5.16472494E-02-3.58221899E-07    3
-4.42055022E-08 2.27345256E-11 4.86353290E+04 1.84194879E+01                   4
C7H7(7251)              C   7H   7          G   100.000  5000.000  942.83      1
 1.92548364E+01 1.35295888E-02-2.96082977E-06 5.29345576E-10-4.56030960E-14    2
 4.47797722E+04-7.76157002E+01 1.45598448E+00 3.42882874E-02 5.11244062E-05    3
-9.93099738E-08 4.27606025E-11 5.05696213E+04 2.01114896E+01                   4
C7H7(7340)              C   7H   7          G   100.000  5000.000  939.78      1
 1.81007353E+01 1.69823365E-02-4.63842278E-06 7.70394900E-10-5.59615822E-14    2
 3.91147899E+04-7.28106778E+01 8.98533780E-01 5.36039509E-02-4.67913092E-06    3
-4.06368712E-08 2.19819370E-11 4.39641301E+04 1.77097488E+01                   4
C7H7(7354)              C   7H   7          G   100.000  5000.000  928.86      1
 2.17677308E+01 9.92402238E-03-3.42329866E-07-2.10430463E-11-6.79284857E-15    2
 2.57203796E+04-9.82659269E+01 1.30241586E+00 3.45892223E-02 6.23152965E-05    3
-1.18550596E-07 5.16930530E-11 3.22601279E+04 1.36948335E+01                   4
C7H7(7355)              C   7H   7          G   100.000  5000.000  939.78      1
 1.81007353E+01 1.69823365E-02-4.63842278E-06 7.70394900E-10-5.59615822E-14    2
 3.91147899E+04-7.28106778E+01 8.98533780E-01 5.36039509E-02-4.67913092E-06    3
-4.06368712E-08 2.19819370E-11 4.39641301E+04 1.77097488E+01                   4
C7H7(7358)              C   7H   7          G   100.000  5000.000  977.14      1
 1.36149039E+01 2.30476255E-02-8.35718724E-06 1.56112963E-09-1.13948979E-13    2
 4.96789068E+04-4.58521520E+01 1.65995947E+00 3.70671582E-02 2.37254235E-05    3
-5.68996366E-08 2.42000618E-11 5.36822732E+04 2.00772626E+01                   4
```

Table B-3. Coefficients for calculating the thermodynamic properties of species in the pathway diagrams of DTE pyrolysis (continued).

```
C7H7(8876)              C   7H   7          G   100.000  5000.000  948.89      1
 1.73157252E+01 1.60255984E-02-4.11951483E-06 7.97763718E-10-6.78978702E-14    2
 4.09509599E+04-7.05225537E+01 2.11643513E+00 1.62681830E-02 9.63970287E-05    3
-1.40711860E-07 5.58917316E-11 4.67090480E+04 1.71496594E+01                   4
C7H8(3291)              C   7H   8          G    10.000  3000.000  590.57      1
-2.46624000E+00 6.20951000E-02-3.84774000E-05 1.14026000E-08-1.29702000E-12    2
 4.08970000E+03 3.55174000E+01 4.04843000E+00-4.96311000E-03 1.90094000E-04    3
-3.12375000E-07 1.63599000E-10 3.72016000E+03 1.09050000E+01                   4
C7H9(2024)              C   7H   9          G    10.000  3000.000  440.11      1
-3.18625000E+00 6.84702000E-02-4.34733000E-05 1.32476000E-08-1.55121000E-12    2
 1.76309000E+04 4.10168000E+01 3.94037000E+00 3.67950000E-03 1.77415000E-04    3
-3.21449000E-07 1.88627000E-10 1.70037000E+04 1.24861000E+01                   4
C7H9(2025)              C   7H   9          G    10.000  3000.000  408.68      1
-2.52355000E+00 6.69984000E-02-4.22560000E-05 1.28111000E-08-1.49441000E-12    2
 1.75155000E+04 3.74016000E+01 3.94238000E+00 3.73416000E-03 1.89866000E-04    3
-3.65712000E-07 2.29978000E-10 1.69868000E+04 1.19908000E+01                   4
C7H9(2151)              C   7H   9          G    10.000  3000.000  391.04      1
-2.19466000E+00 6.65475000E-02-4.20309000E-05 1.27717000E-08-1.49365000E-12    2
 1.68507000E+04 3.54456000E+01 3.94447000E+00 3.71676000E-03 1.99109000E-04    3
-3.98552000E-07 2.61611000E-10 1.63708000E+04 1.15954000E+01                   4
C7H9(2153)              C   7H   9          G   100.000  5000.000 1008.25      1
 1.03346658E+01 3.49616360E-02-1.38262699E-05 2.61922559E-09-1.88497015E-13    2
 1.58308471E+04-3.10413345E+01 1.90087054E+00 3.09750935E-02 4.78140417E-05    3
-7.49741208E-08 2.81848550E-11 1.94348093E+04 1.91547567E+01                   4
C7H9(2229)              C   7H   9          G    10.000  3000.000  522.29      1
-2.59550000E+00 6.89280000E-02-4.48671000E-05 1.40017000E-08-1.67289000E-12    2
 1.83367000E+04 3.67249000E+01 3.92063000E+00 4.75061000E-03 1.80439000E-04    3
-3.25908000E-07 1.86072000E-10 1.78508000E+04 1.13844000E+01                   4
C7H9(2230)              C   7H   9          G   100.000  5000.000 1035.38      1
 1.02368357E+01 3.46935795E-02-1.38655270E-05 2.59748398E-09-1.84016888E-13    2
 2.78189248E+04-2.88047346E+01 1.63844411E+00 4.00065684E-02 1.88652744E-05    3
-4.45086214E-08 1.74755651E-11 3.10951748E+04 2.01996101E+01                   4
C7H9(2597)              C   7H   9          G   100.000  5000.000  942.07      1
 1.77908167E+01 2.13081381E-02-6.07903616E-06 1.03574333E-09-7.56083945E-14    2
 2.23843353E+04-6.63637476E+01 1.00074481E+00 4.83146627E-02 2.14295791E-05    3
-6.83274311E-08 3.15725525E-11 2.75129124E+04 2.40662919E+01                   4
C7H9(6326)              C   7H   9          G   100.000  5000.000 1047.87      1
 1.37878433E+01 2.96336713E-02-1.17792938E-05 2.18572969E-09-1.53733826E-13    2
 3.77035383E+04-4.15346476E+01 9.14150889E-01 5.71206814E-02-2.01274492E-05    3
-1.22247311E-08 7.98944359E-12 4.15904494E+04 2.68484547E+01                   4
C7H9(6641)              C   7H   9          G   100.000  5000.000  987.01      1
 1.41700453E+01 2.77146222E-02-9.97510020E-06 1.76733760E-09-1.22174842E-13    2
 3.72366577E+04-4.32568386E+01 8.37330893E-01 5.93947373E-02-2.41507683E-05    3
-1.16022997E-08 9.07578036E-12 4.09573557E+04 2.64070658E+01                   4
C7H9(6645)              C   7H   9          G   100.000  5000.000  964.15      1
 1.22363278E+01 2.97465612E-02-1.03403048E-05 1.74677121E-09-1.15788362E-13    2
 3.96359145E+04-3.16269286E+01 8.40998058E-01 6.30360850E-02-4.03710889E-05    3
 7.46540677E-09 2.30286354E-12 4.24833606E+04 2.63042202E+01                   4
C8H7(8283)              C   8H   7          G   100.000  5000.000 1051.14      1
 1.29751110E+01 2.99877692E-02-1.28381494E-05 2.50949013E-09-1.82336914E-13    2
 4.11238054E+04-4.37949839E+01 1.44541064E+00 4.27038037E-02 1.34801032E-05    3
-4.23829147E-08 1.72018278E-11 4.52690530E+04 2.05923443E+01                   4
C8H9(6454)              C   8H   9          G   100.000  5000.000 1110.23      1
 1.12355843E+01 3.75493481E-02-1.60122209E-05 3.05070250E-09-2.15873429E-13    2
 2.17370654E+04-3.27859354E+01 1.28178111E+00 4.84831350E-02 2.89561655E-06    3
-2.85272553E-08 1.14488999E-11 2.54836059E+04 2.31952814E+01                   4
```

Table B-3. Coefficients for calculating the thermodynamic properties of species in the pathway diagrams of DTE pyrolysis (continued).

```
C8H9(8217)              C   8H   9          G   100.000  5000.000 1110.35      1
 1.14203226E+01 3.61924093E-02-1.50061849E-05 2.81723326E-09-1.97700447E-13    2
 2.78335606E+04-3.35192509E+01 1.18072832E+00 5.15692395E-02-6.71919574E-06    3
-1.96064128E-08 8.77960827E-12 3.14334771E+04 2.29238611E+01                   4
CH3(228)                C   1H   3          G   100.000  5000.000  660.44      1
 3.22169594E+00 5.22645989E-03-1.64124783E-06 2.58224319E-10-1.62579155E-14    2
 1.65213098E+04 3.53938016E+00 3.94800569E+00 8.27589278E-04 8.34935674E-06    3
-9.82640255E-09 3.80106734E-12 1.64253714E+04 3.36652119E-01                   4
CH4(1246)               C   1H   4          G   100.000  5000.000 1084.12      1
 9.08269242E-01 1.14540800E-02-4.57173500E-06 8.29190911E-10-5.66314272E-14    2
-9.71997598E+03 1.39930745E+01 4.20541463E+00-5.35556659E-03 2.51123028E-05    3
-2.13762551E-08 5.97522768E-12-1.01619433E+04-9.21277081E-01                   4
H(7)                    H   1              G   100.000  5000.000 4879.80      1
 4.28461071E+00-1.45494649E-03 4.44804306E-07-6.04359642E-11 3.07921551E-15    2
 2.37230923E+04-1.18931307E+01 2.50000000E+00-3.01680531E-12 3.74582141E-15    3
-1.50856878E-18 1.86626471E-22 2.54742178E+04-4.44972899E-01                   4
H2(219)                 H   2              G   100.000  5000.000 1959.09      1
 2.78812665E+00 5.87691847E-04 1.58986586E-07-5.52691197E-11 4.34276123E-15    2
-5.96121152E+02 1.12964916E-01 3.43536449E+00 2.12707098E-04-2.78617661E-07    3
 3.40261375E-10-7.76017659E-14-1.03135986E+03-3.90841876E+00                   4
S(1039)                 C   7H  11          G   100.000  5000.000  950.94      1
 1.49287695E+01 2.98341376E-02-9.43172596E-06 1.68819755E-09-1.23885854E-13    2
 1.46036242E+04-5.31976673E+01 1.62504826E+00 3.01335007E-02 7.78951935E-05    3
-1.21086019E-07 4.83353194E-11 1.96504958E+04 2.35483908E+01                   4
S(10914)                C  10H   9          G   100.000  5000.000 1094.23      1
 1.44134151E+01 4.36578901E-02-1.97408078E-05 3.88406192E-09-2.80490164E-13    2
 3.30370532E+04-5.69948382E+01 7.53934324E-01 5.47951181E-02 1.81740702E-05    3
-5.16174314E-08 1.98028521E-11 3.83489410E+04 2.07471048E+01                   4
S(1110)                 C   7H  10          G   100.000  5000.000  960.58      1
 1.78943721E+01 2.43012805E-02-8.01423855E-06 1.41741038E-09-1.01048466E-13    2
 8.18560891E+03-6.78089323E+01 5.40177840E-01 6.14551766E-02-1.12032398E-05    3
-3.44221091E-08 1.91301482E-11 1.31395195E+04 2.36489302E+01                   4
S(11126)                C  10H   9          G    10.000  3000.000  544.99      1
-4.65161000E+00 9.01411000E-02-6.07034000E-05 1.93162000E-08-2.33266000E-12    2
 2.71848000E+04 4.56072000E+01 3.89159000E+00 6.34791000E-03 2.27970000E-04    3
-4.04814000E-07 2.24798000E-10 2.65668000E+04 1.24503000E+01                   4
S(11344)                C  10H   8          G    10.000  3000.000  581.28      1
-2.55933000E+00 7.97241000E-02-5.16554000E-05 1.58185000E-08-1.84313000E-12    2
 1.29877000E+04 3.40631000E+01 4.11550000E+00-1.18741000E-02 3.02555000E-04    3
-5.25571000E-07 2.89125000E-10 1.29832000E+04 1.21184000E+01                   4
S(1146)                 C   7H  11          G   100.000  5000.000 1011.64      1
 1.32525197E+01 3.50663883E-02-1.32012036E-05 2.37832188E-09-1.64861368E-13    2
 8.65365745E+03-4.12150953E+01 7.55848202E-01 5.99969483E-02-1.38676983E-05    3
-2.11034792E-08 1.15495084E-11 1.24347903E+04 2.54102154E+01                   4
S(11912)                C  10H  10          G   100.000  5000.000 1194.75      1
 1.50939933E+01 4.42736328E-02-1.85625348E-05 3.44175024E-09-2.37865667E-13    2
 5.71739621E+04-4.02508295E+01 2.56428670E-02 7.53145976E-02-3.31681242E-05    3
-2.00461474E-09 3.74678037E-12 6.21596881E+04 4.09232649E+01                   4
S(12303)                C   8H   6          G   100.000  5000.000  963.80      1
 1.63479345E+01 1.96730465E-02-6.59813328E-06 1.25360777E-09-9.55576600E-14    2
 2.99125264E+04-6.23153792E+01 1.55290426E+00 3.53461915E-02 4.01801902E-05    3
-8.03327562E-08 3.38367617E-11 3.48883583E+04 1.95351587E+01                   4
S(12311)                C   8H   7          G   100.000  5000.000 1090.84      1
 1.18686890E+01 3.18010024E-02-1.38622261E-05 2.69138097E-09-1.93194076E-13    2
 4.03341004E+04-3.75961688E+01 1.48076812E+00 4.37983693E-02 5.52167548E-06    3
-3.10837579E-08 1.25730262E-11 4.41529356E+04 2.05389048E+01                   4
```

Table B-3. Coefficients for calculating the thermodynamic properties of species in the pathway diagrams of DTE pyrolysis (continued).

```
S(12337)                C   8H   7          G   100.000  5000.000 1800.46      1
 1.77214797E+01 2.40291231E-02-9.75271562E-06 1.72639368E-09-1.13658272E-13    2
 4.19344492E+04-7.17920633E+01 7.18594482E-01 6.18039734E-02-4.12239770E-05    3
 1.33795354E-08-1.73175014E-12 4.80570012E+04 2.02353015E+01                   4
S(12510)                C   8H   5          G   100.000  5000.000  952.99      1
 1.63646658E+01 1.59670949E-02-4.79626944E-06 8.71747952E-10-6.63387652E-14    2
 6.08989527E+04-5.94979227E+01 1.50843103E+00 3.89133847E-02 2.11181522E-05    3
-6.06516484E-08 2.74572250E-11 6.55200926E+04 2.08487737E+01                   4
S(12511)                C   8H   5          G   100.000  5000.000  952.99      1
 1.63646658E+01 1.59670949E-02-4.79626944E-06 8.71747952E-10-6.63387652E-14    2
 6.08989527E+04-5.94979227E+01 1.50843103E+00 3.89133847E-02 2.11181522E-05    3
-6.06516484E-08 2.74572250E-11 6.55200926E+04 2.08487737E+01                   4
S(12512)                C   8H   5          G   100.000  5000.000  952.99      1
 1.63646658E+01 1.59670949E-02-4.79626944E-06 8.71747952E-10-6.63387652E-14    2
 6.08989527E+04-6.01910698E+01 1.50843103E+00 3.89133847E-02 2.11181522E-05    3
-6.06516484E-08 2.74572250E-11 6.55200926E+04 2.01556265E+01                   4
S(14220)                C   5H   5          G   100.000  5000.000 1071.06      1
 7.36862629E+00 1.95182608E-02-7.32845026E-06 1.29024003E-09-8.70717796E-14    2
 2.94180007E+04-1.81999344E+01 2.41060753E+00 3.07884821E-02-1.29640939E-05    3
-1.51852769E-09 2.04292522E-12 3.08956887E+04 8.00024195E+00                   4
S(14222)                C   5H   6          G   100.000  5000.000  948.17      1
 1.23880689E+01 1.33342946E-02-3.50202662E-06 6.76646291E-10-5.69850499E-14    2
 1.06912171E+04-4.47923158E+01 2.99618097E+00 2.16819780E-03 9.45074549E-05    3
-1.24725569E-07 4.79019442E-11 1.47551998E+04 1.20570163E+01                   4
S(1785)                 C   7H  10          G    10.000  3000.000  406.26      1
-2.61898000E+00 6.88083000E-02-4.18875000E-05 1.23226000E-08-1.40337000E-12    2
 6.02703000E+03 3.66707000E+01 3.93322000E+00 4.30268000E-03 1.96257000E-04    3
-3.78428000E-07 2.39028000E-10 5.49459000E+03 1.09614000E+01                   4
S(2023)                 C   7H  10          G    10.000  3000.000  410.08      1
-2.75432000E+00 6.94353000E-02-4.25957000E-05 1.26264000E-08-1.44776000E-12    2
 5.71562000E+03 3.71988000E+01 3.93497000E+00 4.17536000E-03 1.96155000E-04    3
-3.75578000E-07 2.35257000E-10 5.16709000E+03 1.08908000E+01                   4
S(2150)                 C   7H  10          G    10.000  3000.000  432.16      1
-3.46759000E+00 7.23999000E-02-4.58172000E-05 1.39695000E-08-1.63956000E-12    2
 6.98834000E+03 4.01657000E+01 3.93810000E+00 3.86964000E-03 1.91993000E-04    3
-3.52802000E-07 2.10486000E-10 6.34811000E+03 1.06490000E+01                   4
S(5864)                 C  10H  12          G   100.000  5000.000 1006.12      1
 1.80178457E+01 4.18474268E-02-1.65156464E-05 3.14361331E-09-2.27736332E-13    2
 4.64114712E+03-6.70855766E+01 1.85741689E-01 6.26549192E-02 2.71362037E-05    3
-7.52597279E-08 3.15483550E-11 1.07645053E+04 3.16512409E+01                   4
S(5899)                 C  10H  11          G   100.000  5000.000 1030.87      1
 1.70262852E+01 4.10222636E-02-1.66103328E-05 3.15018201E-09-2.25592632E-13    2
 3.38059871E+04-5.97823861E+01 1.40354322E-01 6.73793652E-02 2.02422160E-06    3
-4.57537119E-08 2.05715104E-11 3.93684102E+04 3.22891435E+01                   4
S(5910)                 C  10H  13          G   100.000  5000.000 2226.43      1
 2.96646916E+01 3.35291826E-02-1.39030396E-05 2.36982640E-09-1.47507106E-13    2
 3.47779508E+03-1.37241879E+02 4.14002974E-01 7.93513303E-02-4.02406594E-05    3
 8.89859080E-09-7.28165242E-13 1.81706455E+04 3.10337611E+01                   4
S(6149)                 C  14H  14          G   100.000  5000.000  999.02      1
 2.48935655E+01 5.21874155E-02-2.05803339E-05 3.97140902E-09-2.91929439E-13    2
 4.82111223E+03-1.05677076E+02-1.12271835E+00 8.12346886E-02 4.85969422E-05    3
-1.17460045E-07 4.89312592E-11 1.37678932E+04 3.85724890E+01                   4
S(6287)                 C   8H  10          G    10.000  3000.000  378.14      1
-2.62723000E+00 7.39489000E-02-4.60899000E-05 1.38184000E-08-1.59588000E-12    2
 1.21650000E+03 3.79855000E+01 3.93256000E+00 4.57740000E-03 2.29019000E-04    3
-4.71073000E-07 3.18895000E-10 7.20269000E+02 1.27159000E+01                   4
```

Table B-3. Coefficients for calculating the thermodynamic properties of species in the pathway diagrams of DTE pyrolysis (continued).

```
S(6420)                 C  10H  10          G   100.000  5000.000  993.07      1
 1.74633872E+01 3.76584117E-02-1.44964447E-05 2.74936158E-09-2.00074894E-13    2
 2.49660912E+04-6.81564169E+01 5.24422095E-01 5.53809188E-02 3.50228011E-05    3
-8.17081545E-08 3.39546705E-11 3.08208175E+04 2.59854978E+01                   4
S(6455)                 C  10H  11          G   100.000  5000.000 1000.55      1
 1.80171658E+01 3.94340565E-02-1.55401763E-05 2.97821239E-09-2.17450617E-13    2
 2.15715371E+04-6.83848147E+01 3.94333061E-01 5.73118883E-02 3.64768524E-05    3
-8.41980567E-08 3.46867907E-11 2.77296634E+04 2.97957510E+01                   4
S(6457)                 C  10H  11          G   100.000  5000.000 1002.97      1
 1.80043500E+01 3.81893440E-02-1.47399482E-05 2.76768774E-09-1.98994366E-13    2
 3.56414089E+04-6.40957997E+01 1.36592837E-01 6.62882618E-02 7.78550073E-06    3
-5.51100718E-08 2.49221545E-11 4.13964343E+04 3.29809513E+01                   4
S(8404)                 C  10H  10          G   100.000  5000.000  972.57      1
 2.10080576E+01 3.10484886E-02-1.09530409E-05 2.04924054E-09-1.51208531E-13    2
 1.50369506E+04-8.52554393E+01 1.23746998E-01 6.28929151E-02 2.32931967E-05    3
-7.85663877E-08 3.52592657E-11 2.16554559E+04 2.80599881E+01                   4
S(8550)                 C  10H  11          G   100.000  5000.000 1097.32      1
 1.51924763E+01 4.65434795E-02-1.97252553E-05 3.74498439E-09-2.64852339E-13    2
 2.50846906E+04-5.88943712E+01 1.40150115E-01 6.97538143E-02-8.17624498E-06    3
-2.95638262E-08 1.33139214E-11 3.02941930E+04 2.38073729E+01                   4
S(8587)                 C  10H  10          G   100.000  5000.000 1019.60      1
 1.59497105E+01 4.11481311E-02-1.66539292E-05 3.17782647E-09-2.29142498E-13    2
 8.05927153E+03-6.45163997E+01 5.26883123E-01 5.75432253E-02 2.41202874E-05    3
-6.59138972E-08 2.71157825E-11 1.34970937E+04 2.14328598E+01                   4
S(8635)                 C  10H   9          G   100.000  5000.000 1021.10      1
 1.65826273E+01 3.78362927E-02-1.55721240E-05 3.02468785E-09-2.20875972E-13    2
 2.21452979E+04-6.54622863E+01 6.46544262E-01 5.42684368E-02 2.78560162E-05    3
-6.94431658E-08 2.83223677E-11 2.77975790E+04 2.34942037E+01                   4
S(8636)                 C  10H   9          G   100.000  5000.000 1046.26      1
 1.61600965E+01 3.91973697E-02-1.64056174E-05 3.14981332E-09-2.26405198E-13    2
 2.64522934E+04-6.27354362E+01 4.09571001E-01 6.23346661E-02 3.58291207E-06    3
-4.34599100E-08 1.90047533E-11 3.17775647E+04 2.36626011E+01                   4
S(8877)                 C  10H   8          G   100.000  5000.000 1009.62      1
 1.87137182E+01 3.13457407E-02-1.24659658E-05 2.39168846E-09-1.74352421E-13    2
 1.84343701E+04-7.84594852E+01 2.76682450E-01 6.42279528E-02-1.64853663E-06    3
-4.41526666E-08 2.11073623E-11 2.42042360E+04 2.08024760E+01                   4
S(8896)                 C  10H   9          G   100.000  5000.000 1044.33      1
 1.57639104E+01 3.87655918E-02-1.62171165E-05 3.13169677E-09-2.26196821E-13    2
 1.91631320E+04-6.02024778E+01 5.74985341E-01 5.83862644E-02 1.09800356E-05    3
-4.95820110E-08 2.08556126E-11 2.44381018E+04 2.38004674E+01                   4
S(9095)                 C  10H   9          G   100.000  5000.000 1022.58      1
 1.54028263E+01 3.86934320E-02-1.56146197E-05 2.98010912E-09-2.14878102E-13    2
 3.06795037E+04-5.61948445E+01 6.77267590E-01 5.55865475E-02 1.93191040E-05    3
-5.87246531E-08 2.43881617E-11 3.58195153E+04 2.55832307E+01                   4
```

Table B-4. The molecular structures of species in the pathway diagrams of DTE pyrolysis.

Label	Stoichiometry	Multiplicity	Structure	SMILES
ALLENE(51)	C_3H_4	1		C=C=C
ALLYL(3)	C_3H_5	2	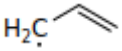	[CH2]C=C
C2H2(501)	C_2H_2	1		C2H2
C2H3(5)	C_2H_3	2	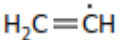	C2H3
C2H4(227)	C_2H_4	1	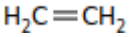	C2H4
C2H5(502)	C_2H_5	2	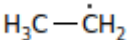	C2H5
C2H6(1571)	C_2H_6	1	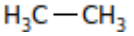	C2H6
C3H3(217)	C_3H_3	2	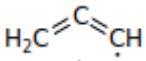	C3H3
C3H4(759)	C_3H_4	1		C#CC
C3H5(53)	C_3H_5	2		C=[C]C
C3H5(54)	C_3H_5	2	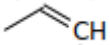	[CH]=CC
C3H6(84)	C_3H_6	1		C=CC
C3H7(231)	C_3H_7	2	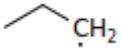	[CH2]CC
C3H7(232)	C_3H_7	2		C[CH]C
C4H5(176)	C_4H_5	2	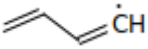	CH2CHCHCH
C4H6(57)	C_4H_6	1	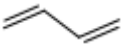	C=CC=C
C4H6(500)	C_4H_6	1		C#CCC
C4H6(239)	C_4H_6	1		CH3CHCCH2
C4H7(9)	C_4H_7	2		[CH2]CC=C
C4H7(181)	C_4H_7	2	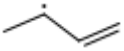	C=C[CH]C
C4H7(246)	C_4H_7	2	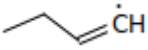	[CH]=CCC
C4H7(247)	C_4H_7	2		C[C]=CC
C4H8(248)	C_4H_8	1		C=CCC
C4H8(251)	C_4H_8	1		CC=CC
C4H8(2010)	C_4H_8	1		CC=CC
C4H9(1337)	C_4H_9	2	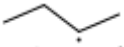	C[C]CC
C5H5(6350)	C_5H_5	2	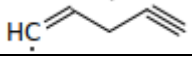	C[CH]CC

Table B-4. The molecular structures of species in the pathway diagrams of DTE pyrolysis (continued).

Label	Stoichiometry	Multiplicity	Structure	SMILES
C5H5(7360)	C_5H_5	2		[CH]=CCC#C
C5H9(984)	C_5H_9	2	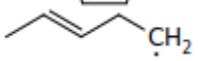	[C]1=CC=CC1
C5H9(1283)	C_5H_9	2	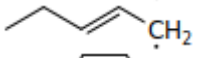	[CH2]CC=CC
C6H5(5026)	C_6H_5	2		C=C[CH]CC
C6H6(3530)	C_6H_6	1		[c]1ccccc1
C6H6(5025)	C_6H_6	1		C1=CC=CCC=1
C6H6(5543)	C_6H_6	1	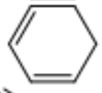	c1ccccc1
C6H6(6617)	C_6H_6	1		[C]1C=CC=CC1
C6H6(6621)	C_6H_6	1		C=C=CC=C=C
C6H6(6622)	C_6H_6	1		C#CCC=C=C
C6H6(7615)	C_6H_6	1		C#CCCC#C
C6H6(7686)	C_6H_6	1		C#CC=CC=C
C6H7(2228)	C_6H_7	2		[CH]1C=CC=CC1
C6H8(951)	C_6H_8	1		C1=CCC=CC1
C6H10(119)	C_6H_{10}	1	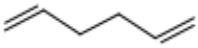	C=CCCC=C
C6H11(200)	C_6H_{11}	2	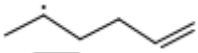	C=CCC[CH]C
C7H7(5027)	C_7H_7	2	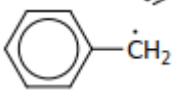	[CH2]c1ccccc1
C7H7(5028)	C_7H_7	2	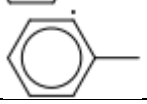	Cc1[c]cccc1

Table B-4. The molecular structures of species in the pathway diagrams of DTE pyrolysis (continued).

Label	Stoichiometry	Multiplicity	Structure	SMILES
C7H7(5029)	C_7H_7	2	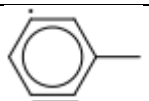	Cc1c[c]ccc1
C7H7(5030)	C_7H_7	2	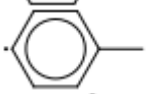	Cc1cc[c]cc1
C7H7(5790)	C_7H_7	2	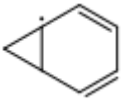	C1=C[C]2CC2C=C1
C7H7(5801)	C_7H_7	2		C1=CC2C=C[C]1C2
C7H7(6190)	C_7H_7	2	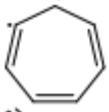	[C]1=CC=CC=CC1
C7H7(7251)	C_7H_7	2	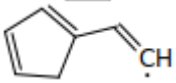	[CH]=CC1=CC=CC1
C7H7(7340)	C_7H_7	2	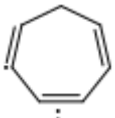	[C]1=CCC=CC=C1
C7H7(7354)	C_7H_7	2	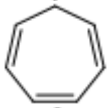	[CH]1C=CC=CC=C1
C7H7(7355)	C_7H_7	2	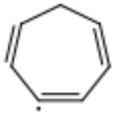	[C]1=CC=CCC=C1
C7H7(7358)	C_7H_7	2	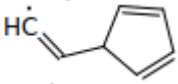	[CH]=CC1C=CC=C1
C7H7(8876)	C_7H_7	2	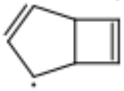	[CH]1C=CC2C=CC12
C7H8(3291)	C_7H_8	1	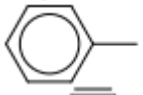	Cc1ccccc1
C7H9(2024)	C_7H_9	2	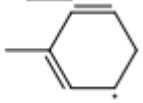	CC1=C[CH]CC=C1
C7H9(2025)	C_7H_9	2	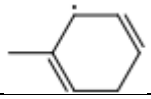	CC1=CCC=C[CH]1

Table B-4. The molecular structures of species in the pathway diagrams of DTE pyrolysis (continued).

Label	Stoichiometry	Multiplicity	Structure	SMILES
C7H9(2151)	C_7H_9	2	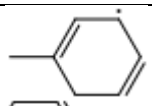	CC1=C[CH]C=CC1
C7H9(2153)	C_7H_9	2	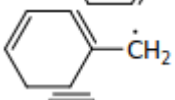	[CH2]C1=CC=CCC1
C7H9(2229)	C_7H_9	2	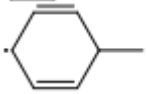	CC1C=C[CH]C=C1
C7H9(2230)	C_7H_9	2	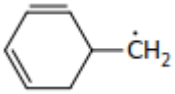	[CH2]C1C=CC=CC1
C7H9(2597)	C_7H_9	2	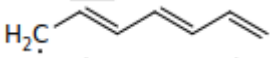	[CH2]C=CC=CC=C
C7H9(6326)	C_7H_9	2	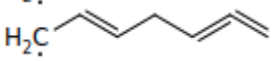	C=C=CC[CH]C=C
C7H9(6641)	C_7H_9	2		C=C=C[CH]CC=C
C7H9(6645)	C_7H_9	2	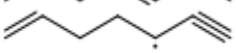	[CH]=C=CCCC=C
C7H10(507)	C_7H_{10}	1		C=CC=CC=CC
C7H11(2)	C_7H_{11}	2	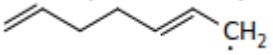	[CH2]C=CCCC=C
C7H11(24)	C_7H_{11}	2	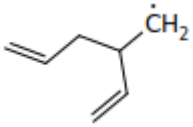	[CH2]C(C=C)CC=C
C7H11(72)	C_7H_{11}	2		C=CC[CH]C=CC
C7H11(73)	C_7H_{11}	2	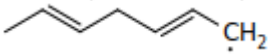	C=C[CH]CC=CC
C7H11(77)	C_7H_{11}	2	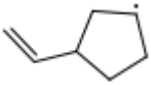	C=CC1C[CH]CC1
C7H11(517)	C_7H_{11}	2	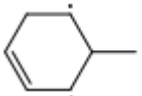	CC1[CH]CC=CC1
C7H11(523)	C_7H_{11}	2	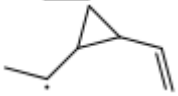	C=CC1CC1[CH]C
C7H11(683)	C_7H_{11}	2	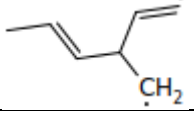	[CH2]C(C=C)C=CC

Table B-4. The molecular structures of species in the pathway diagrams of DTE pyrolysis (continued).

Label	Stoichiometry	Multiplicity	Structure	SMILES
C7H11(945)	C_7H_{11}	2	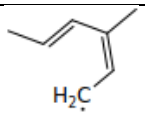	C=C[C](C)C=CC
C7H11(949)	C_7H_{11}	2	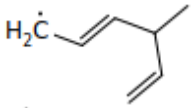	[CH2]C=CC(C)C=C
C7H12(93)	C_7H_{12}	1		C=CCCC=CC
C7H12(257)	C_7H_{12}	1	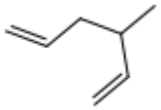	C=CCC(C)C=C
C8H7(8283)	C_8H_7	2	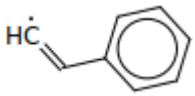	[CH]=Cc1ccccc1
C8H9(6454)	C_8H_9	2	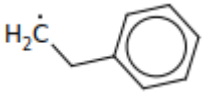	[CH2]Cc1ccccc1
C8H9(8217)	C_8H_9	2	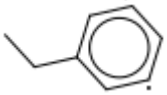	CCc1c[c]ccc1
C10H16(1)	$C_{10}H_{16}$	1	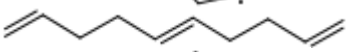	C=CCCC=CCCC=C
C10H16(17)	$C_{10}H_{16}$	1	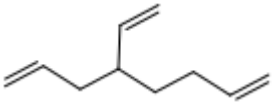	C=CCCC(C=C)CC=C
CH3(228)	C_1H_3	2		CH3
CH4(1246)	C_1H_4	1		CH4
H(7)	H_1	2		H
H2(219)	H_2	1		H2
S(1039)	C_7H_{11}	2	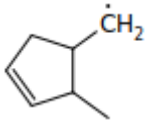	[CH2]C1CC=CC1C
S(1110)	C_7H_{10}	1	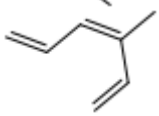	C=CC=C(C)C=C
S(1146)	C_7H_{11}	2	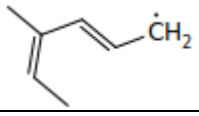	[CH2]C=CC(C)=CC

Table B-4. The molecular structures of species in the pathway diagrams of DTE pyrolysis (continued).

Label	Stoichiometry	Multiplicity	Structure	SMILES
S(1785)	C_7H_{10}	1	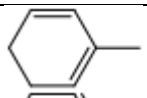	CC1=CCCC=C1
S(2023)	C_7H_{10}	1	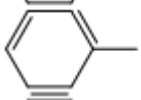	CC1=CC=CCC1
S(2150)	C_7H_{10}	1	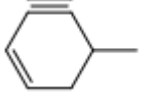	CC1C=CC=CC1
S(5864)	$C_{10}H_{12}$	1	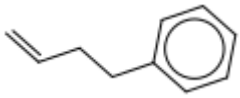	C=CCCc1ccccc1
S(5899)	$C_{10}H_{11}$	2	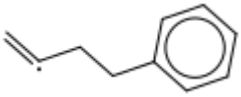	C=[C]CCc1ccccc1
S(5910)	$C_{10}H_{13}$	2	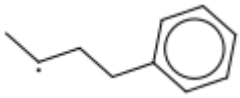	C[CH]CCc1ccccc1
S(6149)	$C_{14}H_{14}$	1	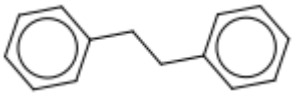	c1ccc(CCc2ccccc2)cc1
S(6287)	C_8H_{10}	1	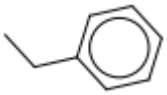	CCc1ccccc1
S(6420)	$C_{10}H_{10}$	1	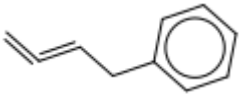	C=C=CCc1ccccc1
S(6455)	$C_{10}H_{11}$	2	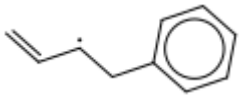	C=C[CH]Cc1ccccc1
S(6457)	$C_{10}H_{11}$	2	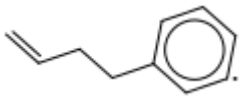	C=CCCc1c[c]ccc1
S(8404)	$C_{10}H_{10}$	1	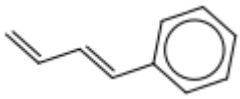	C=CC=Cc1ccccc1
S(8550)	$C_{10}H_{11}$	2	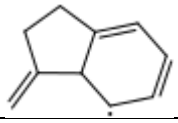	C=C1CC[C]2C=CC=CC21

Table B-4. The molecular structures of species in the pathway diagrams of DTE pyrolysis (continued).

Label	Stoichiometry	Multiplicity	Structure	SMILES
S(8587)	$C_{10}H_{10}$	1	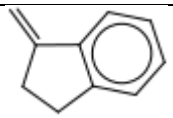	C=C1CCc2ccccc21
S(8635)	$C_{10}H_{9}$	2	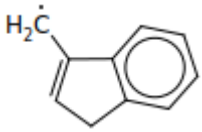	C=C1[CH]Cc2ccccc21
S(8636)	$C_{10}H_{9}$	2	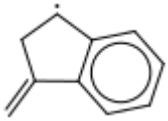	C=C1C[CH]c2ccccc21
S(8877)	$C_{10}H_{8}$	1	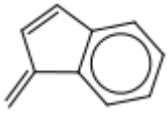	C=C1C=Cc2ccccc21
S(8896)	$C_{10}H_{9}$	2	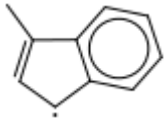	CC1=C[CH]c2ccccc21
S(9095)	$C_{10}H_{9}$	2	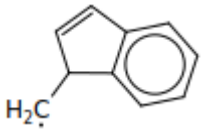	[CH2]C1C=Cc2ccccc21
S(10914)	$C_{10}H_{9}$	2	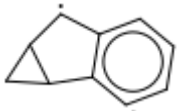	[CH]1c2ccccc2C2CC12
S(11126)	$C_{10}H_{9}$	2	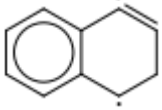	[CH]1CC=Cc2ccccc21
S(11344)	$C_{10}H_{8}$	1		c1ccc2ccccc2c1
S(11912)	$C_{10}H_{10}$	1	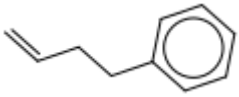	C=C[C]Cc1ccccc1
S(12303)	$C_{8}H_{6}$	1	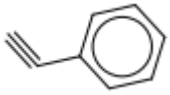	C#Cc1ccccc1
S(12311)	$C_{8}H_{7}$	2	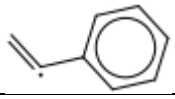	C=[C]c1ccccc1

Table B-4. The molecular structures of species in the pathway diagrams of DTE pyrolysis (continued).

Label	Stoichiometry	Multiplicity	Structure	SMILES
S(12337)	C_8H_7	2	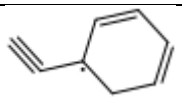	[CH]=C=C1C=CC=CC1
S(12510)	C_8H_5	2	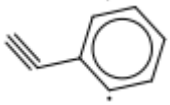	C#Cc1[c]cccc1
S(12511)	C_8H_5	2	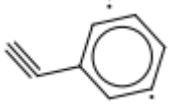	C#Cc1c[c]ccc1
S(12512)	C_8H_5	2	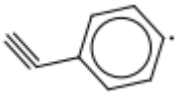	C#Cc1cc[c]cc1
S(14220)	C_5H_5	2		[CH]1C=CC=C1
S(14222)	C_5H_6	1		C1=CCC=C1

List of Symbols, Abbreviations, and Acronyms

2/3D	Two-/Three-Dimensional
AP	Ammonium Perchlorate
ARL	Army Research Laboratory
CFD	Computational Fluid Dynamics
CONP	Constant-Pressure
CPU	Central Processing Unit
DEVCOM	U.S. Army Combat Capabilities Development Command
DoW	Department of War
D/P-GC/MS	Desorption/Pyrolysis-Gas Chromatograph/Mass Spectroscopy
DTE	1,5,9-decatriene
EM	Energetic Material
EODT	6-ethenyl-2,8,12,16-octadectetraene
FID	Flame Ionization Detector
GC	Gas Chromatograph
He	Helium
HTPB	Hydroxyl-Terminated Polybutadiene
MEP	Minimum Energy Path
ML	Machine Learning
MS	Mass Spectrometer
NLR	National Laboratory of the Rockies
PAH	Polycyclic Aromatic Hydrocarbon
PDE	Partial Differential Equation
PPM	Parts per Million
QM-ESM	Quantum Mechanics-Based Electronic Structure Method
RMG	Reaction Mechanism Generator
SME	Subject Matter Expert
TCD	Thermal Conductivity Detector
UQ	Uncertainty Quantification

1 (PDF)	DEFENSE TECHNICAL INFORMATION CTR DTIC OCA
1 (PDF)	DEVCOM ARL FCDD RLB CB TECH LIB